Research Dissertation

For

Enhancing vehicle dynamics through real-time tyre temperature analysis

In fulfilment of the requirements for the degree:

Magister Technologiae: Engineering: Mechanical

By

Trevor Stroud
8799091

Promoter:	Mr K.H. Du Preez
Co-Promoter:	Prof T.I. van Niekerk

Author's declaration

I Trevor Stroud hereby declare that:

- At no time during the registration for the Magister Technologiae Degree has the author been registered for any other university degree
- The work done in this dissertation is my own; and
- All sources used or referred to have been documented and recognized.

Date:

Signed: ___________________________ Place: **Port Elizabeth**

Abstract

Vehicle suspension optimisation is a complex and difficult task, as there are a variety of factors influencing the dynamic performance of a vehicle. During suspension development, the optimisation of a selected few of these factors is often to the detriment of others, as they are all inter-related. In addition, expertise in vehicle setup and suspension tuning is scarce, and is limited to experienced racing teams and large automotive manufacturers with extensive research and development capabilities. The motivation for this research was therefore to provide objective and user-friendly methodologies for vehicle suspension optimisation, in order to support student projects like Formula Student, while having relevance to the needs of the South African automotive industry and racing community.

With the onset of digital data acquisition, it has become feasible to take real-time measurements of tyre temperatures, to provide information on how a tyre is performing at a specific point on the track. Measuring the tyre surface temperature can provide a useful indication on whether the tyre is loaded equally or not, and what suspension adjustments should be made to improve tyre load distribution.

The researcher focussed this study on three crucial areas, namely the analysis of tyre operating temperatures, tyre camber settings and tyre pressures. This test data was then used to provide insights into the shortcomings of a particular vehicle suspension setup, and provide guidance for improvement.

The results of the study revealed that for the DibaOne Formula Student vehicle, as tested on the Celso Scribante Short Circuit, the tyre operating temperature was 43.04°C, with an average warm-up time of 3.51minutes. After testing a range of camber settings on the front wheels, the ideal camber angle was found by comparing the temperature distribution across each tyre, and finding the most even distribution of temperature, which occurred at -1.5° of camber. To determine the best tyre pressure for the vehicle, tyre temperatures were once again analysed to find the best temperature distribution across the surface of the tyre. The most suitable tyre pressures for the vehicle were found to be 70Kpa in their cold condition.

Additional sensors fitted to the vehicle allowed the plotting of a G-G Diagram to analyse the maximum performance envelope of the vehicle, the understeer gradient which highlighted the balance of the vehicle, and GPS track data was used to measure lap times, speeds and distances.

The objective of this research was to use tyre temperatures to determine the optimum suspension settings for a race vehicle, and the results of this study demonstrated that this objective was successfully achieved.

Acknowledgements

I would firstly like to thank our Vice Chancellor Prof Derek Swartz for catching the vision of the Formula Student project, and enabling its success, thereby laying the foundation for this research. I would also like to thank the former Dean of the Faculty of Engineering, the Built Environment and Information Technology, Prof Henk de Jager, who also supported both the project and myself personally, inspiring me to complete this research. I would then like to thank Mr Sarel Schoombie for his wisdom and guidance, and Prof Pat McGrath for his support in providing me with the time to complete this study. I would especially like to thank my supervisor Mr Karl du Preez for his mentorship, and for always expecting the best from me. To my co-supervisor Prof Theo van Niekerk, thank you for your unwavering faith in me, and for facilitating much of the funding needed to set up the research platform.

Finally, I would like to thank my wife Prof Louise Stroud, for her love, support, guidance and insight into the academic research process, which enabled me to find my way, and persevere on this journey, to finally complete this research study.

Table of Contents

List of Figures

List of Tables

1. Introduction

1.1 Background to this Research

The NMMU Racing Formula Student team started at the end of 2008, under the leadership of the researcher, and after designing and building their first “Formula Student” vehicle, the NMMU Racing team competed in the German Formula Student completion in August 2011. The development and manufacture of a second formula student race car has since commenced, and incorporates much of the valuable engineering knowledge gained.

The researcher chose to focus this study on vehicle dynamics and suspension optimisation, primarily to expand the body of local knowledge available in this field. This research hopes to support the Formula Student project in the Nelson Mandela Metropolitan University by generating and documenting specific academic knowledge in the field of vehicle design and testing. In addition, this research project serves to support the South African motor industry due to its automotive-specific focus.

Vehicle suspension optimisation is a complex and difficult task as there are a variety of factors influencing the dynamic performance of a vehicle. During suspension development, the optimisation of a selected few of these factors is often to the detriment of others, as these factors are all inter-related. In addition, expertise in vehicle setup and suspension tuning is scarce, and is limited to experienced racing teams and large automotive manufacturers with extensive research and development capabilities.

The motivation for this research was therefore to provide objective and user-friendly methodologies for vehicle suspension optimisation, in order to support student projects like Formula Student, while having relevance to the needs of the South African automotive industry and racing community.

1.2 Vehicle Development Cycle

Figure 1 below illustrates a typical vehicle development cycle, consisting of vehicle modelling, vehicle dynamic simulation, testing, data analysis and refining. Due to the fact that the Formula Student vehicle was already built at the time of conducting this research, the first two phases of the development cycle had already been completed. The focus of this study was therefore on the development of a vehicle data acquisition system to facilitate the optimisation of the dynamic performance of the NMMU Racing Formula Student vehicle.

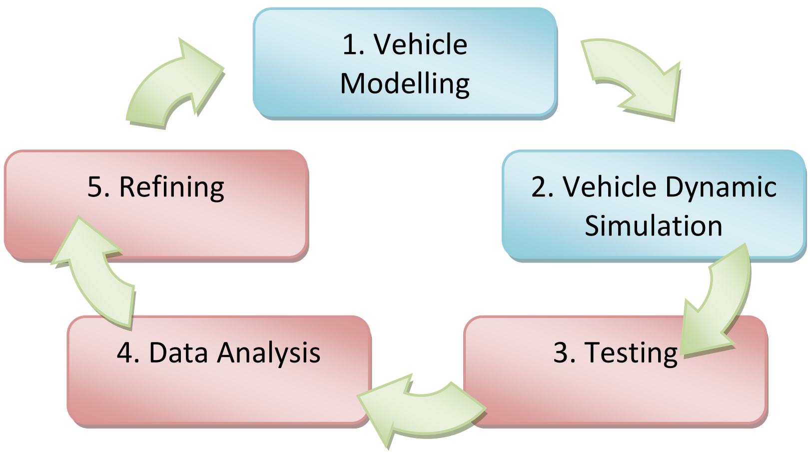

Figure 1: Vehicle Development Cycle

1.4 The Formula Student Competition

The Formula student competition is an international design competition requiring students to research, design and build a functional “Formula Student” single-seater racing car according to strict rules formulated by the Society of Automotive Engineers (SAE), with the ultimate goal of competing against other university teams from around the world.

Due to the nature of the Formula Student competition, which consists of various dynamic and static events, the main priority in the design of the vehicle is optimising vehicle dynamics including cornering, acceleration and braking. The tracks used in the competition are narrow and have very tight corners, which limit the maximum speeds attained by the formula student cars. The maximum speed attained in the dynamic events, typically does not exceed 80km/h, and although the use of aerodynamic aids has historically been largely ignored, more and more vehicles are incorporating wings and diffusers into their designs to maximise down-force, thereby improving cornering speeds. The Formula Student dynamic events are listed below:

a) Acceleration

The objective of the acceleration event is to evaluate the car’s acceleration performance in a straight line on flat pavement [1], and is conducted on a 75m course.

b) Skid-Pad

The objective of the skid-pad event is to measure the car’s cornering ability on a flat surface while making a constant-radius turn. As shown in Figure 2 below, the vehicle is required to drive on two concentric circles 15.25 m in diameter, in a figure of eight pattern [1].

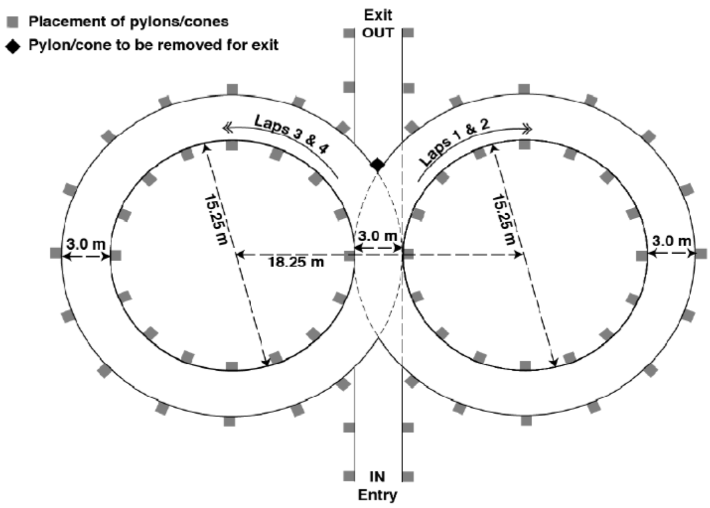

Figure 2: Formula Student Skidpan Layout

Source: 2011 Formula SAE Rules. SAE International. 2010 [1]

c) Autocross

The objective of the autocross event is to evaluate the car's manoeuvrability and handling qualities on a tight course without the hindrance of competing cars. The autocross course combines acceleration, braking and cornering into one event [1].

d) Endurance

The endurance event is designed to evaluate the overall performance of the car and to test the car’s durability and reliability [1]. Figure 3 below shows NMMU Racing’s “DibaOne” on the Formula Student Germany endurance course, which is the longest and most challenging event as the cars drive approximately 22km at race-pace, with a compulsory driver change mid-way through.

Figure 3: Formula Student Germany Endurance Track

2. Research Proposal

2.1 Problem Statement

The main research problem was to develop an objective and repeatable measurement system, which could provide the required data to make reliable inferences regarding the shortcomings of a particular vehicle suspension setup, and provide guidance for potential improvements.

2.2 Research Aims

The main aim of this research was to provide a means by which the NMMU Racing Formula Student vehicle could be dynamically optimised, to improve vehicle handling on a race circuit. In addition, this research aimed to expand the body of knowledge available to the Nelson Mandela Metropolitan University in the field of vehicle dynamics.

In order to achieve these aims, the researcher had to accomplish the following:

- Establish the historical and current methodologies employed in vehicle dynamic research and testing, through an extensive literature survey. The researcher also engaged with industry experts and attended seminars related to this field.
- Create a research platform through the manufacture of a Formula Student racing vehicle, and the sourcing and installation of the required data acquisition system and sensors.

- Design and carry out the appropriate vehicle tests and accurately record vehicle test data.
- Analyse test data in order to reach a conclusion that proves or disproves the research hypothesis.
- Record research findings and document the study in an appropriate academic format.

2.3 Hypothesis

Tyre temperatures of a Formula Student race car can be used to determine the vehicle's optimum suspension setting.

This hypothesis is based on the idea that vehicle tyres, being the sole means of contact between the vehicle and the track, experience all of the forces encountered during acceleration, braking and cornering, and develop heat due to the frictional forces from both the track surface, and tyre internal friction. These temperatures can be used to determine the appropriate suspension adjustments required for best performance.

2.4 Literature Review

2.4.1 Understanding Vehicle Acceleration

Pat Clarke, head judge at the "Formula Student Germany" competition in his column "Pat's Corner" [2] likened the process of suspension tuning to a variation on Rubik's cube, where you manage to get one or two sides right, only to destroy your progress in trying to solve the other sides. A typical example could be when your vehicle experienced under-steer going in to a corner, and after making adjustments to resolve this problem, find that the vehicle then over-steered going out of the corner.

According to Milliken & Milliken [3] "Vehicle dynamics is the branch of engineering which relates tyre and aerodynamic forces to overall vehicle accelerations, velocities and motions, using Newton's laws of motion. It encompasses the behaviour of the vehicle as affected by driveline, tyres, aerodynamics and chassis characteristics". This is a particularly complex subject to study due to the large number of variables at work during the motion of a motor vehicle. Milliken & Milliken [3] goes on to say that although the focus in racing and road car design is different, the same fundamental engineering principles apply.

In order to maximise the dynamic performance of a motor vehicle, both the longitudinal and lateral dynamics are of interest. Millikin & Millikin [3] states that the objective of studying the dynamics of a vehicle in a corner is "to use the cornering forces of all four tyres to achieve maximum lateral acceleration while balancing the front and rear tyres, so that the car neither runs wide ("understeers") nor tightens ("oversteers") the intended turn".

With the development of modern computerised data acquisition systems, it is now possible to measure and analyse these dynamic forces experienced by a vehicle under various conditions. In addition, analytical techniques can be used to predict the performance of a vehicle by simulating various configurations in the virtual environment.

According to Milliken & Milliken [3] the velocity of a circuit racing car should never be constant, unless held for some particular reason, or limited by the maximum speed of the vehicle. Peter G. Wright, Technical Director of Team Lotus said “Driving a car as fast as possible (in a race) is all about maintaining the highest possible acceleration level in the appropriate direction” [3].

Race car performance is not only about lateral acceleration, but according to Rouelle [4] it is also about longitudinal, vertical and yaw acceleration. It is about maintaining the maximum possible tyre grip in the appropriate direction, on every part of the track [4].

For this reason, racing car requirements are best expressed in terms of acceleration, which is defined as a change in velocity with time. It is also convenient to express vehicle acceleration in terms of the gravitational acceleration of a body falling to the ground. 1G of acceleration is therefore equal to 9.81 m/s^2.

When considering a vehicle that negotiates a corner of a given radius, the vehicle needs to be moving forward as well as sideways. Lateral acceleration is therefore defined as “the change in lateral speed with time” [3].

Combining lateral and longitudinal acceleration vectors into a resultant acceleration facilitates the plotting of a “G-G” diagram for a particular vehicle negotiating various corners on a racing circuit, as illustrated in Figure 4 below. The combination of all plotted resultant accelerations, when outlined by a boundary line, shows the “G-G” boundary at which a particular vehicle can achieve maximum acceleration. The objective of the racing driver is therefore to spend as much time on this boundary as possible, as it represents the maximum acceleration, braking and cornering ability of the vehicle with a particular configuration. It follows that in order to improve the performance of the vehicle, the G-G diagram needs to be increased as much as possible, while providing vehicle control and stability characteristics that allow the driver to operate the vehicle at these limits.

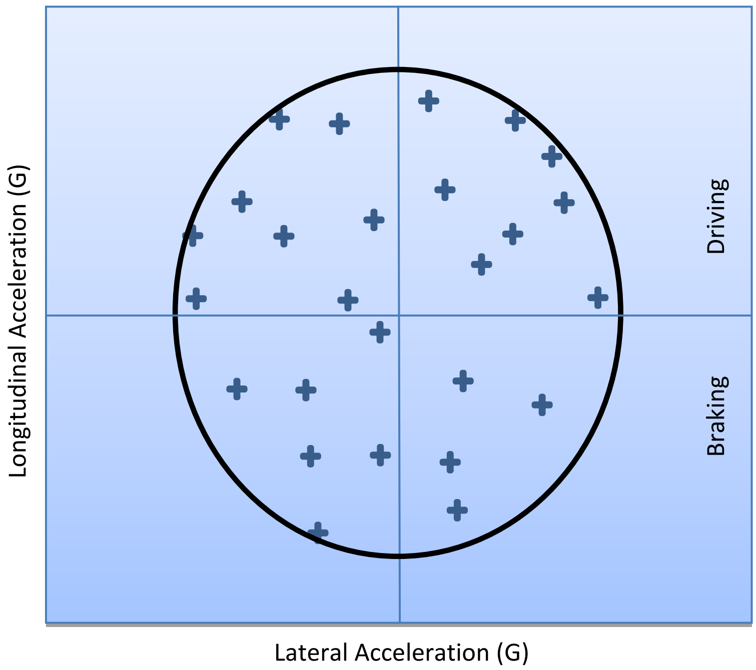

Figure 4: A Typical “G-G” Diagram

2.4.2 Understanding Suspension and Steering Geometry

a) Camber Angle

The camber angle (Figure 5) of a wheel is the angle of the wheel centre line to the vertical as viewed from the front or rear of the vehicle [5]. A wheel leaning outboard is considered to have positive camber, while a wheel leaning inboard is considered to have negative camber. A slight negative camber is desirable during cornering to compensate for tyre flex. Racing tyres are typically designed to operate with higher levels of camber than road tyres due to the higher lateral forces experienced.

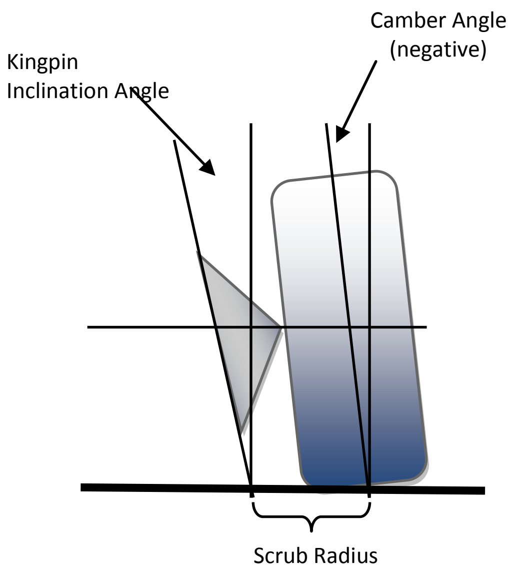

Figure 5: Camber Angle, Kingpin Inclination and Scrub Radius

b) Castor Angle

The castor angle (Figure 6) is the inclination angle of the steering axis of the front wheel to the vertical, when viewed from the side [5]. The line of action of steering axis must lie in front of the centre line of the tyre contact patch to produce a self-aligning castor effect, which improves vehicle stability at speed. Castor also helps counteract negative kingpin inclination (KPI) effects during steering. Note that leaning the car forward reduces the castor effect, as does hard braking. Castor also increases steering effort and creates negative camber on turn-in for the outside wheel. A combination of castor and slip angle variation while driving is what produces steering "feel" for the driver.

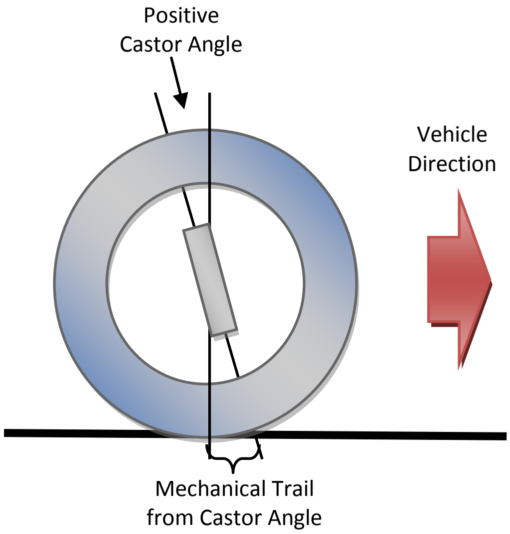

Figure 6: Castor and Mechanical Trail

c) Toe-In and Toe-Out

When viewed from above, front wheels facing inwards produce toe-in, while front wheels facing outwards produce toe-out (Figure 7) [5]. Toe is measured by comparing the horizontal distance between front and rear of the wheel rim. Toe-in improves vehicle dynamic stability as an upset force is corrected by the car automatically. Toe-out with suspension upward movement should be avoided due to the dynamic instability it causes.

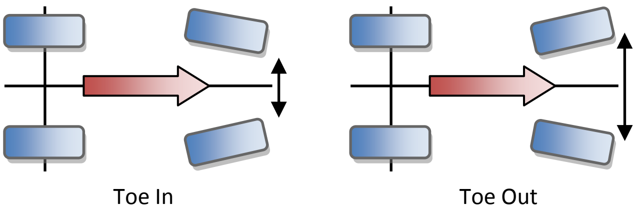

Figure 7: Toe-in and Toe-Out

d) Kingpin Inclination (KPI)

The angle of the steering axis to the vertical, when viewed from the front, is called kingpin inclination [6]. This angle is used to improve or reduce the scrub radius (kingpin offset) of the steered wheels which in turn reduces steering effort. Too much KPI causes undesirable wheel camber changes with steering movement. KPI also produces a self-aligning torque in the steering system, which tends to keep the steered wheels facing straight-ahead.

e) Scrub Radius

Scrub Radius, also called kingpin offset (KPO), is the distance between the steering axis where it cuts the ground, and the centre of the wheel patch [6]. Too large a scrub radius causes high steering effort, however some KPO is desirable to provide steering feel, or feedback to the driver. Centre point steering is when KPO = 0, resulting in no steering feel.

f) Ackerman Steering

For full Ackerman geometry, the rearward (or forward) facing arms of the steering links taper inward to meet at the rear axle (Figure 8). This allows the inboard and outboard wheels to turn through different angles during steering, but steer around the same turning circle centre [5]. The outer wheel does the majority of steering during a corner due to weight transfer.

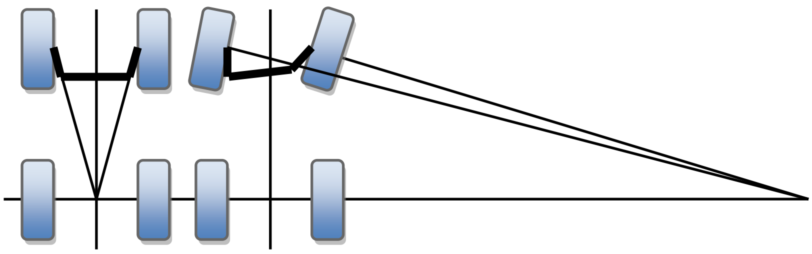

Figure 8: Ackerman Geometry

Racing cars typically do not run with full Ackerman geometry due to high tyre slip angles (Figure 9), requiring the wheels to remain parallel for the initial turning angle, during a high-speed corner, and then progress to mild Ackerman geometry with increased steering, usually required for lower speed corners.

Steering angles are only really important when entering a corner. Corner entry understeer can be reduced by adding mild static toe-out, however too much will lead to a dynamically unstable vehicle [6].

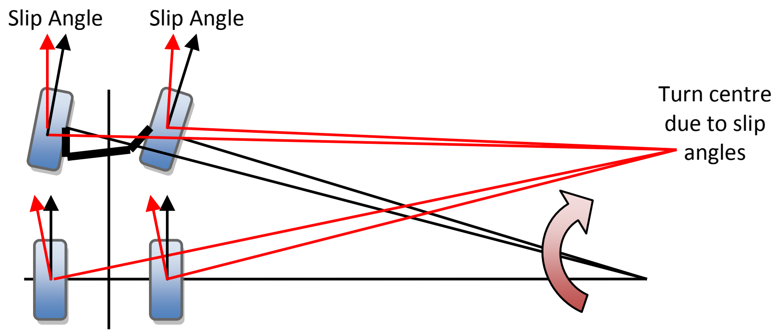

Figure 9: Ackerman Geometry Modified by Slip Angles

g) Instantaneous Centre

Due to the tyre slip angles, the vehicle travels around its Instantaneous centre in a corner, rather than the geometric centre given by the vehicle's Ackerman geometry. The instantaneous centre is determined by tracing lines perpendicular to the individual wheel slip angle velocity vectors (Figure 9) [4].

h) Wishbone Suspension Design

Longer suspension wishbones minimize camber and track changes with suspension movement and are therefore desirable. The lower wishbones are typically 1.2 to 1.5 times longer than upper wishbones to produce negative camber with suspension upward movement (bump), or positive camber with downward movement (droop) [7]. This counteracts the positive camber created during body roll in a corner and is usually achieved by locating the lower wishbone mounting inboard of the upper mounting (Figure 10).

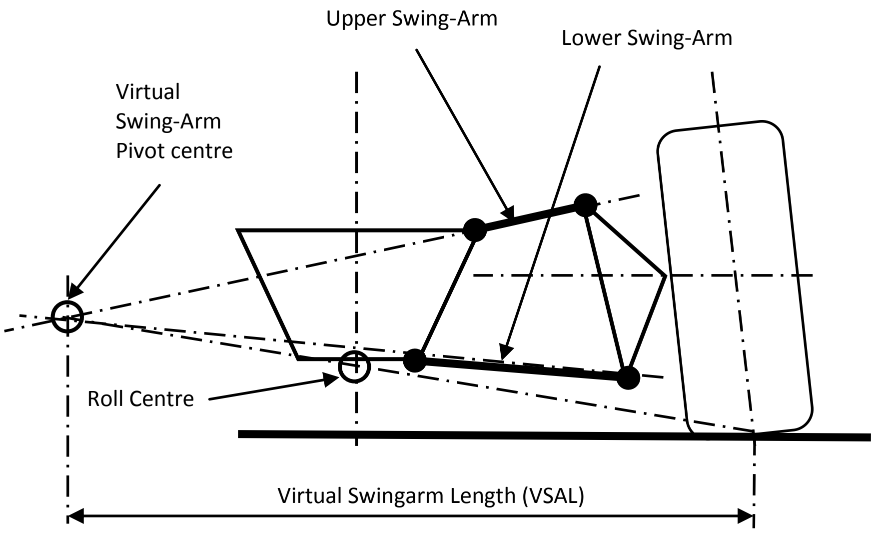

Figure 10: Virtual Swingarm Length and Roll Centre

To further assist in controlling wheel camber changes with body roll, inboard suspension mounting points are either designed with the lower wishbone inner higher than outer mounting point, or by locating the upper wishbone inner mounting point lower than its corresponding outer mount. Too much negative camber in wheel bump movement is also undesireable, as it is leads to ineffective traction under braking and acceleration (dive and squat).

Extending the centre lines along the upper and lower wishbones provides the location of the instantaneous centre of the virtual swing-arm (Figure 10) [4]. The virtual swing-arm length measured from the instantaneous centre to the wheel contact patch, gives rise to the variation in camber in bump and droop suspension motion. Using an infinitely long virtual swing-arm produces camber angle change equal to body roll, while with a virtual swing-arm length equal to half the track width, no camber change is experienced with body roll [4].

Inboard wishbone mountings should be as wide apart as possible to reduce loading on suspension pivots while the lower mounts should be wider than upper due to the higher loading experienced by the lower wishbones, particularly during braking in traditional push-rod or direct-actuation suspension designs [7].

i) Bump Steer

Bump steer is the undesirable effect of the wheel steering angle change during suspension movement. To eliminate bump steer the inner track rod pivot (steering arm) must lie on the same plane as the inner suspension mountings [6].

j) Anti-dive and Anti-squat

Anti-dive and anti-squat geometry is the resistance to changes in a car's pitch attitude under braking or acceleration, generated by forces in the wishbones [7].

Anti-dive geometry is achieved by tapering the inner wishbone mounting centrelines towards the rear for the front wishbones, and towards the front for the rear wishbones, as viewed from the side. The point of convergence of these lines determines the amount of anti-dive or anti-squat forces. Wishbone inner mounting centre lines can also taper in plan view to achieve the same effect.

k) Roll centre

The roll centre (Figure 11) is the single most dominant kinematic factor in suspension design [4]. Instant centres on the left and right side of the vehicle can be determined by extending the centre lines of the upper and lower wishbones to the point where they converge [6].

The roll centre is the theoretical point about which body roll occurs, and is determined by connecting a straignt line from the instant centre to the centre of the wheel patch. The point at which this line crosses the vehicle centreline is the roll centre.

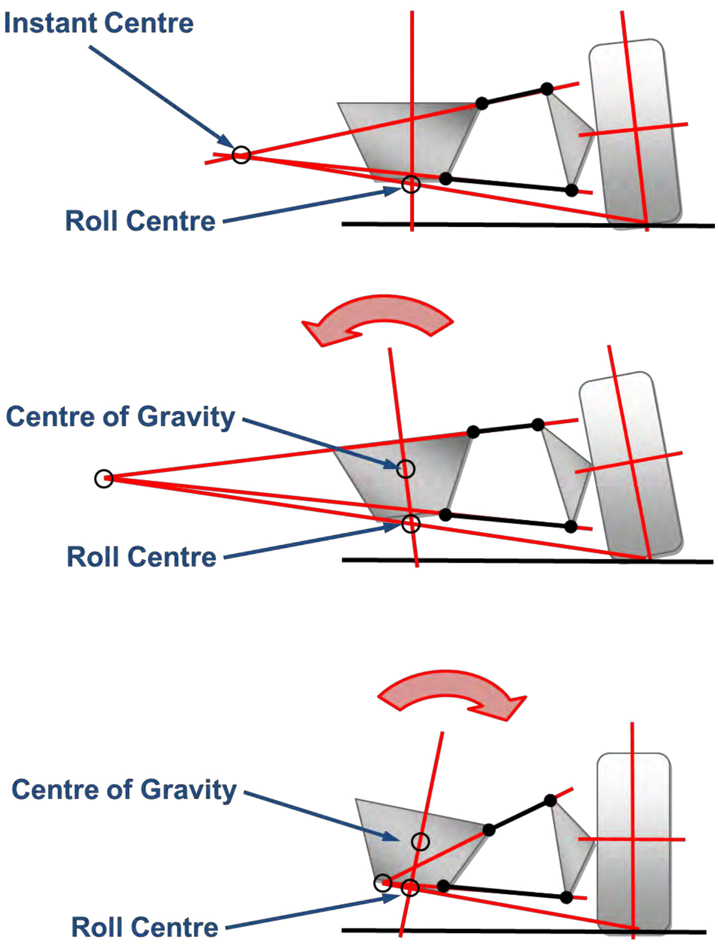

Figure 11: Roll Centre

To minimise body roll during cornering, the roll centre should be close to the vehicle centre of gravity (CG). To prevent jacking forces from lifting the vehicle during cornering however, the roll centre should be as close to the ground as possible, but not below ground level [6].

The roll centre will move around with suspension movement, but to avoid inconsistent handling, the roll centre should not drop below ground level. Roll centres are best optimised using kinematics software packages which simulate suspension parameters for the full range of suspension motion [4].

l) Suspension Springs

The wheel rate is defined as the spring rate divided by the suspension motion ratio. The motion ratio is determined by the suspension design and geometry and is the relationship between the movement at the wheel and the movement at the spring or damper [6].

Wheel rate = Spring rate / Motion ratio

High wheel rates (stiffness) have the effect of limiting body roll, but limit the suspension's ability to follow the undulations on the road (compliance), therefore negatively effecting wheel traction. Rising rate suspension design is when the wheel rate of the suspension increases with increasing suspension travel [6].

Required roll stiffness is usually higher than the optimum bump stiffness. The function of anti-roll bars are therefore to limit body roll by increasing suspension roll stiffness without affecting bump compliance. Anti-roll bars also have the effect of transferring weight from the outboard to the inboard wheel.

2.4.3 The Role of the Vehicle Tyre

As the vehicle tyre is the only means by which a vehicle reacts the forces required to generate acceleration, it follows that understanding tyre behavior is key to the achievement of the largest possible "G-G" diagram. Tyres also transmit the forces required to enhance vehicle stability and control [3].

a) Tyre Behavior

An analysis of the forces and moments, or torques transmitted by a vehicle tyre reveals the following categories [4]:

- Vertical force due to vehicle mass
- Vertical force due to aerodynamic forces
- Vertical force due to road banking
- Longitudinal force due to acceleration (tractive force)
- Longitudinal force due to braking
- Lateral force due to cornering
- Lateral force due to wind or other disturbances

Tyres produce forces of their own, which impact on the overall performance of the vehicle namely [4]:

- Rolling resistance
- Steering or self-aligning torque

The overall grip of a tyre is also based on the coefficient of friction between the tyre tread and the track surface. The coefficient of friction can be influenced by the tyre compound, the roughness of the track, ambient temperature and other factors, such as the amount of rubber left on the track by other vehicle tyres. The frictional force required to transmit the above tractive or cornering forces, is also proportional to the vertical load on the tyre. For a given tyre and track, it follows that the greater the vertical load on the tyre, the more grip a vehicle will have, providing the opportunity for greater acceleration in all directions [3].

The role of the suspension system is therefore to optimally balance the loading at the respective tyre contact patches, while controlling the variation in tyre camber with suspension movement to ensure that the tyre contact patch pressure distribution is optimised [4].

A closer look at the tyre contact patch pressure distribution is useful for interpreting the effects of such factors as camber and tyre pressure on the ability of a tyre to transmit the required forces. Tyres themselves form a significant part of the suspension system of a vehicle, in that they have their own stiffness and damping characteristics. Tyres also deform due to the various loads applied to them. These loads include the following [4]:

- Vertical deformation due to vertical load
- Asymmetrical vertical deformation due to camber changes
- Lateral deformation due to cornering load, with associated vertical deformation
- Longitudinal deformation due to acceleration and braking
- Torsional deformation due to steering and tyre slip angle

Tyre forces and moments are also a function of the tyre slip angle, which is the angular measurement of the difference between the expected direction of the tyre (steered direction) and the real tyre direction [8]. In order for a tyre to provide the required grip when cornering, deformation of the contact patch occurs, causing the tyre slip angle. As the slip angle increases, we have [4]:

- Lateral tyre deformation
- Torsion around the vertical axis
- Modification of the contact patch

In the same way as the tyre slip angle operates in a lateral direction, the tyre slip ratio operates in a longitudinal direction, under braking and acceleration. The slip ratio is the relationship between the tyre's tangential speed and the vehicle's longitudinal speed.

A tyre slip ratio is caused by the following three factors [4]:

- Wheel spin
- The movement of the contact patch in relation to the wheel rim
- The longitudinal deformation of the contact patch

A useful way to view a tyre's slip angle and slip ratio variation, with longitudinal and lateral force variation, is to plot a friction ellipse, which provides a graphic representation of the tyre's performance capabilities.

Tyre pressure management is crucial to effective tyre performance, as a particular tyre will provide the optimum contact patch pressure distribution on the track when the internal pressure is optimised. Tyre pressure is however influenced by the operating temperature of the tyre, which increases from its "cold" condition at ambient temperature, to its "warm" condition during extended operation. Various operating conditions such as acceleration, braking and cornering serve to increase the temperature of the tyre due to increased frictional heat generated between the track and the tyre, as well as internal stresses in the tyre itself. The relationship between the tyre pressure and internal temperature is governed to a large extent by the ideal gas equation PV=nRT. Assuming that the volume of gas in the tyre does not change significantly, the above equation can be shown as P1/T1 = P2/T2.

This equation can be modified to provide guidance on the ideal “cold” pressure for the tyre to provide the best “warm” pressure for particular ambient conditions [4].

b) The Continental Formula Student Tyre

The NMMU Racing team utilized the purpose built 2010 Continental 205/510 R 13 Formula Student tyre for “DibaOne”, and plans to use the 2011 model tyre in “DibaTwo”. This tyre was developed by Continental in Hannover Germany, specifically for the use of Formula Student teams, and is available in a racing slick (smooth), and wet-weather (grooved) versions. This tyre has been extensively tested by Continental and the Tyre Testing Consortium, and tyre performance data is available to Formula Student teams for analysis and simulation. All vehicle testing for this research study was conducted using the 2011 Continental Formula Student tyre, and key specifications are shown in Table 1 below. Additional tyre data can be found in Appendix A.

TIRE SIZE	**205/510 R 13**
Max. Circumference [mm]	1575
Diameter [mm]	501,3
Section Width [mm]	205.0 ± 0.2
Weight [kg]	4.6
Test rim size	7 J x 13
Test inflation pressure	0.8bar
Recommended “hot” inflation pressures:	
- static wheel load of approx. 65 kg	0.69bar
- static wheel load of approx. 85 kg	0,76 to 0,83 bar

Table 1: 2011 Continental Formula Student Tyre Specifications

Source: Information about Continental‘s Formula Student / Formula SAE tire. 2011 [9]

Figure 12 shows the radial pressure distribution graphs comparing the tyre’s contact patch at 0°, 1.5° and 3° camber, under 1400N of vertical load. Increasing camber shows not only that the tyre contact patch area reduces from $128cm^2$ to $120cm^2$, but the mean pressure increases from 129kpa to 132kpa, thereby decreasing the available grip, while increasing the stress on the tyre, and therefore the corresponding tyre temperature.

This camber variation versus tyre temperature distribution were analysed during testing. The graphs also indicate that to gain the most grip from the tyre, camber should be kept as close to 0° as possible.

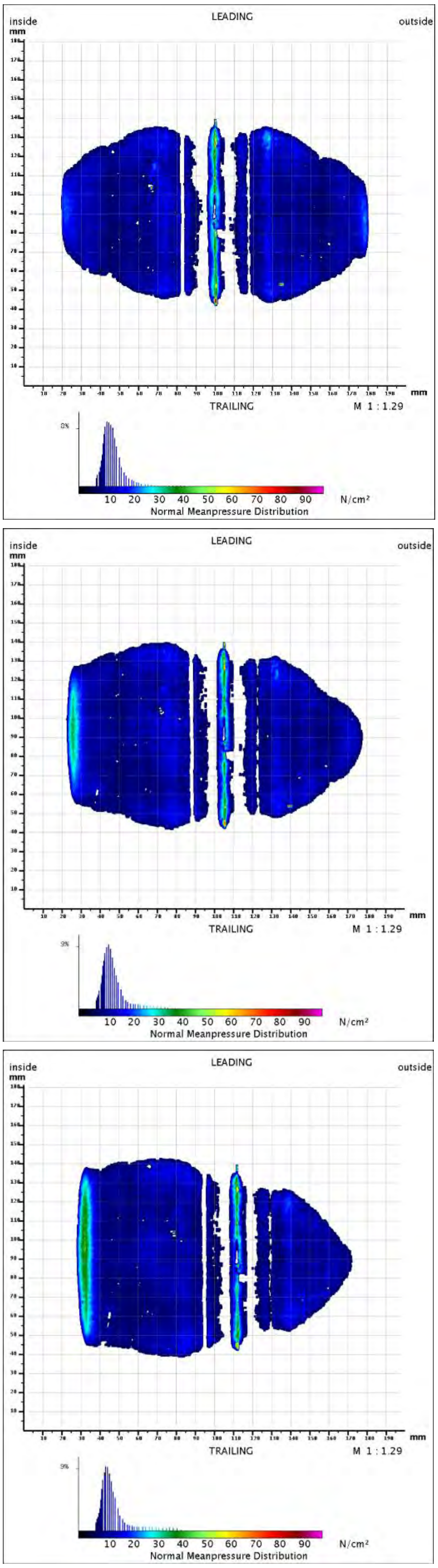

Fz = 1400 N; IA = 0,0°; p=0,8bar
Length: 97 mm
Width: 160 mm
Gross Area: 128 cm²
Mean Pressure: 129 kPa

Fz = 1400 N; IA = 1,5°; p=0,8bar
Length: 98 mm
Width: 155 mm
Gross Area: 123 cm²
Mean Pressure: 130 kPa

Fz = 1400 N; IA = 3,0°; p=0,8bar
Length: 104 mm
Width: 144 mm
Gross Area: 120 cm²
Mean Pressure: 132 kPa

Figure 12: Static Footprint Radial Pressure Distribution

Source: Information about Continental‘s Formula Student / Formula SAE tire. 2011 [9]

Figure 13 illustrates the increasing lateral grip of the tyre with increasing vertical load. The loads applied to the tyre are Fz3=1400N , Fz4=798N , Fz5=602N , Fz8=1106N . What is also notable is that the graphs level off as steering angle increases, so that with 1400N of vertical load for example, no more than 3000N of lateral grip is available, under any steering angle. Lateral grip is therefore constant from around 8° steering angle upwards.

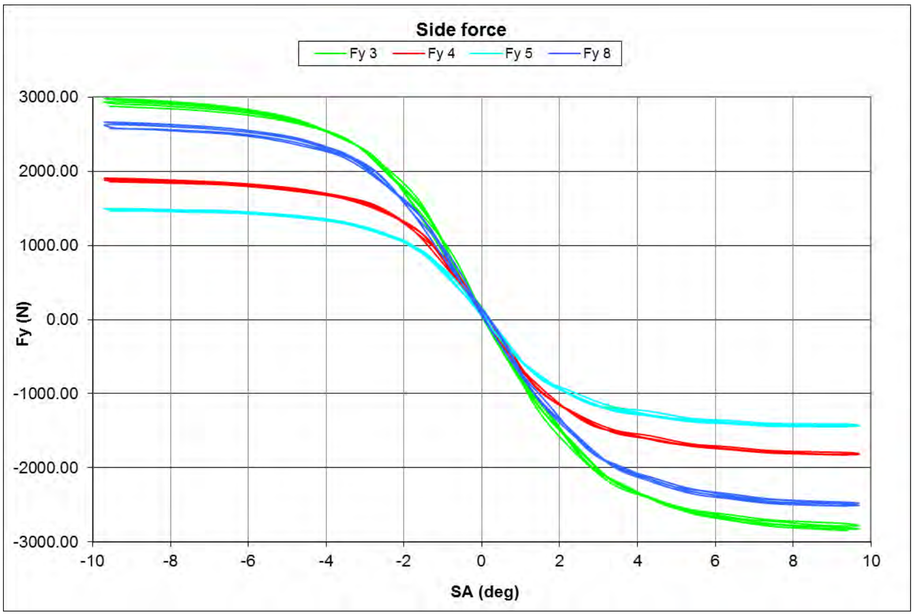

Figure 13: The Influence of Tyre Loads on Lateral Grip

Source: Information about Continental‘s Formula Student / Formula SAE tire. 2011 [9]

The influence of camber variation on the lateral grip of the tyre can be seen in Figure 14. Comparing at 0°, 1.5° and 3° camber with 1400N of vertical load, the highest lateral grip on average was at 1.5° camber as this was the best compromise between the two directions of lateral grip.

Suspension design should therefore focus on maintaining as close to 1.5° camber as possible under all conditions of suspension movement such as bump, rebound, roll and pitch, as well as when steering into a corner, with associated camber variation due to kingpin and castor angles.

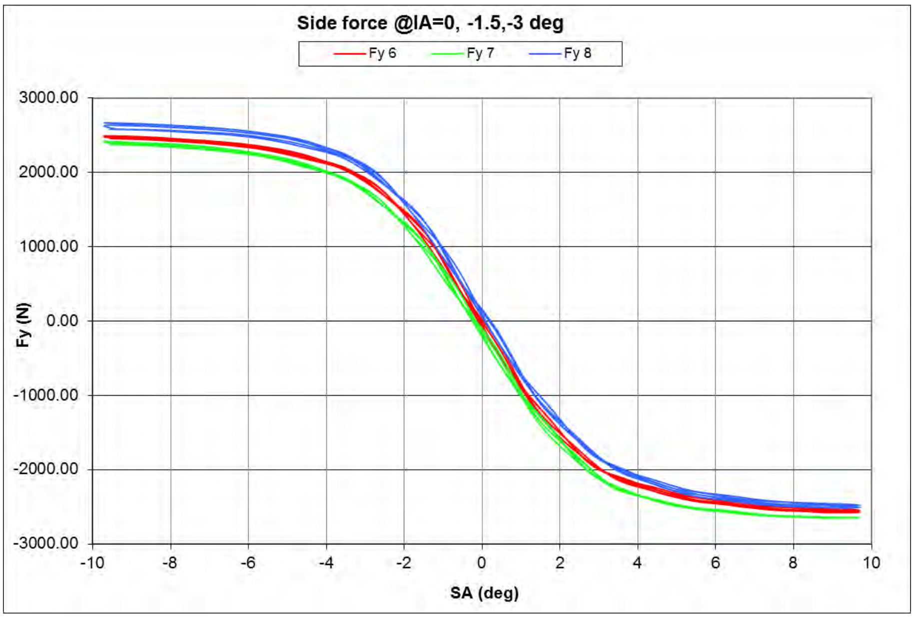

Figure 14: The Influence of Camber on Lateral Grip

Source: Information about Continental's Formula Student / Formula SAE tire. 2011 [9]

The available lateral grip in the tyre is also influenced by the temperature of the tyre, and Figure 15 below shows tests conducted at 33°, 36° and 40° average temperatures. The highest lateral grip at steering angles above 2° was achieved at 40° operating temperature. This parameter will be evaluated further during vehicle testing to confirm the optimum tyre operating temperature.

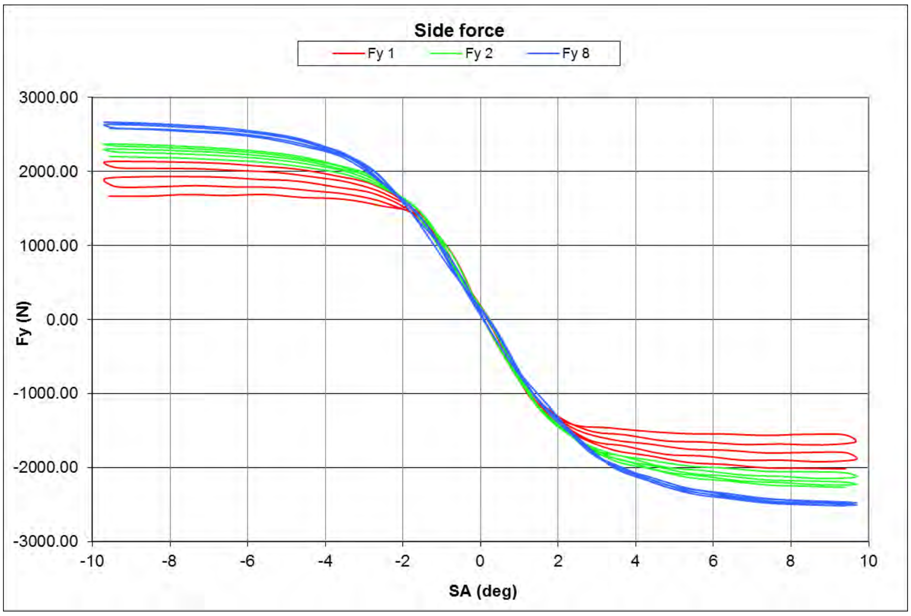

Figure 15: The Influence of Compound Warm-up on Lateral Grip

Source: Information about Continental's Formula Student / Formula SAE tire. 2011 [9]

The Normalized graph shown in Figure 16 below takes lateral forces into consideration in combination with the applied vertical load.

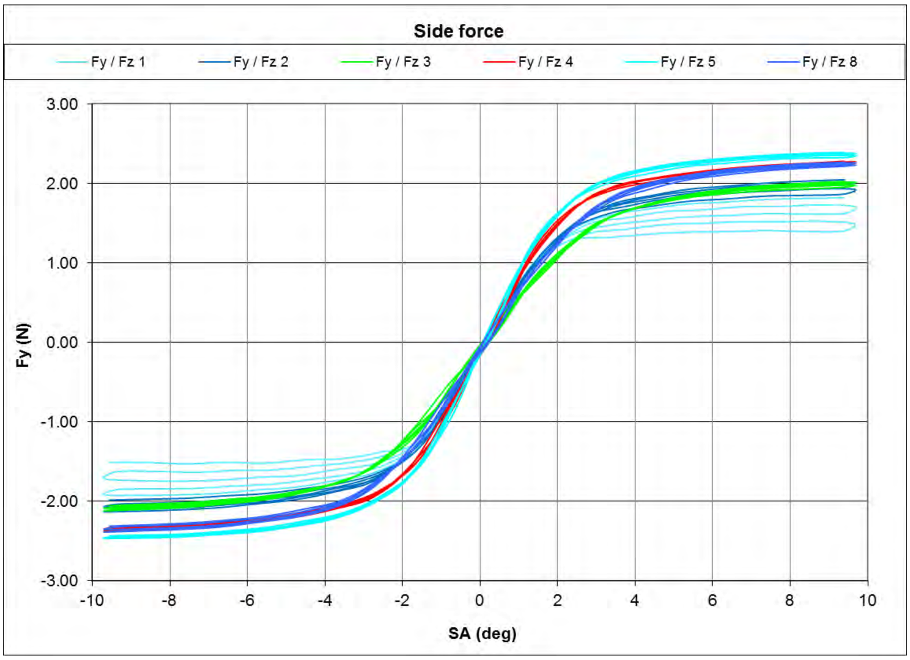

Figure 16: The Influence of Different Loads (Normalized)

Source: Information about Continental's Formula Student / Formula SAE tire. 2011 [9]

The highest normalized lateral force is experienced with a vertical force of 602N (Fy/Fz5) applied to the tyre. This graph is useful for estimating the optimum vehicle weight which should be approximately four times 602N, which is 2408N (245.5Kg). Figure 16 does not take into consideration the dynamic loading on the tyre, but shows the importance of controlling weight transfer during cornering and acceleration or braking events, through effective management of the vehicle centre of gravity, roll axes and anti-roll mechanisms.

The tyre aligning torque, shown on Figure 17 below, affects the steering sensitivity of the vehicle and should be considered in combination with the steering scrub radius, to optimise steering feel and driver feedback. High steering loads make a vehicle difficult and tiring to control, however too little steering feedback makes a vehicle unpredictable and difficult to control at the limit of adhesion.

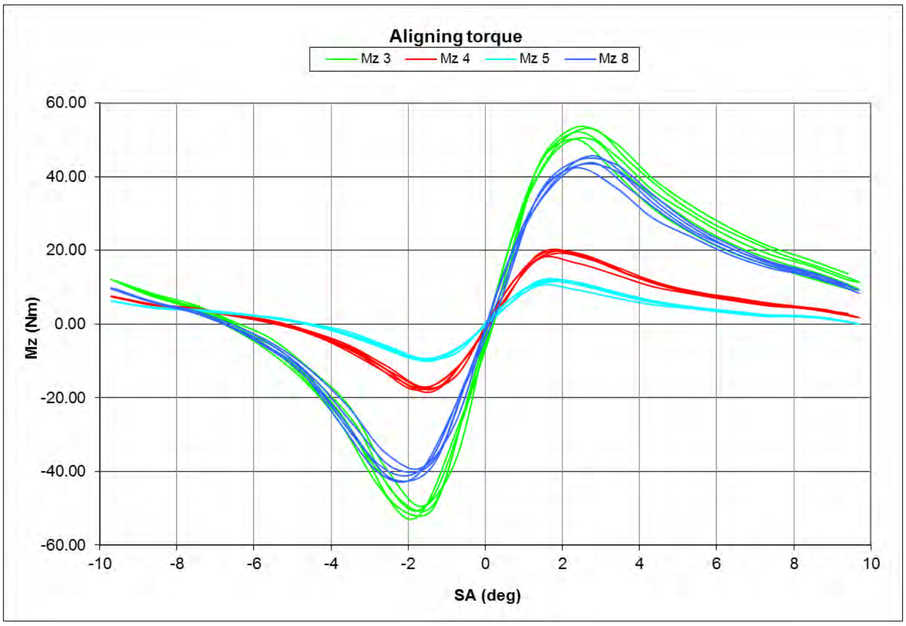

Figure 17: Tyre Aligning Torque

Source: Information about Continental's Formula Student / Formula SAE tire. 2011 [9]

2.4.4 Vehicle Simulation

a) Optimum K

A kinematic analysis of the suspension design for DibaOne was conducted using Optimum K software, and the key parameters are shown in Appendix C. Figure 18 shows the suspension kinematics for DibaOne simulated in Optimum K, along with the roll-centre, instantaneous centres and roll axes. Kinematic analysis is useful to optimise these parameters in order to minimise camber variation and stabilise roll axes and other factors.

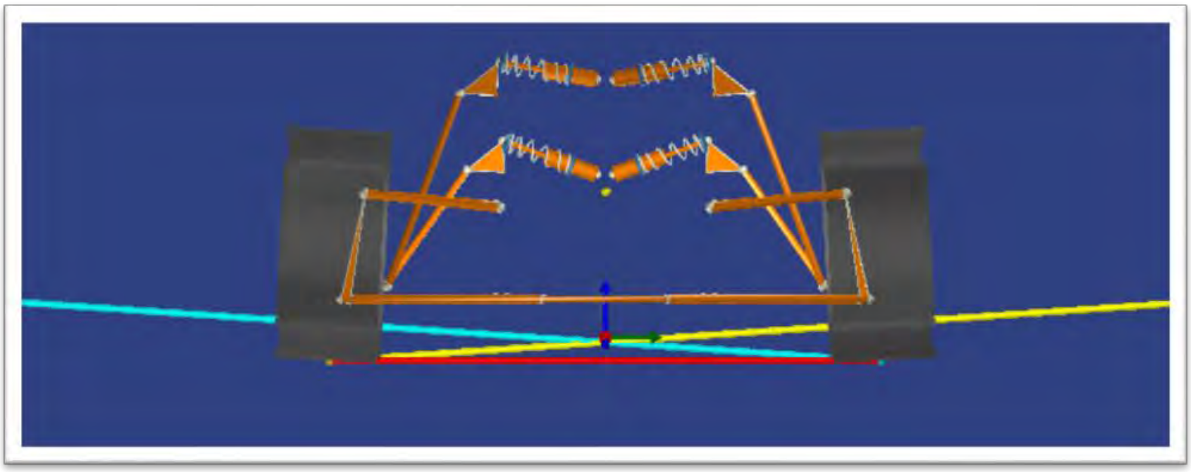

Figure 18: Optimum-K Kinematics Geometry for DibaOne

The process to be followed when conducting a kinematic simulation in Optimum K is as follows:

- Create a model of the suspension design by entering the respective co-ordinates of the key suspension components in the software.
- Apply various heave, pitch, roll and steering motions to the model, or a combination of the above to simulate the behaviour of the suspension.
- Analyse the movement of any point or axis on the model, such as the roll axis, pitch axis, camber, toe, damper movement etc. and create graphs to visualise its behaviour.

- Run multiple iterations of designs to optimise parameters before transferring suspension points into CAD software.

b) MSC Adams/Car software

Adams/Car, part of the MD Adams 2012 suite of software, is a specialized environment for modelling vehicles [10]. It allows you to create virtual prototypes of vehicle subsystems and analyze them much like you would analyze the physical prototypes.

Using Adams/Car, you can quickly create assemblies of suspensions and full vehicles, and then analyse them to understand their performance and behaviour. Adams/car differs from Optimum K in that forces and flexile bodies can be simulated.

Although an Adams/Car model was created, no analysis was conducted, as it was beyond the scope of this research study.

Appendix B shows the design priorities that were used to guide the engineering design and simulation process of DibaTwo, which enabled the focus on key areas of the vehicle design that were critical to its success.

2.4.5 Tyre Temperature Measurement for Suspension Optimisation

"The most critical performance factor for any race car is tyre management. Every other element on the car, from aerodynamics to suspension geometry, ends up being transmitted to the tarmac through the four small patches of rubber. Yet the race engineer's knowledge of how the tyres have performed has traditionally been limited to temperature readings taken manually when the car returns to the pits" [11]. With the onset of digital data acquisition and track side telemetry, it has become feasible to take real-time measurements of tyre temperatures, to provide information on how a tyre is performing at a specific point on the track.

With the goal being to optimise the use of each of the four tyres, as well as each part of a specific tyre's contact patch, measuring the tyre surface temperature can provide a useful indication on whether the tyre is loaded equally or not. This knowledge can be extremely useful in suspension set-up. Once set-up alterations have been made to equalise temperatures across the tread, it is reasonable to assume that the car is making best use of the tyres [11].

"What is extremely useful is the immediacy of the indication of the optimum camber and optimum tyre pressure," says Durand [11]. "How we were loading the tyres optimally in a stabilised way not only middle of the corner, but also on corner entry and exit. All this Information is extremely valuable" [11].

In an SAE Technical Paper entitled "Surface Temperature of Running Tires Using Infrared Scanning" Conant, Hall, and Walter [12] developed an infrared line scanning system to measure surface temperatures of automobile tyres under operating conditions. This experiment demonstrated statistically the individual and interactive effects on tyre temperature profiles, of changes in tyre speed, inflation pressure, and wheel load. These effects were shown to be different at different radial positions on a given tyre and were quite dependent on tyre construction.

Trivisonno [13] in his SAE Technical Paper entitled "Thermal Analysis of a Rolling Tire", measured tyre surface temperature distributions using infrared sensors. The results of this study gave the complete distribution of temperatures and rates of heat generation in the tyre, and were used to calculate power loss and shoulder temperature.

Although the research in [12] and [13] above demonstrated the usefulness of analysing tyre surface temperatures to evaluate tyre dynamic performance, all experiments were conducted on tyre testing machines, and not on a vehicle driving on a track. Their research also did not relate tyre performance to a vehicle application, where specific suspension settings would impact on tyre performance.

2.5 Delimitation of research

There are three general approaches to vehicle dynamics optimisation, namely:

- Driver feedback
- Simulation in the virtual environment
- Vehicle testing using data acquisition systems

The focus of this research was on developing a vehicle data acquisition system, along with an effective test methodology to provide objective feedback on vehicle dynamic performance. This research was limited to three variables in suspension tuning, namely:

- Tyre operating temperatures
- Wheel camber
- Tyre pressures

This information was analysed to provide a correlation between measurement data and suspension settings, which ultimately guided the vehicle tuning process. To further focus the study, the wheel camber and tyre pressure tests analysed data from the front tyres only, due to the significance of load transfer to the front wheels when cornering.

3. Research Methods

One of the strategies the researcher explored in this study is the measurement of the distribution of tyre temperature gradient across the width of a vehicle tyre while driving through various corners at various speeds. Vehicle cornering performance can be measured with a combination of vehicle speed, lateral acceleration and yaw speed/acceleration. In addition to track testing, skid pan testing allows for the evaluation of steady-state cornering performance of a vehicle, and provides useful results due to the exclusion of variables such as driving technique and varying track corner geometry. These strategies are in line with accepted techniques in vehicle dynamic testing [3].

The researcher will discuss the research methodology in three sections: 1) the establishment of a research platform, utilising the NMMU Racing Formula Student vehicle and various test facilities, 2) designing and installing a data acquisition system, and 3) developing a research and testing strategy, which makes most efficient use of the data captured.

3.1 Research Platform

3.1.1 NMMU Racing Formula Student Vehicle

The NMMU Racing Formula Student vehicle shown in Figure 19, is a single-seater racing vehicle designed according to international Formula Student specifications. It is powered by a 600cc Honda engine, mounted behind the driver for a front/rear weight distribution of 45/55%. The suspension design employed is a double-wishbone or short-long arm SLA suspension configuration providing accurate control of the wheel movements under all driving conditions. Due to its independent nature it also allows tuning of the individual wheel movement and steering geometry.

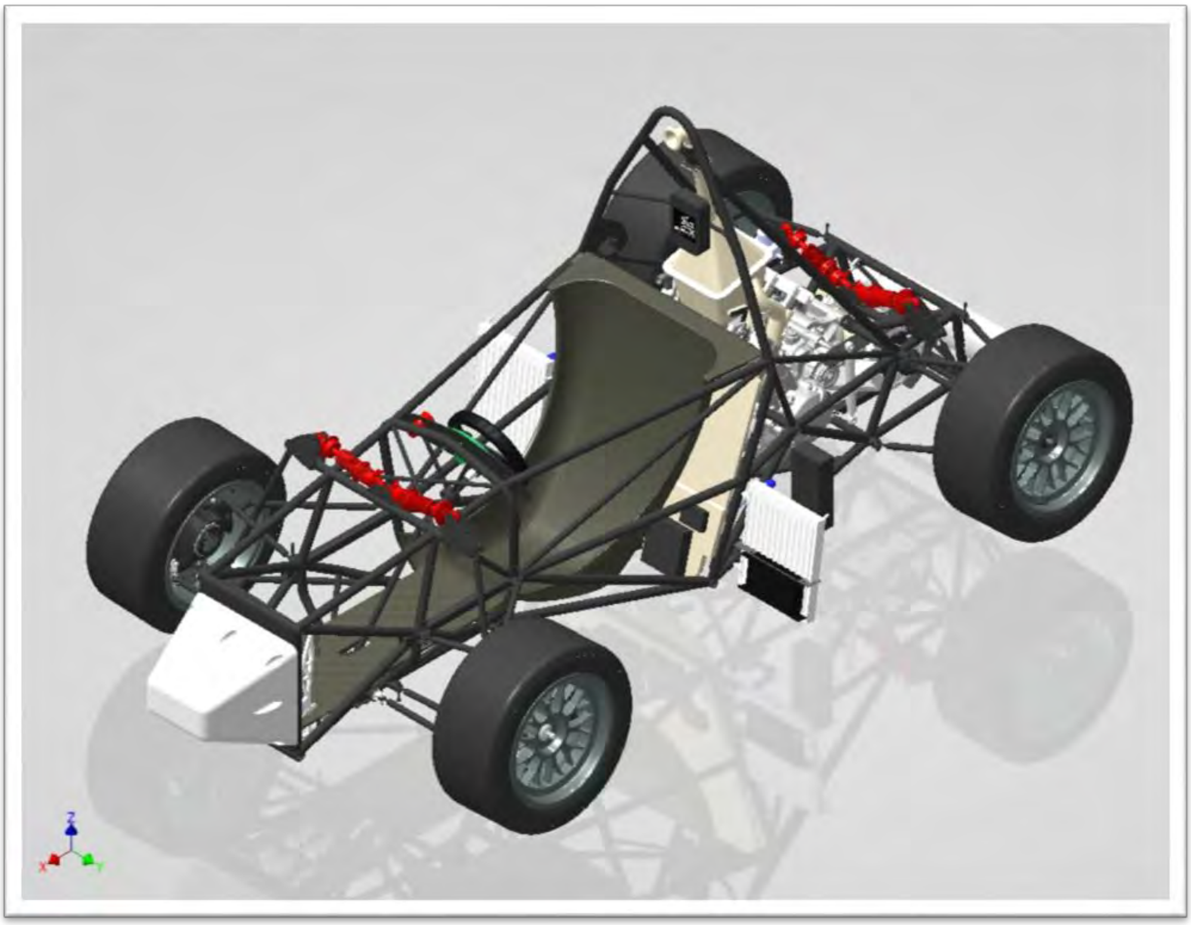

Figure 19: NMMU Racing DibaOne Frame and Suspension

Table 2 shows the key specifications of NMMU Racing's DibaOne, as used for all vehicle testing on this research project.

Specification	DibaOne
Wheelbase	1700mm
Track width – front	1220mm
Track width – rear	1200mm
Overall height	1360mm
Overall mass (without driver)	283kg
0 – 100km/h	6sec

Table 2: DibaOne Technical Specifications

3.1.2 Test Facilities Utilised

The researcher utilised two test facilities for vehicle testing, each selected for their suitability for the required tests, availability, provision of a safe environment to operate the vehicle and repeatability of track conditions. These two facilities were the Celso Scribante Short Circuit in Schoenmakerskop Road Port Elizabeth, and the Volkswagen South Africa (VWSA) Skidpad in Uitenhage.

a) Celso Scribante Short Circuit

The Celso Scribante Short Circuit is the home of the Algoa Kart and Motorcycle Club, and is regularly used for local and national kart racing. The circuit is well-maintained and is available most week-days, as racing is typically held on weekends. The circuit was designed for kart racing, and as such has approximately 1km track distance, with many "optional" corners allowing the circuit to be altered for different events. The track also has extensive run-off areas and tyre barriers to minimise the possibility of injury in the event that a vehicle unexpectedly left the track. Figure 20 shows data being downloaded after a test run on the Celso Scribante Short Circuit.

Figure 20: Downloading Data at Celso Scribante Short Circuit

The testing conducted for this research utilised all available corners, resulting in a track length of 1024m. This approach was selected due to its close approximation of a typical Formula Student event, which has very tight corners and minimal straight sections. This fact makes traditional vehicle racing circuits, such as the Aldo Scribante Raceway unsuitable due to its long straights and large radius corners. The track configuration used had twelve right-hand and six left-hand corners when driven in a clockwise direction (Figure 21 and 22). Having double the amount of right-hand corners would tend to skew any tyre temperature tests, and all testing was therefore balanced by driving an equal number of clockwise and anti-clockwise laps. An average was then taken between the two directions, for further analysis and interpretation. The two most consistent drivers were also selected for driving duties to attempt to limit test data variances with differing driving styles.

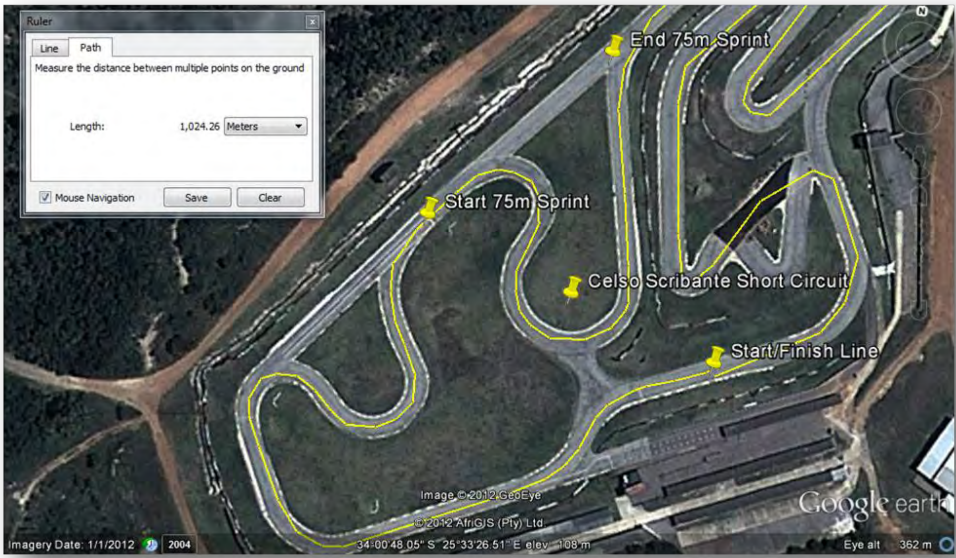

Figure 21: Google Earth View of Celso Scribante Short Circuit

The Motec data acquisition system, along with i2 software, facilitated the use of GPS data to visualise the track, and plot vehicle position, along with the ability to overlay vehicle variables such as speed and acceleration on the track map (Figure 23 and 24). Beacons were also programmed to log the start/finish line for further analysis by lap.

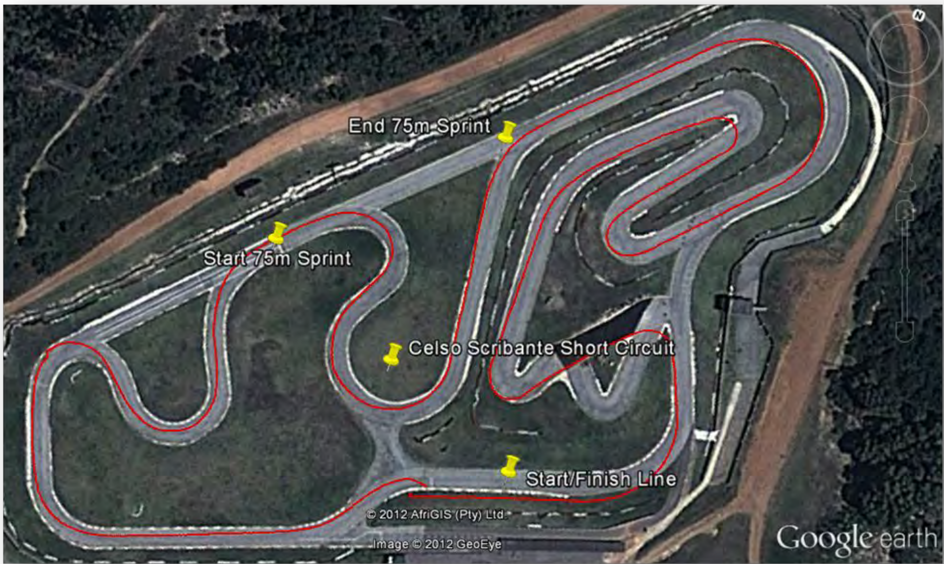

Figure 22: GPS Track Data Overlaid on Google Earth Image

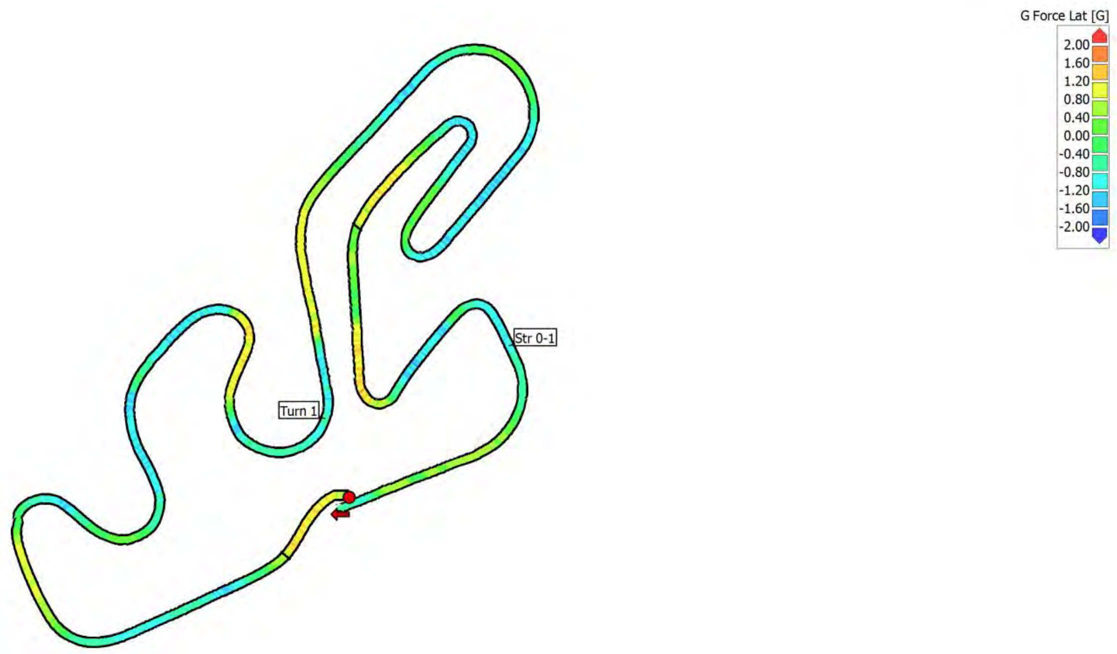

Figure 23: Vehicle Lateral Acceleration Plotted on GPS Track Map

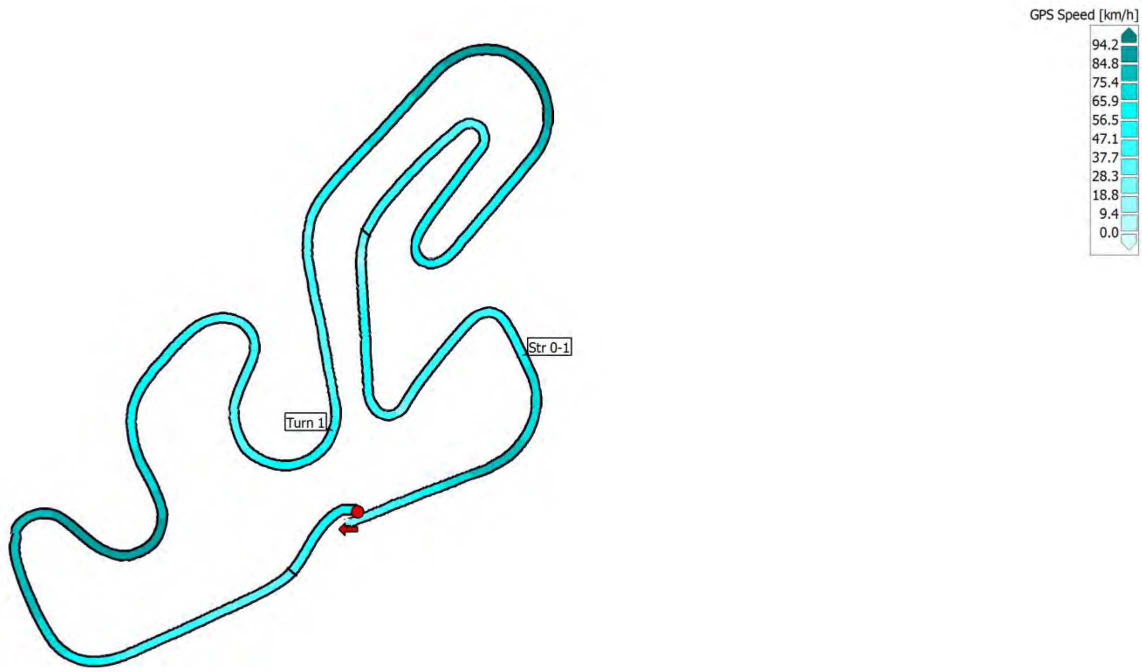

Figure 24: Vehicle Speed Plotted on GPS Track Map

b) VWSA Skid Pan

The VWSA Skid Pad is part of the greater VWSA track testing facilities, which also include a high-speed track, various rattle and suspension test surfaces and workshop facilities. The track is located near VWSA plant in Uitenhage, and is approximately 60m in diameter, as shown in Figure 25.

Figure 25: VWSA Skid Pad

Two diameters were selected for testing, namely 30m and 50m, as shown in Figure 26, and tests were conducted in a clockwise and anti-clockwise direction to average-out any vehicle symmetry variances that could result in uneven suspension performance.

The skidpan surface was ageing, however, and during testing the researcher encountered problems with the surface, including loose gravel and bumps. Although the gravel was largely eliminated during testing, the bumps upset vehicle stability when approaching the tyre adhesion limit. This caused the vehicle to over or under steer prematurely, when de-stabilised by a bump, and therefore limited the maximum recorded lateral acceleration during the test. Higher lateral accelerations were measured on the Celso Scribante Short Circuit than the VWSA Skidpan.

Figure 26: "Google Earth" Image of VWSA's Skidpan

3.1.3 Vehicle Preparation and Setup

The reliability of each test was underpinned by ensuring that the vehicle was accurately measured and adjusted before commencing testing. A detailed log was maintained by the researcher, to record all pertinent set-up data. The "NMMU Racing Setup and Testing Record" datasheets are shown in Appendix F (Vehicle Setup Datasheet for Wheel Camber Test) and Appendix H (Vehicle Setup Datasheet for Tyre Pressure Test).

Vehicle setup is the subject of much discussion in vehicle dynamic literature, due to the fundamental influence it has on vehicle performance. Vehicle parameters recorded during vehicle setup include:

- Front and rear camber angles
- Front and rear ride heights
- Front castor angles
- Spring stiffness
- Front and rear toe measurement
- Front and rear corner weights
- Front and rear damper bump and rebound settings
- Tyre pressures
- Anti-roll bar setup
- Vehicle overall weight with and without driver
- Front and rear sprockets (final drive ratio)

In addition to the above vehicle data, other information such as date, test location, weather conditions, drivers, test description and additional comments were recorded. The goal of recording this detail was to ensure that each test conducted could have a traceable record of conditions and settings, to assist in subsequent data analysis.

It must also be noted that the vehicle setup was conducted with a driver in the vehicle, as the addition of the driver significantly affected not only vehicle weight, but suspension deflection, ride heights and camber angles.

a) Vehicle Ride Height

The first step in vehicle setup is to ensure that the vehicle ride height is adjusted correctly. The ride height must be accurately measured and adjusted to ensure that the suspension has the required range of movement from bump (fully compressed) to rebound (fully extended), and that the vehicle is not lower on one side. Ride height is a function of the vehicle weight balanced by the suspension spring force, through the suspension motion ratio. A stiffer spring will tend to raise ride-height, while a softer spring would lower ride height.

Setting ride height is therefore not simply a matter of adjusting the push-rods longer or shorter, but first finding the balance point of the suspension and adjusting the damper travel to be at its mid-point at this balance point. This is achieved through the correct spring selection, and spring-seat preload adjustment. Ride height can then be set without changing damper travel, by adjusting individual push-rod lengths.

Ride height can also be used to compensate for track conditions, as a bumpy track would require a higher setting, for example, to avoid unnecessary contact between the underbody and the road surface. Excessive ride height raises the centre of gravity of the vehicle causing added body roll when cornering. It could even result in an unstable over-turning moment, which encourages the vehicle to lift the inside wheels in a corner. This tendency was experienced on DibaOne when conducting initial testing subsequent to the 2011 Formula Student event in Germany, and as a result, ride heights were significantly reduced in line with original design intent.

b) Wheel Alignment

The second step in vehicle setup is to ensure that the wheels are properly aligned, set to the correct angles, and longitudinally symmetrical. Basic camber and castor measurements were taken using a hand-held digital camber gauge shown in Figure 27, however to ensure wheel alignment symmetry, a full-vehicle electronic wheel-alignment machine was required.

Tiger Wheel and Tyre provided the use of their wheel alignment equipment, and with the assistance of the wheel-alignment technician, DibaOne was measured and adjusted to ensure symmetrical camber, toe, castor and track alignment.

Figure 27: Digital Camber/Castor Gauge with AccuLevel and Quick Set Adapter

Source: www.longacreracing.com [14]

c) Vehicle Load Distribution

In order to fully utilise the available grip from all four tyres, the weight distribution needs to be adjusted to be as even as possible. Fore/aft weight distribution is largely determined by the location of major components such as the engine, gearbox and driver, and as such is built into the design. Lateral weight distribution, however should be as symmetrical as possible to ensure predictable cornering performance on both left and right turns. An equal lateral weight distribution also ensures safe vehicle handling under braking conditions so as to avoid causing the vehicle to spin around unexpectedly when braking hard.

To set the vehicle load distribution, it was placed on four scales (Figure 28) which measured the load applied on each wheel. The suspension push-rods were then adjusted to increase or decrease the load on a tyre until the lateral loading was within two to three kilograms. The vehicle load was usually distributed diagonally so that the font left and rear right tyres were either both higher, or lower than their counterparts. If it was found that one side of the vehicle was heavier, as opposed to a diagonal split, either the vehicle contained some asymmetrically placed mass, or the vehicle was located on an inclined surface when measuring the loads. The vehicle steering should always be centralised when measuring wheel loads, as steering castor causes a static load distribution change when the steering is turned.

Figure 28: Longacre Accuset Vehicle Scales

Source: www.longacreracing.com [14]

d) Trackside Setup

Other important setup parameters were tyre pressures, damper settings, anti-roll bars and toe settings, which were usually adjusted at the track, according to test feedback. Typically, the front wheels were set with a mild toe-out configuration to assist with “turn-in” or corner entry grip, while the rear wheels were set with toe-in to ensure dynamic stability of the rear of the car.

3.2 Data Acquisition System

Figure 29 shows the installation of the test sensors on the NMMU Racing Formula Student vehicle DibaOne, most notably the three infrared tyre temperature sensors over each tyre.

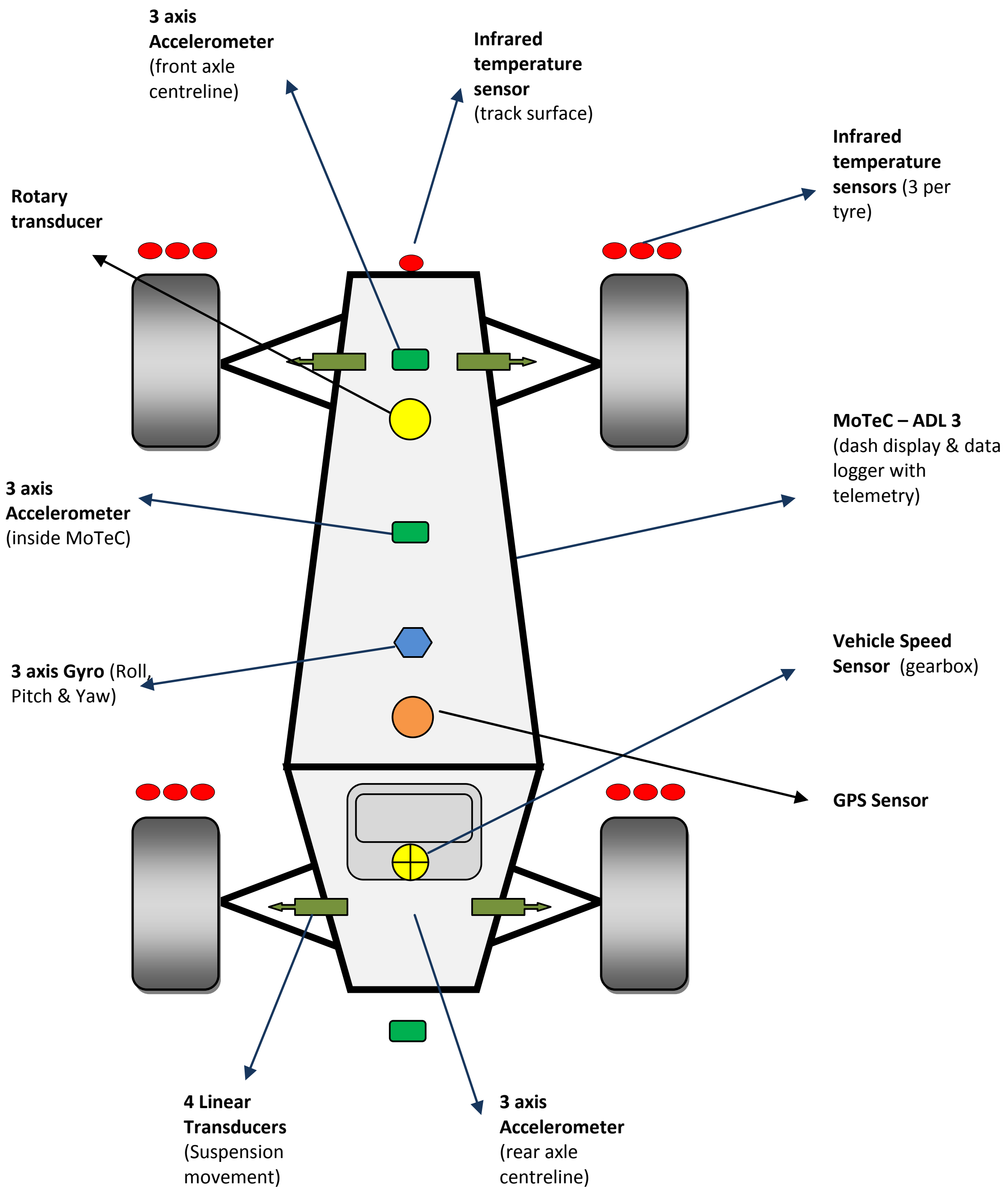

Figure 29: Data Acquisition System

3.2.1 Data Capture

The heart of the data acquisition system was the MoTeC Advanced Dash Logger (ADL3), shown in Figure 30, which combined a comprehensive configurable dashboard display with programmable data logging and control capabilities. It is a flexible, professional system that is designed to be scalable to meet the future needs of the project. The ADL3 comes with 16MB of data logging memory, which can be upgraded to 250MB if needed [15].

Figure 30: MoTeC Advanced Dash Logger (ADL3)

Source: MoTeC ADL3/EDL3 User Manual. V 1.1 May 2009 [15]

The ADL3's screen layout is fully configurable to display a multitude of data channels, warning alarms, lap times, fuel calculations, minimum corner speeds and maximum speeds. Four auxiliary outputs can be used to control external devices.

MoTeC's i2 data analysis software provides all the tools for comprehensive analysis of logged data, and an optional telemetry system was purchased for real time viewing of data while the vehicle is on the track.

a) Input Types

A range of sensors to suit different types of measurement such as temperatures, pressures, speed can be connected to the MoTec ADL3 Data Logger. Each type of measurement generates a different electrical signal that requires a suitable input type. Each sensor therefore needs to be connected to the type of input on the MoTec ADL3 designed to suit that type of sensor [15].

MoTeC devices have the following input types available:

- Analogue Voltage Inputs
- Analogue Temperature Inputs
- Switch Inputs
- Digital Inputs
- Wheel Speed Inputs

In addition to sensors connected to the inputs, the ADL3 has internal sensors available for battery voltage, 3-axis G force and device temperature [15].

Analogue Voltage inputs are normally used to measure the signals from analogue voltage type sensors, which are sensors with variable voltage outputs. Typical examples include:

- Rotary or linear potentiometers
- Signal conditioned 3-wire pressure sensors
- Thermocouple amplifiers
- Accelerometers

These inputs can also be used to measure two wire variable resistance sensors if an external pull-up resistor is connected from the input to the 5V sensor supply. Additionally, on/off switch signals may be connected, which may also require an external pull-up resistor [15].

Analogue Temperature inputs are identical to Analogue Voltage inputs, except that they contain a 1000 ohm resistor which is connected internally from the input pin to the 5 V sensor supply. This allows the Analogue Temperature inputs to be used with two wire variable resistance sensors such as:

- Two wire thermistor temperature sensors
- Two wire variable resistance pressure sensors

Additionally, on/off switch signals may be connected [15].

Switch inputs are generally used for the external switches required to operate the display. These inputs have a 4700 ohm resistor connected internally from the input pin to the 5 V sensor supply so that a switch can be simply connected between the input pin and 0 V. They can also be connected to a brake switch or other types of switch [15].

Digital Inputs are identical to Switch Inputs except that they include the following additional measurement methods:

- Frequency: The frequency of the input signal is measured
- Period: The time between successive pulses is measured
- Pulse width: The low time of the pulse is measured
- Count: Counts the number of pulses
- Beacon: For connection of a lap beacon [15]

Speed Inputs are identical to Digital Inputs except that they can also be configured to suit Variable Reluctance (Magnetic) sensors e.g. some wheel speed sensors. Because the amplitude of the signal from these sensors varies with speed of rotation, variable trigger levels are required, which must vary with the frequency of the input signal. The Speed Inputs can also be used with Hall Effect type wheel speed sensors.

The Pulse Width measurement method measures the high time of the pulse rather than the low time as measured by the Digital Inputs [15].

b) Input Specifications

- 10 x Analogue voltage inputs (24 optional), some are high resolution inputs
- 4 x Analogue temperature inputs (8 optional)
- 4 x Digital inputs
- 4 x Speed inputs with voltage measuring capability
- 4 x Switched inputs
- Compatible with VIM input expanders

c) Output Specifications

- 4 x PWM, digital or switched outputs (8 optional)
- Compatible with up to 2 E888/E816 input/output expanders

d) Internal Sensors

- 3 axis G sensor
- Dash temperature sensor
- Sensor supply voltage
- Battery voltage

e) Calculations

The ADL3 has special and user definable general purpose calculations available. These calculated channels allow the recording of data on a separate channel, derived from one or more data input channels. The types of calculations available are listed below.

- **Lap Time and Number**
- **Speed and Distance**
- **Lap Gain / Loss**
- **Gear Detection**
- **Fuel Prediction**
- **Running Min / Max**
- **Tables**
- **Timers**
- **User Conditions**
- **Channel Maths**
- **Advanced Maths**
- **Bit Combine**
- **PID Control** [15]

f) Display

The ADL3 display is a high contrast, high temperature, custom made LCD display. The display contains a Bar Graph, three Numeric Displays, a Centre Numeric Display and a Bottom Alpha/Numeric Display.

3.2.2 Tyre temperature measurement

Three infra-red temperature sensors per tyre were mounted on purpose-built brackets designed to ensure that the sensors consistently focus on a specific area of the tyre while driving. An additional infra-red sensor measured the track surface temperature. As shown in Figures 31 and 32, three sensors per wheel were mounted inline, so as to record the inner, centre and outer circumferential tyre temperature during vehicle motion.

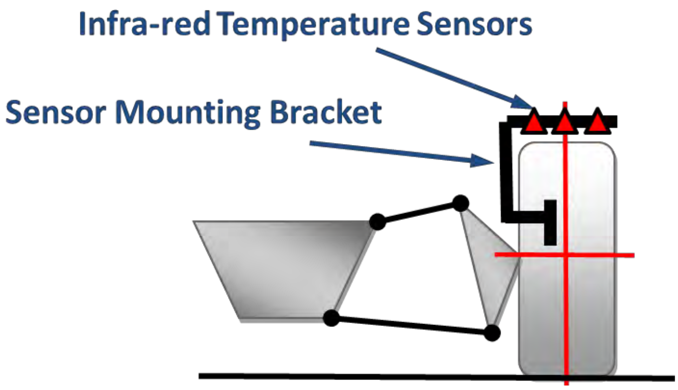

Figure 31: Schematic View of Tyre Temperature Sensor Mounting

Figure 32: Tyre Temperature Sensor Installation

To accommodate the steering movement of the front wheels, special brackets were designed which attach to the suspension uprights, thereby allowing the bracket and sensors to move with the steering movements of the front wheel. This meant that the temperature band being monitored by each sensor would remain constant relative to the tyre, making analysis of tyre temperatures easier.

The optimal distance to measure the tyre surface temperature was 50mm, and the sensor brackets were designed to maintain this position. In addition, the extruded aluminium angle-iron was orientated with the vertical flange protecting the sensors from debris thrown by the tyres during driving. The design of these brackets also took into consideration the fact that they should be transferrable to the next generation Formula Student vehicle.

A single sensor was also mounted to the underside of the vehicle to monitor track temperatures, which assisted in correlating tests over multiple days, or at different times of the day.

3.2.3 Vehicle Acceleration

Vehicle acceleration was measured in three places, with three-axis accelerometers. The MoTeC ADL3 also has a built-in three axis accelerometer, which was centrally mounted in the vehicle (but not at the vehicle centre of gravity), while the second and third sensor were mounted centrally on the front and rear axle centreline. The purpose of these accelerometers was to record vehicle linear acceleration and deceleration, along with pitch, roll and yaw accelerations.

3.2.4 Vehicle Motion

A three axis gyroscope was mounted as close to the vehicle centre of gravity as possible to precisely measure vehicle pitch, roll and yaw movements under various conditions.

3.2.5 Vehicle Location

A global positioning sensor (GPS) was mounted in the vehicle to facilitate the correlation of sensor data with the location of the vehicle on the track.

3.2.6 Suspension Motion

Four linear transducers were located on the suspension dampers to measure suspension movement. Vehicle pitch and roll angles can be determined by converting the linear transducer data using the suspension motion ratio into wheel movement. Individual wheel loads can also be calculated using the spring stiffness and the suspension motion ratio.

3.2.7 Steering Angle

A rotary steering angle sensor was used to measure the driver input into the steering system, thereby providing some correlation between steering angle and vehicle direction. This provided an indication of the vehicle's overall slip angle through a corner.

3.2.8 *Vehicle Speed*

A speed sensor was located in the gearbox, which was calibrated to provide the vehicle instantaneous speed signal. Due to the fact that this sensor was connected only to the rear wheels, interpreting the data during maximum acceleration and braking had to take into account wheel slip.

3.2.9 *Data Acquisition System Technical Specifications*

Table 3 summarises the equipment and sensors used for vehicle dynamic analysis on the NMMU Racing Formula Student vehicle, as well as details of their installation.

	Description	**Part No.**	**Installation**
1	MoTeC ADL3	ADL3	Dash mounted
2	Infrared temp. sensor	NFKL-150	3 per wheel mounted on dedicated aluminium brackets
3	Accelerometer	AC-CAP3	One mounted on each axle centreline
4	Digital gyroscope	GYRN3	One mounted under driver's seat close to vehicle centre of gravity
5	Linear transducer	VLPM Series	One mounted on each of the 4 suspension dampers
6	Rotary transducer	TBD	One mounted to steering rack to measure steering angle
7	GPS sensor	TBD	One sensor located behind the dashboard data logger
8	Connectors & Cables		

Table 3: Data Acquisition System Specifications

3.3 Research Strategy and Experimental Plan

Due to the many factors influencing vehicle dynamic testing, as well as the vast array of variables to be measured, a logical approach was required, which broke down the process into manageable steps. This strategy was also required to allow the researcher to focus on specific aspects for detailed analysis. A three-pronged strategy was used, dividing the vehicle dynamic testing firstly, into an analysis of the tyre operating temperature, secondly an analysis of tyre camber and thirdly, an analysis of tyre pressures. In addition, consequential information was documented such as the creation of the vehicle's G-G diagram, using GPS data for track-based analysis, considering the tyre dynamic load distribution across all four tyres, analysing tyre load distribution versus steering angle, and plotting the vehicle's oversteer gradient, which compared the steering angle to the available lateral acceleration force. Figure 33 illustrates the three research strategies employed to analyse vehicle dynamic data from the research platform.

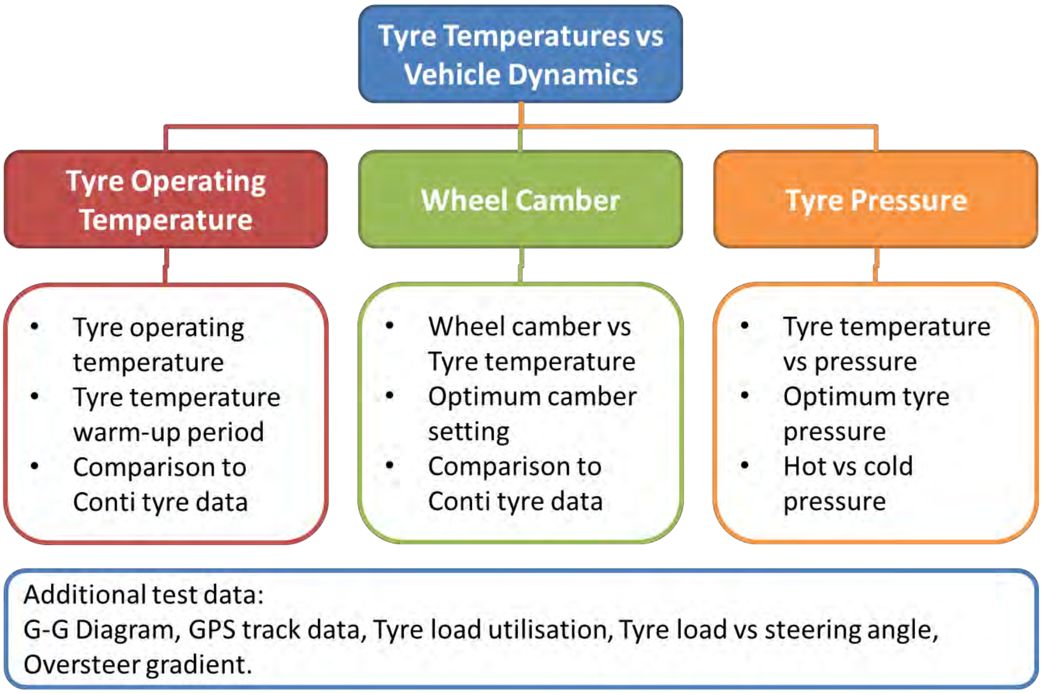

Figure 33: Vehicle Test Strategy

3.3.1 Tyre Operating Temperature

According to Continental Tyre's "Information about Continental's Formula Student / Formula SAE tire" document [9], the 2011 Continental Formula Student tyre tread was formulated to operate at a lower working temperature, resulting in higher levels of grip with cold tyre temperatures and faster tyre warm-up, especially in lower ambient temperatures. There is a risk of overheating the tread on hot days during prolonged use, such as during the Formula Student endurance event, however the new carcass construction was designed to counteract this tendancy. This tyre data also indicated optimum levels of grip at 40°C, and the goal of this test was to establish the tyre operating temperature experimentally. In addition, the time taken to "warm-up" the tyre from ambient temperature to operating temperature was also required.

Utilising the average of the three (inner, middle, outer) tyre temperatures per tyre, an average for all four tyres were plotted for the test, and the stabilised tyre operating temperature determined. Track surface temperature was also measured. The vehicle was tested on the Celso Scribante Short Circuit, and all available corners were used to maximise tyre use. Drivers were instructed to drive smoothly and consistently, but as close to the limit of adhesion as possible. Test results were compared to Continental tyre test data. Tyre temperature channels were smoothed with a three second average to enhance readability.

Tyre operating temperature tests were conducted at a tyre pressure of 80Kpa, a front camber angle of -1.5° and rear camber angle of -0.8°.

3.3.2 Wheel Camber

For tyre camber testing, tyre temperature readings were used to determine which camber setting produced the most even temperature distribution over the tyre, thereby producing the best level of grip.

The three tyre temperatures (inner, middle, outer) were measured, and a calculated channel, which determined the percentage difference between the inner and outer tyre temperatures, was plotted. The ideal camber would be when, on average, the calculated percentage channel reached zero.

The vehicle was tested on the Celso Scribante Short Circuit track, using the smallest radius corners available. All tests were conducted in a clockwise and anti-clockwise track direction, to average-out track-specific influences on tyre temperatures. Camber settings ranging from -1° to -3° were tested at a tyre pressure of 80Kpa. Refer to the Appendix F for the full vehicle setup datasheet. Only front wheel camber was used for this test, as front tyres experience the greatest loads during cornering. Results were compared to tyre test data from Continental Tyres.

3.3.3 Tyre Pressure

For tyre pressure testing, tyre temperature readings were used to determine which tyre pressure setting produced the most even temperature distribution over the tyre, thereby producing the best level of grip.

The three tyre temperatures (inner, middle, outer) were measured and a calculated channel, which determined the percentage difference between the centre temperature and the average of the inner and outer tyre temperatures, was plotted. The ideal pressure would be when, on average, the calculated percentage channel reached zero.

Tyre pressure tests were conducted on the Celso Scribante Short Circuit track, using the outer circuit to minimise stress on the tyres. All tests were conducted in a clockwise and anti-clockwise track direction, to average-out track-specific influences on tyre temperatures. Tyre pressure settings of 60, 70, 80, 90 and 100Kpa were tested. Tyre pressure tests were conducted with a front camber setting of -0.8°. Refer to Appendix H for the full vehicle setup datasheet. All four tyre pressures were changed and tyre temperature data for all four tyres were monitored. Results were compared to tyre test data from Continental Tyres [9].

3.3.4 Additional Test data

In addition to the three focus areas of this research, further vehicle data was available for analysis, providing useful supporting information regarding the performance of the test vehicle on the track.

a) G-G Diagram

Plotting the lateral versus longitudinal acceleration during track testing produced the G-G diagram for DibaOne during track testing, providing the vehicle performance limits for longitudinal and lateral acceleration.

b) Steering Angle versus Lateral Acceleration (Understeer Gradient)

A useful test to improve vehicle balance near the adhesion limit, and to increase lateral acceleration at lower speeds is to drive on a circular skid pan at varying speeds, recording lateral acceleration and steering angle. A graph can then be plotted showing lateral acceleration versus steering angle, also called the “understeer gradient”, providing an insight into the vehicle performance at the limit of adhesion.

c) Tyre Dynamic Load Distribution

Tyre dynamic load distribution was calculated using the average tyre temperature per tyre, and calculating the percentage of the total of all four tyre temperatures. This calculated channel was plotted to show which tyres had the highest average temperature, indicating that it was working the hardest. To establish the effect of castor on static load distribution, a static test was also performed which measured the actual load per wheel under various steering angles. Actual on-track tyre loading was therefore a combination of static load and dynamic load transfer.

d) GPS Data

The GPS receiver fitted to the vehicle (GPS-L10) had a sampling frequency of 10Hz and an accuracy of +-3m, allowing the vehicle location, speed and direction to be recorded. This data was very useful in support of the aforementioned tests, and allowed the plotting of track data for the Celso Scribante Short Circuit and VWSA skid pad.

In addition, various parameters could be plotted on the GPS track via the MoTec i2 software, to allow analysis of vehicle speed and acceleration in relation to track position.

With the addition of virtual GPS beacons, lap times could be automatically calculated, and the track could also be broken down into sections to compare sequential laps or drivers.

4. Experimental Data Results

Test data captured in the course of conducting the various vehicle tests, is reflected in summary form in this chapter. Full details of each test can be found in the relevant Appendices.

4.1 Tyre Operating Temperature

Six different track test warm-up cycles were compared to provide the results in table 4. Table 4 shows an average of 3.51 minutes (3 minutes 31 seconds) to warm up a cold set of tyres an average of 12.55°C to their recommended operating temperature of 40°C. The average track surface temperature was 27.95°C. Detailed graphs from each of the six tests are available in Appendix D. Figure 34 shows the average tyre temperatures for all four tyres and the track surface temperature during the warm-up phase of a typical track test. All tyre temperature channels were smoothed using a running average of 3 seconds.

Test Number	**1**	**2**	**3**	**4**	**5**	**6**	**Average**
Time to 40° (min)	4	2.8	0.8	2.6	6	4.8	**3.51**
Starting Temp (°C)	29	32	33	20.5	26	24.2	**27.45**
Temp increase (°C)	11	8	7	19.5	14	15.8	**12.55**
Track Temp (°C)	n/a	n/a	27.2	29	32.3	23.3	**27.95**

Table 4: Tyre Warm-up Test Results

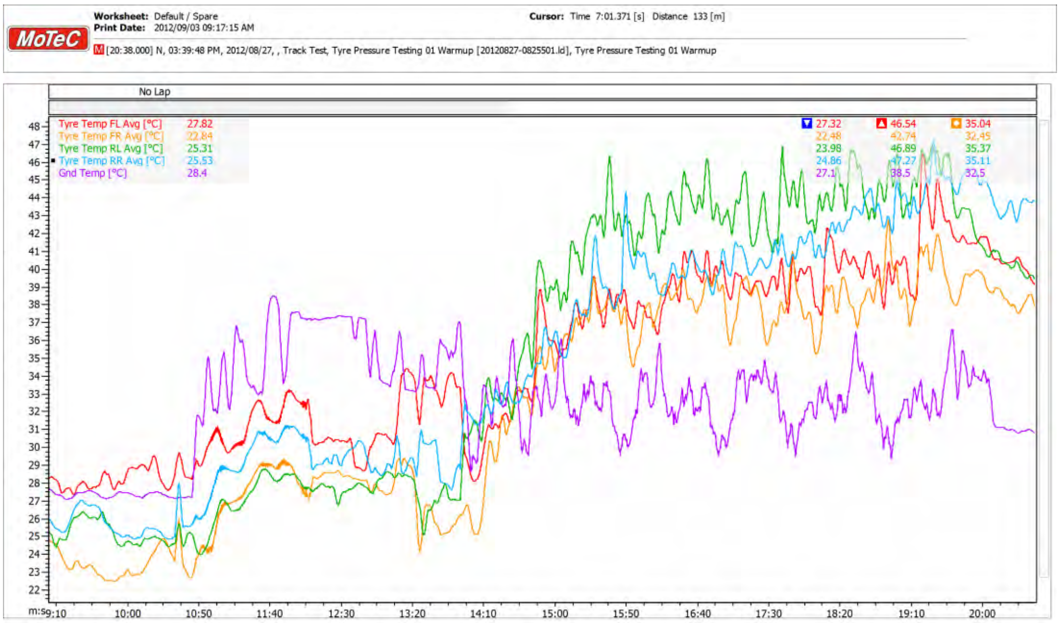

Figure 34: Typical Tyre Average Temperatures During Warm-up

Table 5 below shows the average tyre operating temperatures for all four tyres for six different tests, as well as the track surface temperature. The tyre operating temperature on average was 43.04°C for an average track surface temperature of 27.02°C.

Test Number	1	2	3	4	5	6	Average
Tyre Average Temp (°C)	46.51	43.6	41.7	45.0	42.22	39.2	43.04
Track Temp (°C)	n/a	27.2	27.9	26.1	30.6	23.3	27.02

Table 5: Tyre Operating Temperatures

Figure 36 below shows a typical smoothed graph of stabilised tyre temperatures during testing. Detailed graphs for each of the six tests are available in Appendix E. The two upper windows of the graph show detailed results for the front tyres, while the lower graph shows the calculated average of the three temperature sensor readings (inner, centre and outer) of each of the four tyres. The track surface temperature is also reflected on the lower graph for reference.

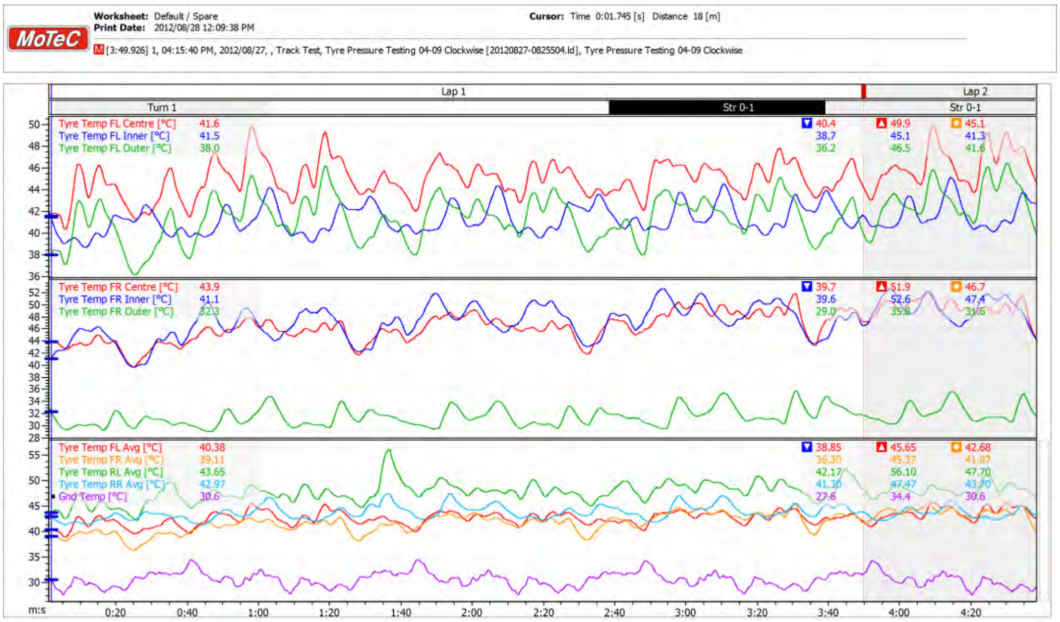

Figure 35: Typical Stabilised Tyre Operating Temperatures

4.2 Wheel Camber

4.2.1 Wheel Camber Tests – First Round

The first round of exploratory testing was designed to cover a broad range of camber settings within the available test window, and to facilitate this, different camber angles were set on the front left and front right wheels for each test (asymmetrical camber settings). As mentioned in chapter 2, wheel camber tests focussed on the analysis of front tyre temperatures due to the significance of load transfer to the front wheels when cornering. The benefit of this approach was to validate the test methodology employed, and to provide an indication of where the focus (in terms of camber angles) of future tests should be. A record of the vehicle setup parameters, such as corner weights, damper settings, ride heights and tyre pressures, is shown in Appendix F.

The first round of tests covered the following camber settings: 0°, -1.2°, -1.7° and -3.0°. These results are shown in table 6, as well as Figure 36 and 37 below. Detailed graphs are also available in Appendix G. Each test consisted of five laps in a clockwise direction around the track, and then five laps in an anti-clockwise direction. The clockwise and anti-clockwise results were then averaged for each camber setting, to eliminate track bias in the temperature readings. All tyre temperature channels were smoothed using a running average of 3 seconds.

Camber	Front Left Wheel				Front Right Wheel		
	Inner	Centre	Outer		Inner	Centre	Outer
-1.2° CW	41.4	47.5	45.7	-1.7° CW	46.8	45.3	34.6
-1.2° ACW	45.0	43.5	39.3	-1.7° ACW	42.0	46.7	38.4
-1.2° Avg	**43.2**	**45.5**	**42.5**	**-1.7° Avg**	**44.4**	**46.0**	**36.5**
0° CW	35.1	42.9	42.3	-3° CW	50.0	39.5	27.6
0° ACW	39.4	42.5	38.5	-3° ACW	44.2	41.7	30.8
0° Avg	**37.3**	**42.7**	**40.4**	**-3° Avg**	**47.1**	**40.6**	**29.2**

Table 6: Front Tyre Temperature Results (Round 1)

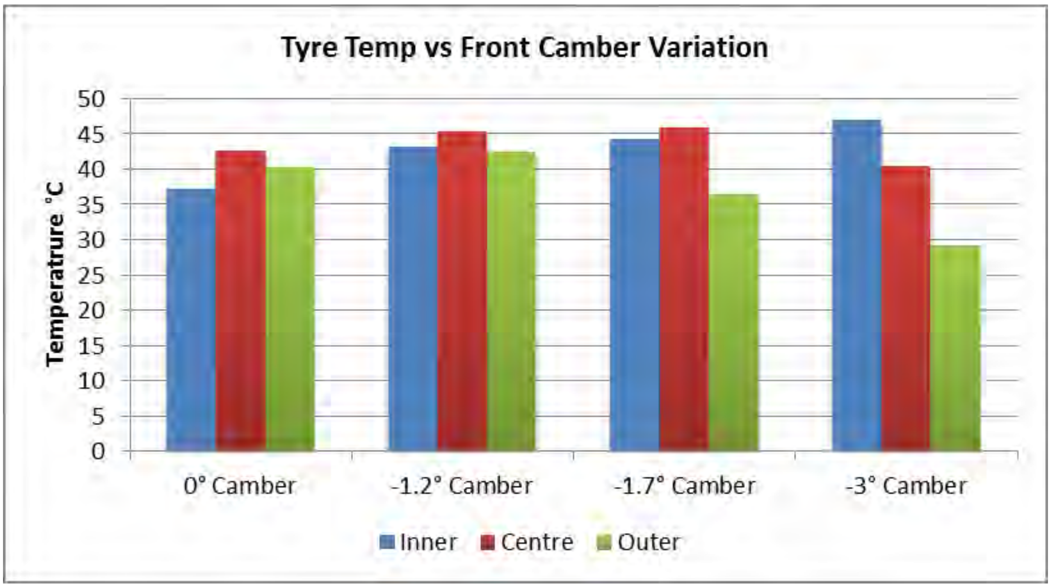

Figure 36: Tyre Temperatures versus Camber Variation (Round 1)

Figure 37 shows the percentage difference between the inner and outer tyre temperature, taken as an average of the clockwise and anti-clockwise results for each data point. The ideal camber setting, where the percentage value crosses the 0% line, was shown to be between 0° and -1.2°, indicating that the tyre was most effectively utilised during the test.

In order to narrow this ideal range however, more data points, and a more accurate picture of the left versus right ideal camber were required. Initial vehicle setup was performed using manual equipment such as a hand-held camber gauge, and in order to improve the accuracy of the test, a digital wheel-alignment process was required.

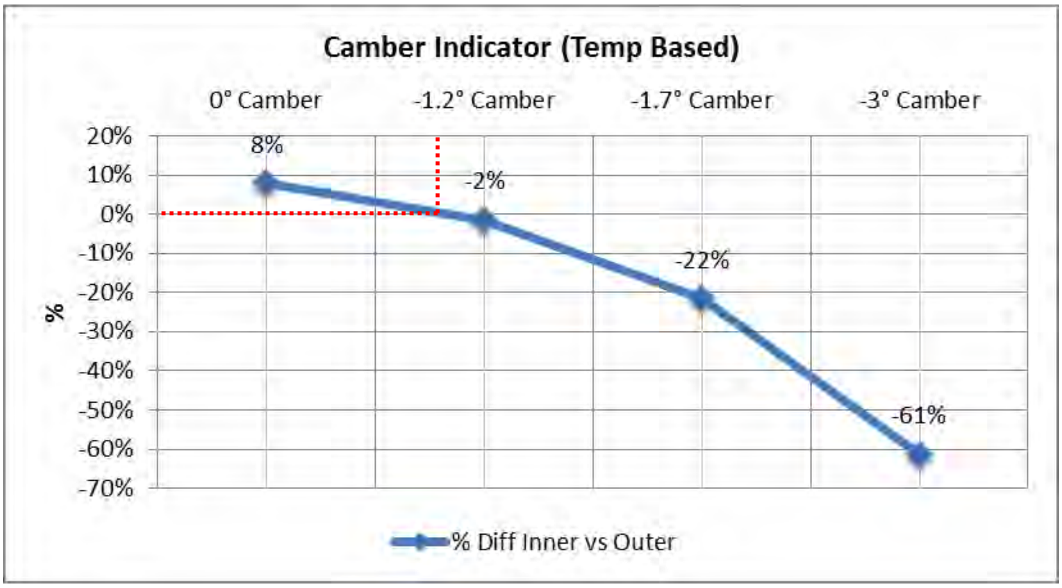

Figure 37: Camber Percentage Indicator based on Temperatures (Round 1)

4.2.2 Wheel Camber Tests – Second Round

A second round of camber testing was therefore conducted after setting wheel alignment accurately on a digital machine. Table 7, 8 and Figures 38 to 41 below summarise the results of the second round of testing with front camber settings of -1.0°, -1.5°, -2.0°, -2.5° and -3.0°. Detailed graphs for each test are included in Appendix G. Due to adjustment limitations the -1.0° and -3.0° test were conducted simultaneously on the front left and right wheels respectively, and no data for the front right -1.0° and front left -3.0° camber points are therefore available. Results for front left and front right camber were analysed separately.

Camber / Direction	Front Left Wheel		
	Inner	Centre	Outer
-2.0° Clockwise	42.8	45.2	40.1
-2.0° Anti-clockwise	46.9	45.4	38.0
-2.0° Avg	**44.9**	**45.3**	**39.1**
-1.5° Clockwise	41.2	53.3	49.0
-1.5° Anti-clockwise	43.7	46.6	40.2
-1.5° Avg	**42.5**	**50.0**	**44.6**
-2.5° Clockwise	41.7	42.7	38.2
-2.5° Anti-clockwise	45.2	43.9	38.3
-2.5° Avg	**43.5**	**43.3**	**38.3**
-1.0° Clockwise	38.1	53.4	49.5
-1.0° Anti-clockwise	41.4	50.9	45.1
-1.0° Avg	**39.8**	**52.2**	**47.3**

Table 7: Tyre Temperatures Versus Camber Variation – Front Left Tyre (Round 2)

Camber / Direction	Front Right Wheel		
	Inner	Centre	Outer
-2.0° Clockwise	50.2	45.5	31.4
-2.0° Anti-clockwise	45.5	45.5	34.7
-2.0° Avg	**47.9**	**45.5**	**33.1**
-1.5° Clockwise	44.0	49.1	35.4
-1.5° Anti-clockwise	40.7	49.0	38.5
-1.5° Avg	**42.4**	**49.1**	**37.0**
-2.5° Clockwise	51.3	44.4	29.9
-2.5° Anti-clockwise	45.1	45.4	34.6
-2.5° Avg	**48.2**	**44.9**	**32.3**
-3.0° Clockwise	48.0	45.3	32.6
-3.0° Anti-clockwise	45.4	47.2	35.3
-3.0° Avg	**46.7**	**46.3**	**34.0**

Table 8: Tyre Temperatures Versus Camber Variation – Front Right Tyre (Round 2)

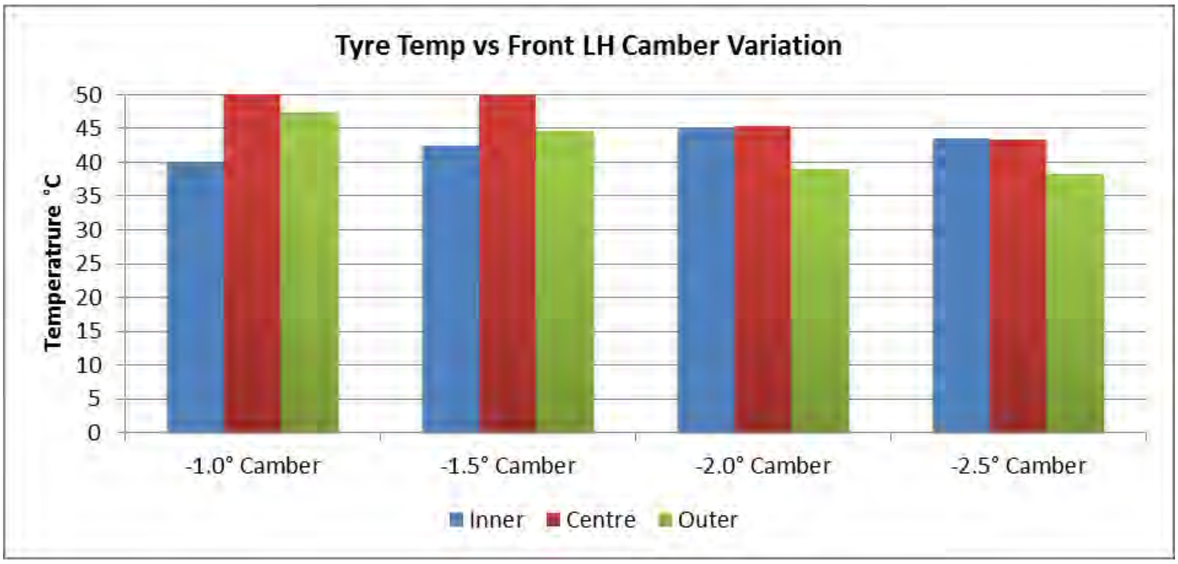

Figure 38: Tyre Temperatures versus Camber Variation – Front Left Tyre (Round 2)

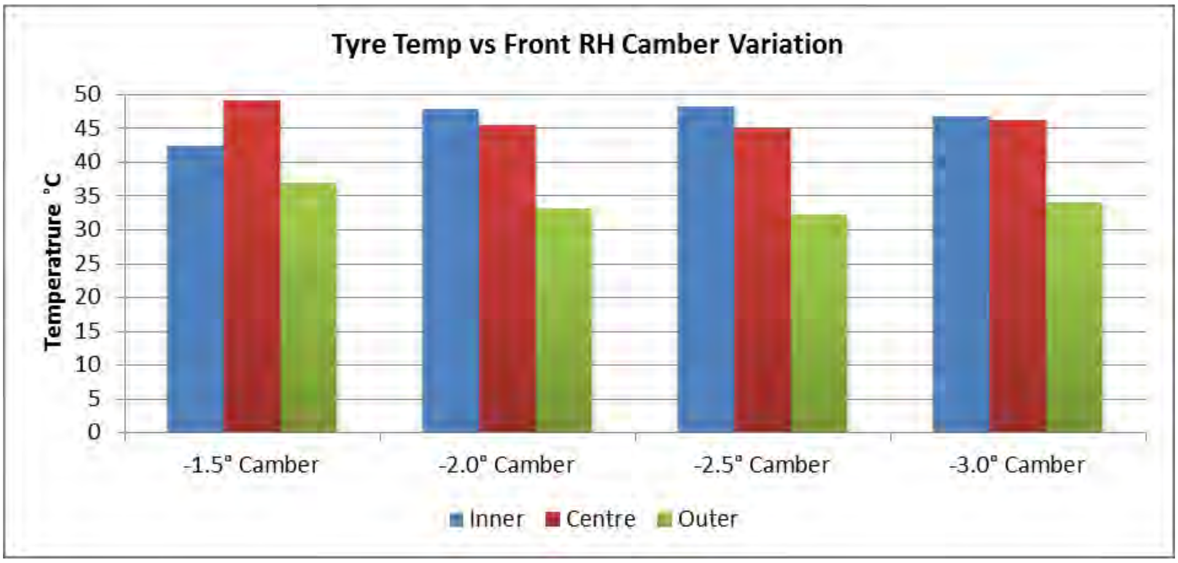

Figure 39: Tyre Temperatures versus Camber Variation – Front Right Tyre (Round 2)

Figures 40 and 41 below show the percentage difference between the outer and inner tyre temperatures for the front left and front right tyres, at each recorded camber setting. The front left tyre results show an ideal camber setting point, where the percentage difference between the outer and inner temperature is 0%, between -1.5° and -2.0°. The front right tyre results however, show a different ideal camber point, which was less than -1.5°.

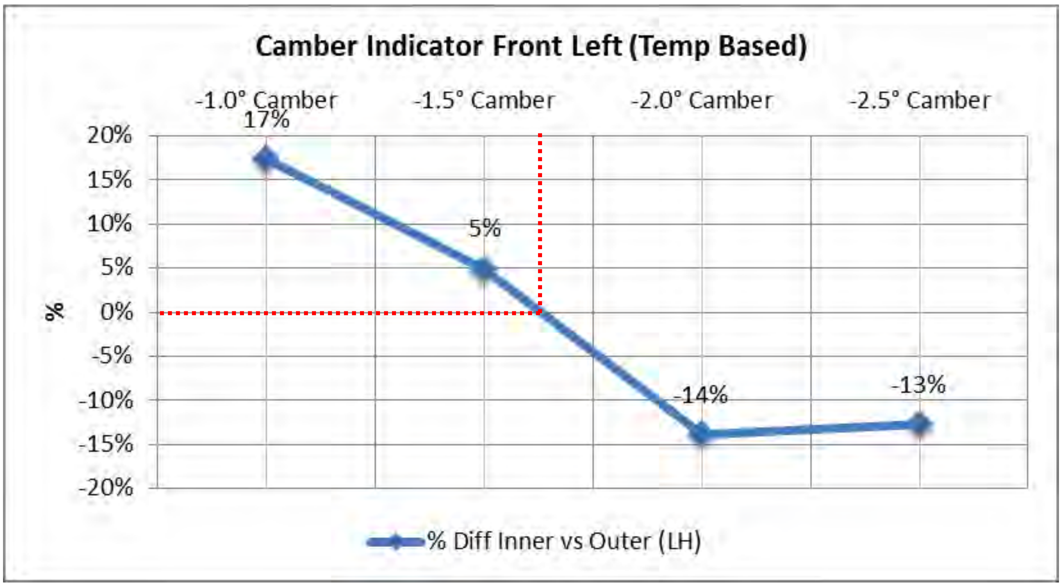

Figure 40: Camber Percentage Indicator based on Temperatures (Front Left Round 2)

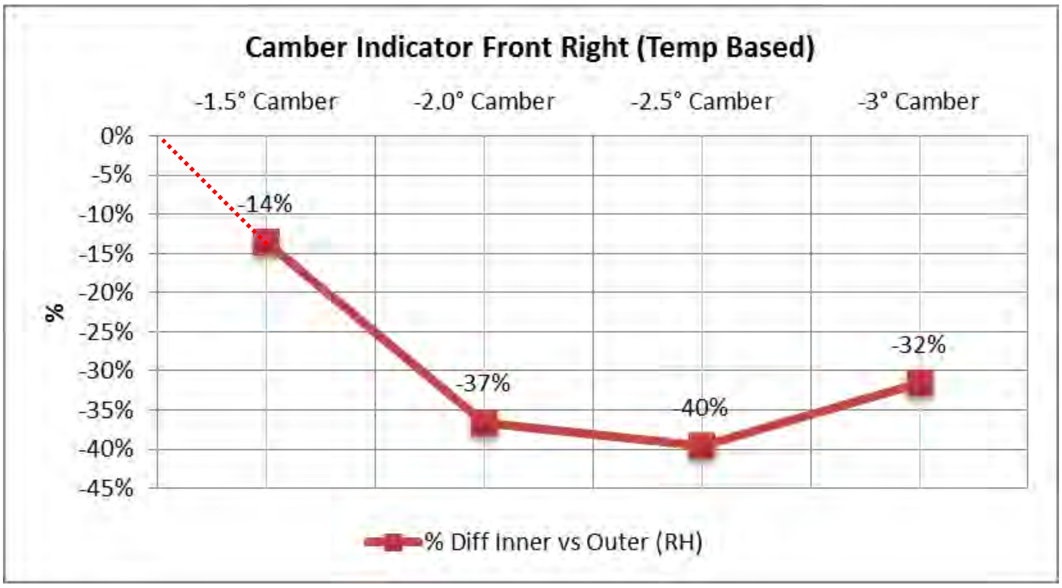

Figure 41: Camber Percentage Indicator based on Temperatures (Front Right Round 2)

4.3 Tyre Pressure

4.3.1 Hot vs Cold Tyre Pressure Tests

Due to the relationship between temperature and pressure, tyre pressures typically increase as the tyre temperature increases. Tyre pressure settings were done with “hot” tyres, and the first tests performed were designed to establish the relationship between “cold” and “hot” tyre pressures. Figure 42 shows the corresponding hot and cold tyre pressures at two pressure points, namely 90Kpa and 60Kpa. Subtracting the hot pressure from the cold pressure, revealed a difference of 10Kpa on average, indicating a 10Kpa increase in tyre pressure as the tyre temperature increased from a cold to a hot condition.

After an initial cold tyre pressure setting, 10Kpa lower than the required data point, all subsequent tyre pressure readings were done on hot tyres, so as to maintain the temperature generated in the tyre while on the track.

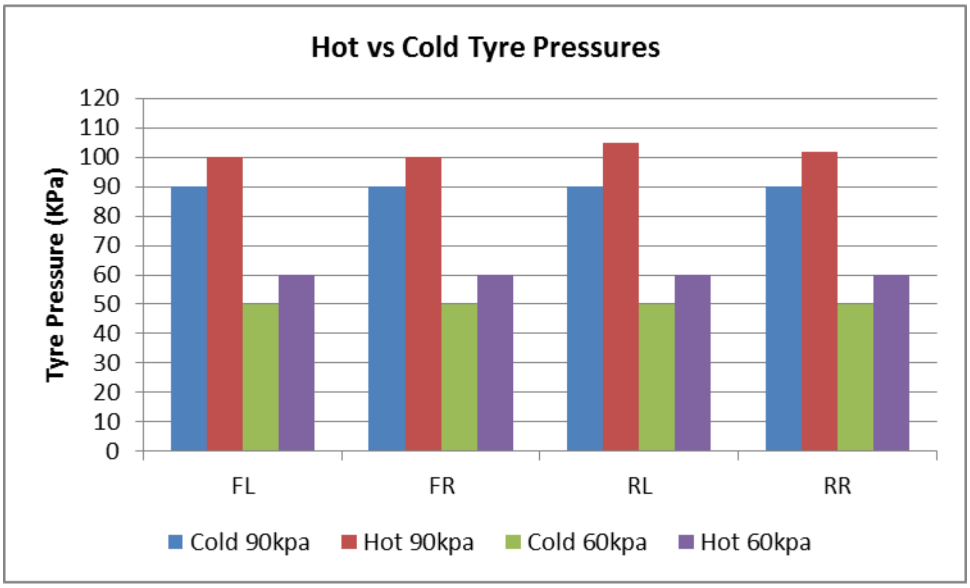

Figure 42: Hot vs Cold Tyre Pressure

4.3.2 Tyre Pressure Setting Tests

Appendix H shows the vehicle setup data for the tyre pressure tests. All parameters reflected on this datasheet were kept constant during the test, except for the adjustment of tyre pressures. Wheel camber was set -0.8° and all four tyre pressures were adjusted for this test, however tyre temperature analysis focussed on front tyres only.

Table 9 below, provides a summary of the results of the tyre pressure tests for the front tyres. Tyre temperature data for each tyre pressure setting was recorded during five laps of clockwise and anti-clockwise testing, and the results averaged to minimise any track bias in the tyre temperature results.

		Front Left Wheel			Front Right Wheel		
Tyre Pressure	**Direction**	**Inner**	**Centre**	**Outer**	**Inner**	**Centre**	**Outer**
100KPa	Clockwise	38.1	56.1	50.1	35.3	52.6	33.0
	100KPa Avg	**38.1**	**56.1**	**50.1**	**35.3**	**52.6**	**33.0**
90KPa	Clockwise	33.6	47.9	44.5	35.9	46.5	30.0
	90KPa Avg	**33.6**	**47.9**	**44.5**	**35.9**	**46.5**	**30.0**
80KPa	Anti-clockwise	41.7	40.7	37.1	37.0	47.8	39.6
	80KPa Avg	**41.7**	**40.7**	**37.1**	**37.0**	**47.8**	**39.6**
70KPa	Anti-clockwise	38.6	52.4	49.2	40.0	48.1	31.3
70KPPa	Clockwise	41.1	41.9	39.3	36.6	47.3	39.6
	70KPa Avg	**39.9**	**47.2**	**44.3**	**38.3**	**47.7**	**35.5**
60KPa	Anti-clockwise	43.2	64.7	60.1	41.3	52.8	33.7
60KPPa	Clockwise	42.1	45.3	43.2	38.0	50.1	41.1
	60KPa Avg	**42.7**	**55.0**	**51.7**	**39.7**	**51.5**	**37.4**

	Front Left Wheel			Front Right Wheel				
Averages	**FL Inner**	**FL Centre**	**FL Outer**	**FR Inner**	**FR Centre**	**FR Outer**	**Front Left %**	**Front Right %**
100KPa	38.1	56.1	50.1	35.3	52.6	33.0	31.8	38.5
90KPa	33.6	47.9	44.5	35.9	46.5	30.0	30.7	35.3
80KPa	41.7	40.7	37.1	37.0	47.8	39.6	25.8	31.2
70KPa	39.9	47.2	44.3	38.3	47.7	35.5	28.0	32.3
60KPa	42.7	55.0	51.7	39.7	51.5	37.4	29.2	33.4

Table 9: Tyre Temperatures vs Tyre Pressures

Figure 43 shows graphically the average clockwise and anti-clockwise tyre temperatures for each tyre pressure setting tested on DibaOne.

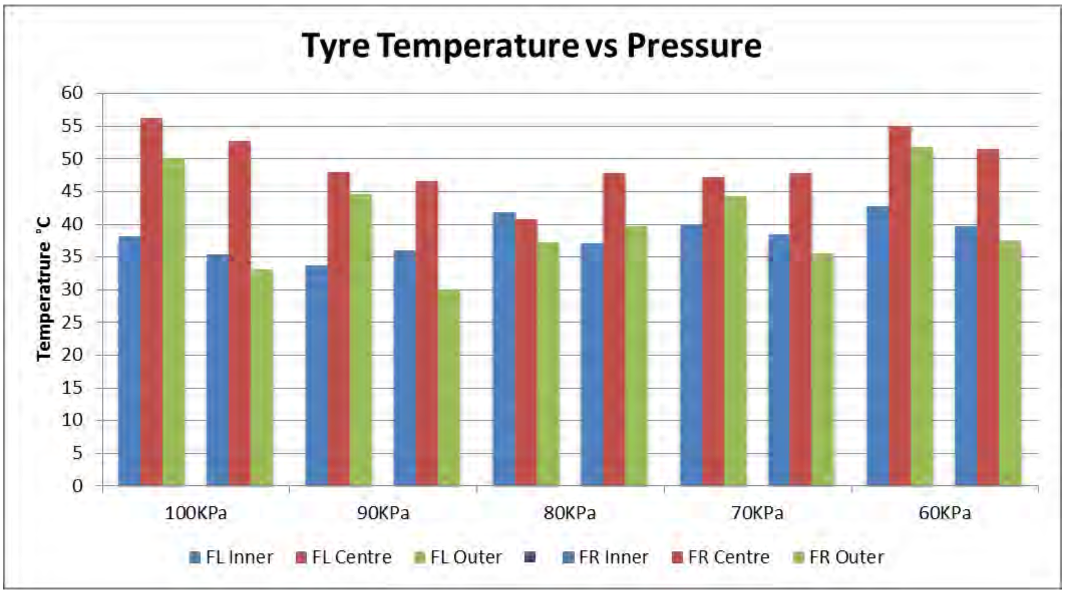

Figure 43: Front Tyre Temperature vs Pressure

Figure 44 shows the percentage difference between the centre tyre temperature and the average of the inner and outer temperatures at hot tyre pressures of 100Kpa, 90Kpa, 80Kpa, 70Kpa and 60Kpa. Although the graph does not reach the 0% line, it does show a downward trend as tyre pressures are reduced to 80Kpa, and upward trend thereafter. The tyre pressure providing the most even spread of tyre temperatures across the front tyres (inner middle and outer temperatures) is therefore 80Kpa. This is true of both left and right front tyres.

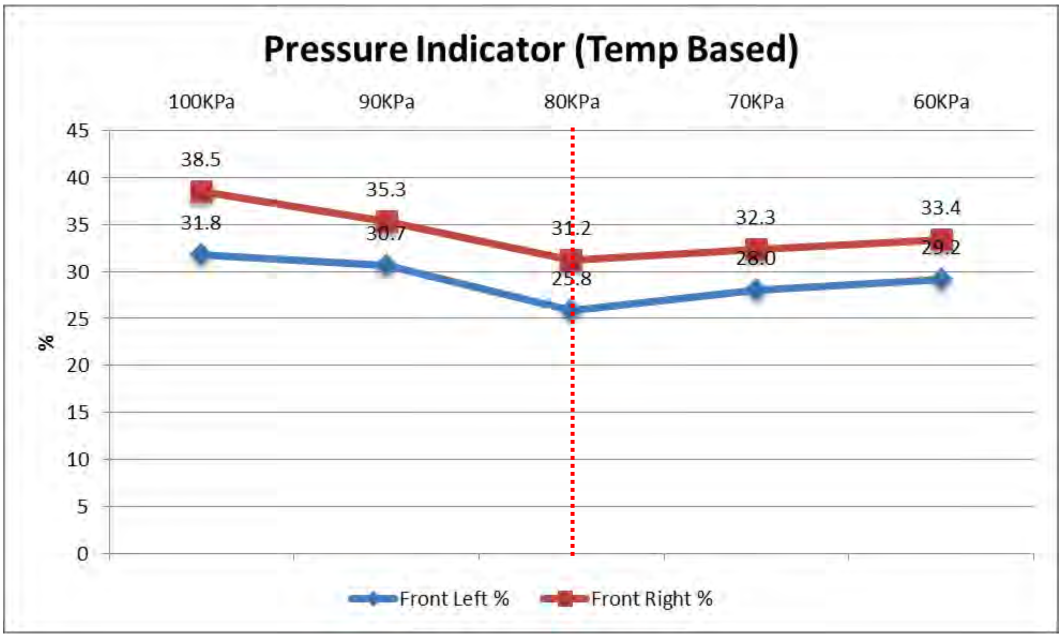

Figure 44: Front Tyre Pressure Indicator

4.4 Additional Test Data

4.4.1 G-G Diagram

The G-G diagrams in Figure 45 and 46 were constructed using the lateral acceleration and longitudinal acceleration data recorded while track testing DibaOne. Figure 45 shows a G-G diagram for a clockwise circuit, while Figure 46 shows an anti-clockwise circuit. A clear shift can be seen when comparing these two graphs, indicating the effect of track layout on the recorded data. The maximum values of acceleration recorded for DibaOne on the Celso Scribante Short Circuit are as follows:

- Maximum lateral acceleration = 1.8G
- Maximum longitudinal acceleration = 0.6G
- Maximum deceleration = 1.4G (braking)

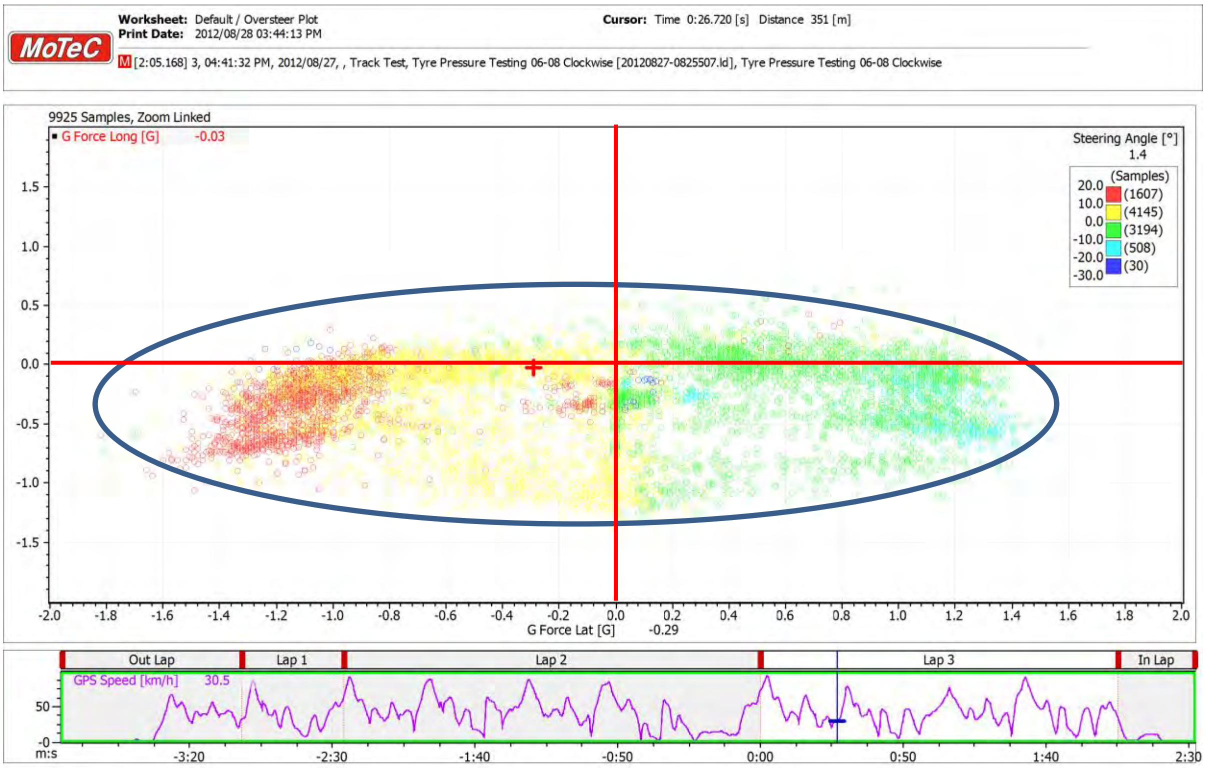

Figure 45: G-G Diagram Clockwise Circuit

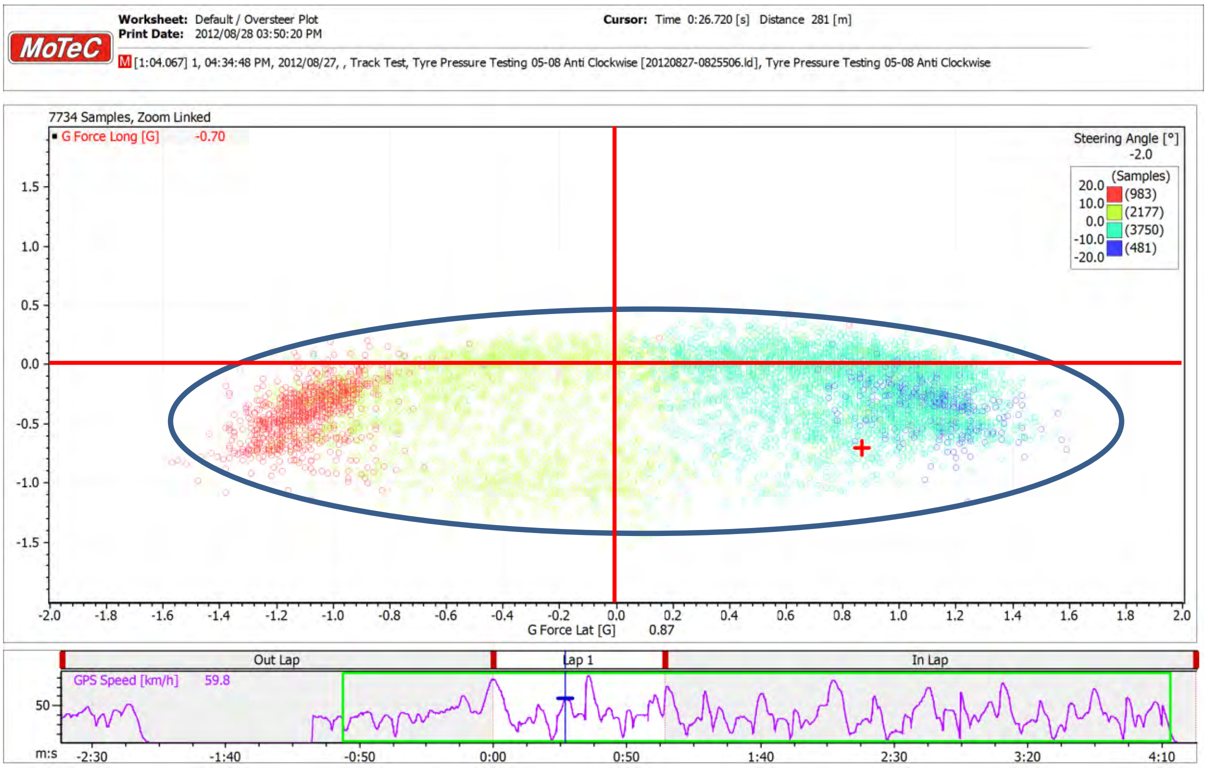

Figure 46: G-G Diagram Anti-Clockwise Circuit

4.4.2 Steering Angle versus Lateral Acceleration (Understeer Gradient)

A useful test to improve vehicle balance near the adhesion limit, and to increase lateral acceleration at lower speeds, is to drive on a circular skid pad at varying speeds, recording lateral acceleration and steering angle. Figure 47 and 48 show lateral acceleration versus steering angle, also called the “understeer gradient” [3], providing an insight into the vehicle performance at the limit of adhesion.

Understeer gradient analysis was performed on data from both the VWSA Skidpad and the Celso Scribante Short Circuit.

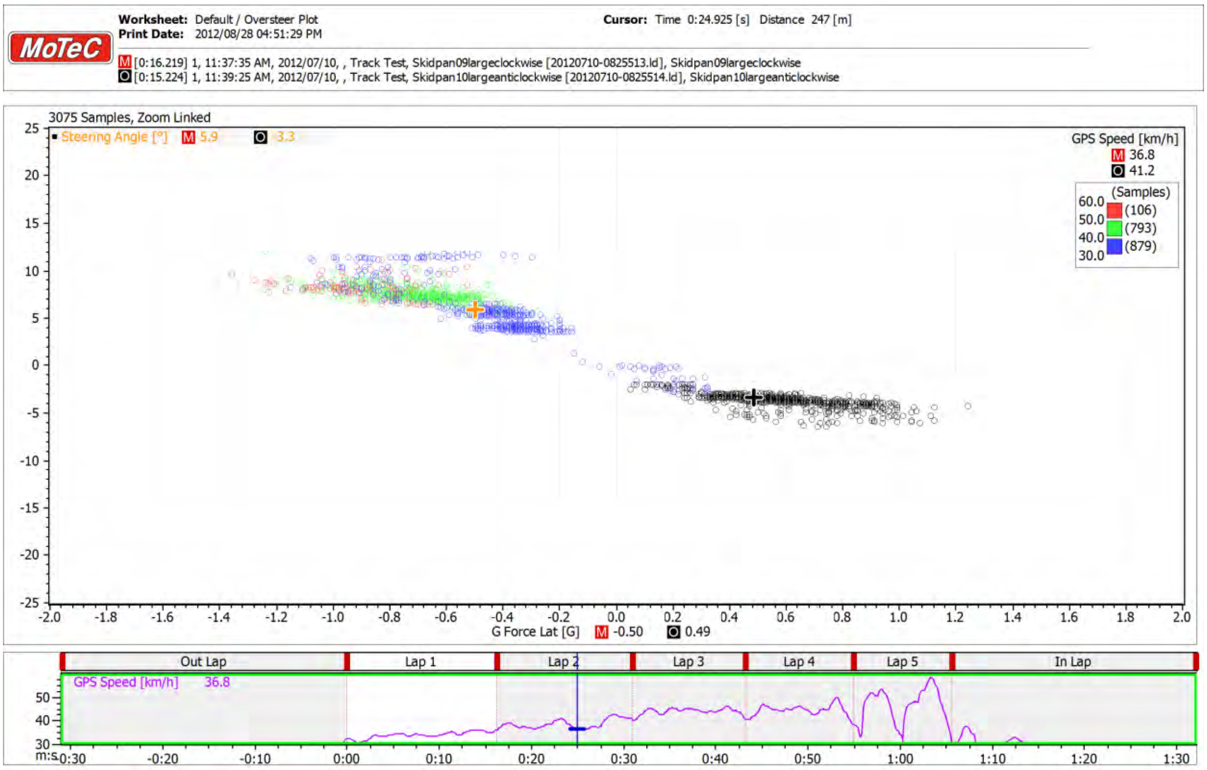

Figure 47: Understeer Gradient on VW Skid Pad

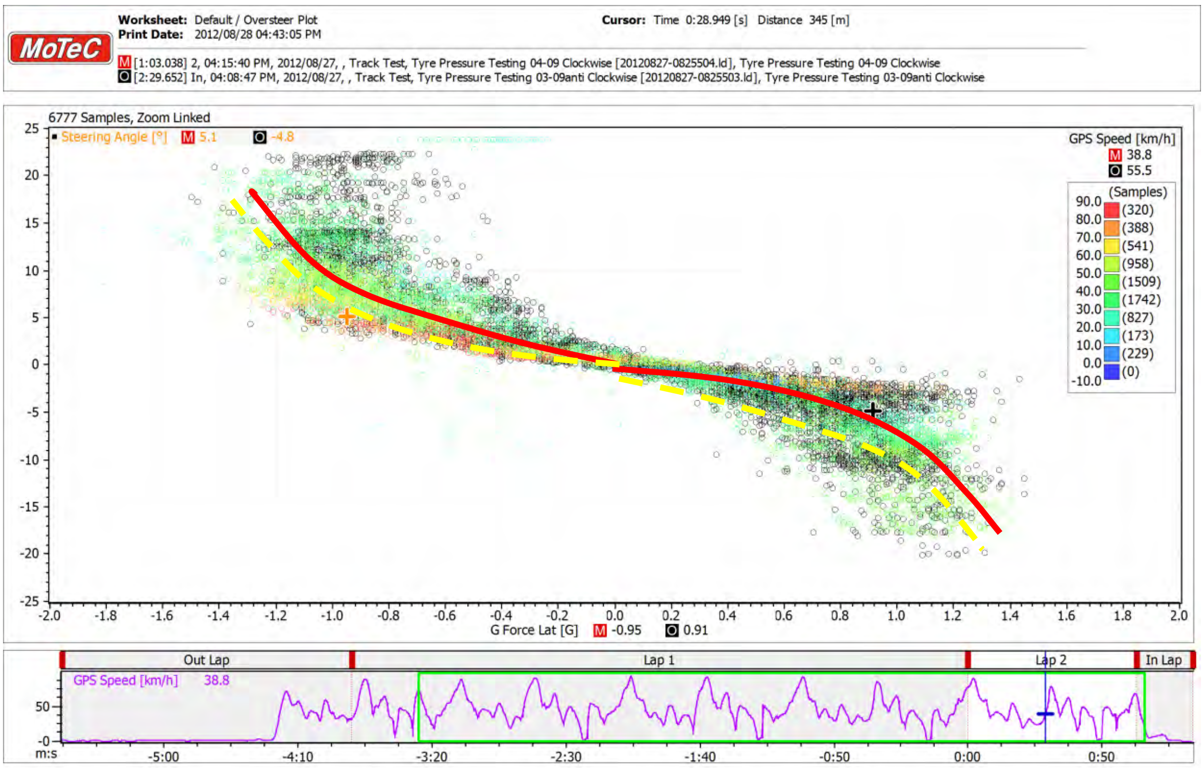

Figure 48: Understeer Gradient on Celso Scribante Short Circuit

4.4.3 Tyre Dynamic Load Distribution

Tyre temperatures vary dynamically due to both static and dynamic weight transfer. Measuring tyre temperatures on the track provides data on the combined effect of static and dynamic weight transfer, however it is useful to analyse these separately, in order to determine the effect of each on vehicle performance. A static weight distribution vs steering angle test was devised, which measured the load on each wheel under different steering angles. As shown in Figure 49, the castor angle and kingpin inclination of the steering system causes a change in weight distribution at different steering angles. Individual wheel loading was measured on vehicle scales and potted against steering angle to quantify the level of static weight transfer.

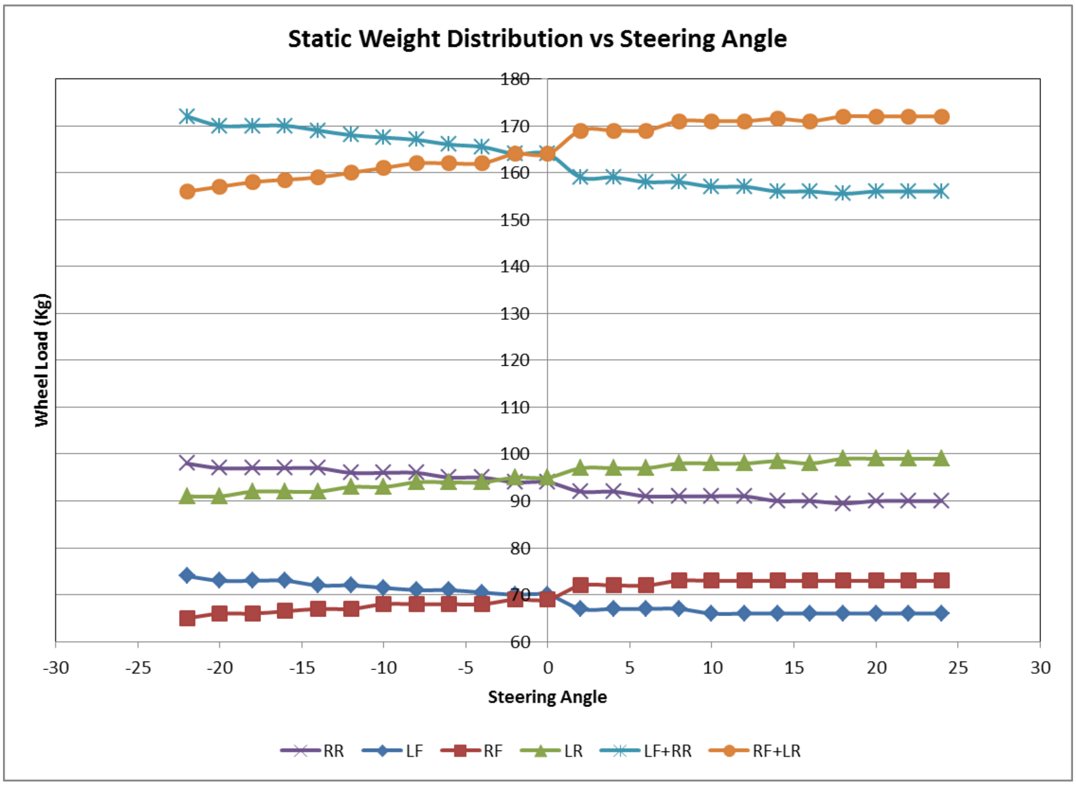

Figure 49: Static Weight Distribution Versus Steering Angle

Figure 50 shows the resultant effect of static weight transfer by subtracting the sum of the diagonal corner weights of the vehicle. The total static weight transfer was therefore calculated to be 16Kg at a maximum steering angle of 24°.

Figure 50: Static Weight Transfer Versus Steering Angle

Figure 51 shows a typical dynamic tyre load distribution during track testing by calculating the percentage of each tyre average temperature in relation to all four tyres. The upper window shows the actual average tyre temperatures, while the lower window shows the percentage of each of the tyre temperatures in relation to the sum of the four tyres.

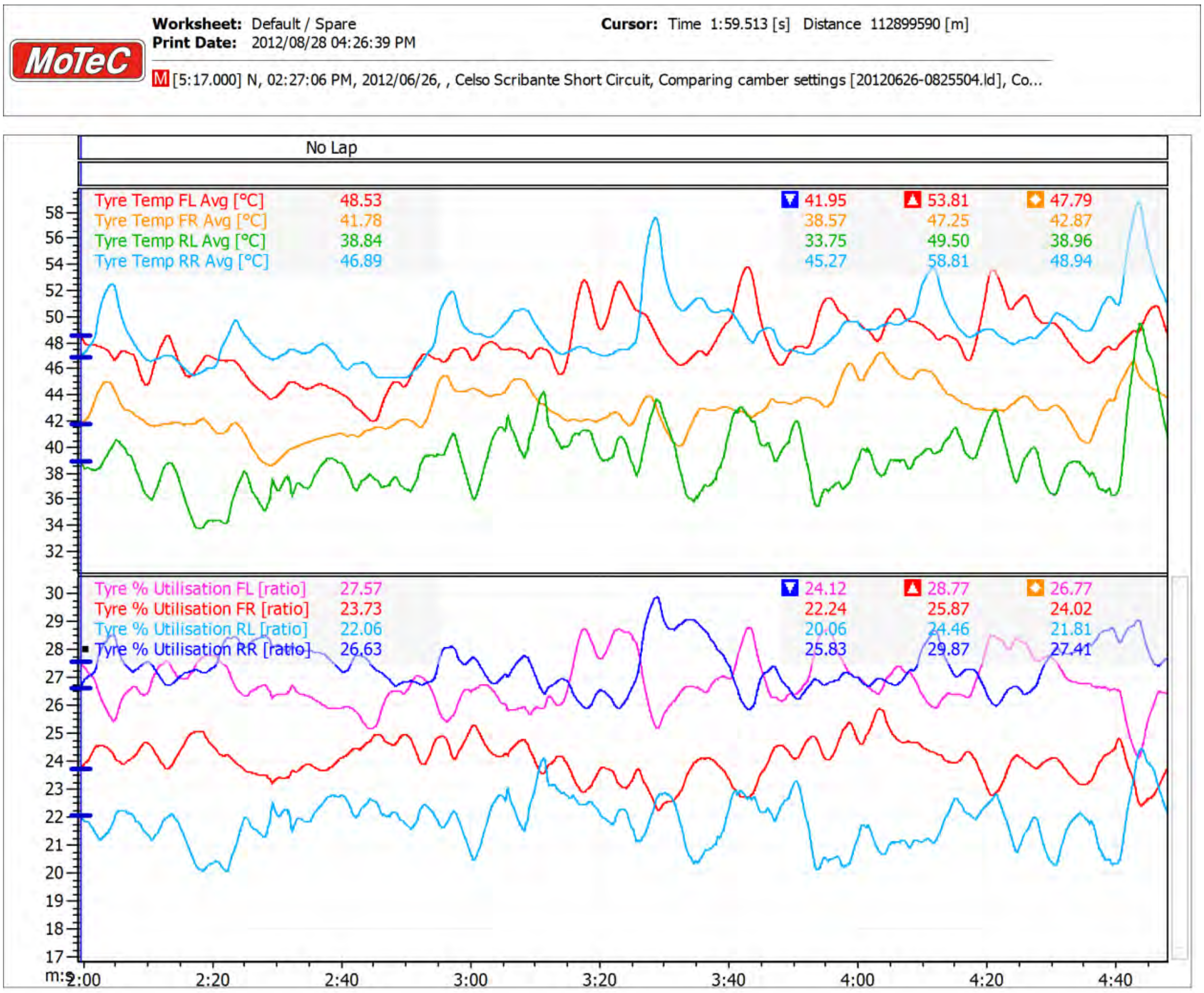

Figure 51: Typical Tyre Dynamic Weight Distribution Based on Temperatures

This graph is useful to analyse the balance of the vehicle when on the track, and clearly shows that despite setting corner weights before testing, weight distribution is not symmetrical in the vehicle when driving on the track.

4.4.4 GPS Track Data

Global Positioning Satellite (GPS) Track Data was recorded during track testing, and analysed using MoTec i2 software. This data provided many opportunities to analyse vehicle performance with parameters such as vehicle position, speed and altitude. The i2 software also provided opportunities to overlay various vehicle data channels onto the GPS data, so that vehicle performance data could be linked to the GPS position on the track. GPS data was recorded for the Celso Scribante Short Circuit, as shown in Figure 52 and 53 below, as well as the VWSA Skidpan.

The GPS receiver (MoTec GPS-L10) samples at a rate of 10Hz with an accuracy of approximately 3m, and care had to be taken when recording GPS data to avoid inaccuracies in measurement.

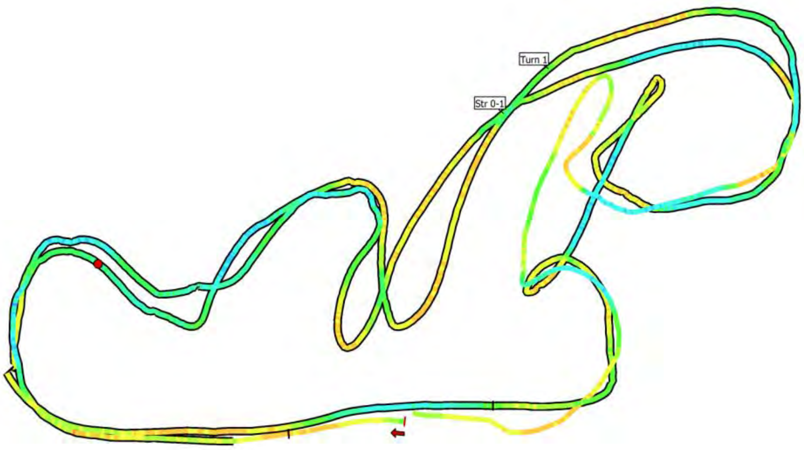

Figure 52: GPS Track Data During High-Speed Testing

Figure 53 shows a data-overlay of vehicle speed, showing the variation of vehicle speed in different colours on the track.

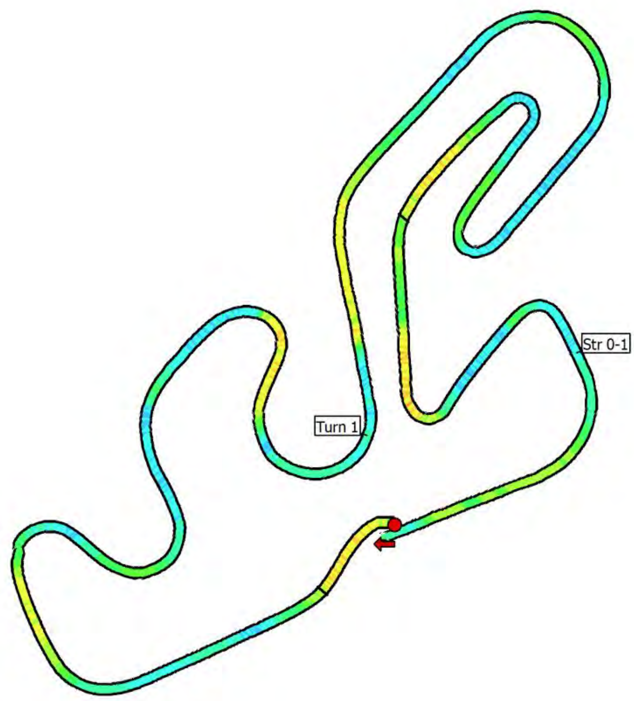

Figure 53: GPS Track Data for Reference Lap

5. Analysis and Discussion

The test results shown in Chapter 4 are discussed below under their respective headings.

5.1 Tyre Operating Temperature

As discussed in chapter 2, heat is generated in vehicle tyres due to the frictional forces between the tyre and the track surface, as well as internal stresses in the tyre carcass. In addition, tyres have been designed and tested by the manufacturer to operate within an ideal temperature range, due to the construction of the carcass and rubber compounds utilised in the tread. It follows therefore, that utilising a given tyre at its ideal temperature would lead to the best performance in the tyre. For this reason it is vitally important to know what the operating temperature of the tyre is, and how long a particular tyre takes to reach this optimum temperature.

The tyre operating temperature and warm-up time is however influenced by many factors, including ambient conditions such as the weather, humidity/rain, track surface temperature and wind. The largest influence on tyre temperatures, is however due to the forces experienced by the tyre during acceleration, braking and cornering, when the tyre converts grip into vehicle acceleration. Both the track and driver have a major role to play in the generation of these forces and temperatures, and varying these two factors alone produces very different test results.

5.1.1 Tyre Warm-Up

The testing conducted in this study utilised the DibaOne Formula Student race car, fitted with Continental racing slick tyres and driven by reasonably competent student drivers. Under these conditions, an average warm-up time for the tyres, from an ambient temperature to 40°C was recorded as 3.51 minutes (3min 31sec). This was an average of 12.55°C increase in the surface temperature of the tyre.

The effect of ambient conditions can clearly be seen in the results in Table 4, where a high track (27.2°C) and tyre starting temperature (33°C) reduced the warm-up time to 0.8 minutes (48sec), while a low track (23.3°C) and tyre starting temperature (24.2°C) extended the warm-up time to 4.8min (4min 48sec)

Figure 34 shows the variation in tyre average temperature over time, illustrating how each of the four tyres warm-up at differing rates. On a clockwise circuit for example, the right hand side tyres may take longer to warm-up than the left hand side tyres, due to lateral weight transfer, which produces higher loading on the outside tyres.

Tyre warm-up can also be accelerated by inducing additional stress on the tyres through weaving on the track, as typically seen before Formula One races, or by driving at higher speeds through the corners, and braking harder. Caution should be exercised when driving on "cold" racing tyres however, as grip is significantly reduced, and the vehicle is more prone to unexpectedly over or under steer in a corner. This problem is less pronounced on road cars, as road tyres are designed to operate through a much larger range of temperatures and road conditions.

5.1.2 Tyre Operating Temperature

Tyre operating temperatures will differ for example, on a track with few, versus a track with many corners, and the data discussed below is relevant only to its specific application. The average tyre operating temperatures shown on Table 5 were mostly higher than the expected value of 40°C, as indicated in the Continental tyre test data (Figure 15). On average the recorded tyre operating temperature was 43.04°C with an average track surface temperature of 27°C.

Ambient conditions played a significant role in this value, with lower track temperatures (23.3°C) recording lower tyre operating temperatures (39.2°C). The higher than expected operating temperature can therefore be attributed to the higher ambient conditions experienced in South Africa, compared to Europe, where the tyres were developed, and the higher than average weight of DibaTwo (330Kg with driver), when compared with other Formula Student cars who are typically 50-80Kg lighter, which placed additional load on the tyres.

5.2 Wheel Camber

Managing the tyre contact patch pressure distribution is vital to maintaining the highest possible level of grip for the tyre. One of the most important factors influencing this pressure distribution is the angle in which the tyre finds itself when contacting the road. This angle is determined by the camber angle of the wheel, which is a function of both the static and dynamic camber produced by the suspension system. Different suspension designs have varying degrees of success in keeping the dynamic wheel camber angle at an ideal value during pitch, heave, roll and yaw movements of the vehicle under the influence of driver and track inputs.

Appendix C shows the simulated results of various suspension movements of DibaOne, and their influence on wheel camber. Figure 57 and 59 are of particular interest to this study, as they illustrate the camber variation of DibaOne's suspension during heave and roll motions. 30mm of suspension bump movement produced 0.8° of front camber change, and for 2° of roll, the front wheel camber changed by 1.5°. With the ineffective anti-roll bars fitted to DibaOne, a significant amount of roll was experienced during testing, producing at least these levels of camber variation when cornering. The roll centre height, roll axis control and centre of gravity height in relation to the roll centre, also have a significant effect on the amount of body roll experienced in a corner. Figure 60 illustrates the simulated positions of these points and of significance is the movement of the roll axis and the height of DibaOne's centre of gravity. These two factors produced excessive cornering body roll in DibaOne and reduced the cornering stability of the vehicle, while increasing the dynamic camber variation.

In addition, Dynamic camber variation is produced by steering castor and KPI angles, further impacting on the wheel camber angle on the track. It is therefore logical to assume a significant camber angle variation on the track, when compared with the applicable static camber setting.

The first round of camber testing was conducted using assymetric camber settings to facilitate the testing process, and provide a means to test a wide range of camber settings in a few tests. The camber settings tested were: 0°, -1.2°, -1.7° and -3.0°. The results shown in Table 6, as well as Figure 37 clearly indicate a trend, which lead the researcher to conclude that the ideal front camber for DibaOne would be between 0° and -1.2°. To reduce external variables to this test as well as to enhance the accuracy of the result, a second round of testing was performed on DibaOne covering static camber settings of: -1.0°, -1.5°, -2.0°, -2.5° and -3.0°. Some of the factors that were addressed in the second round of testing were, a more accurate vehicle setup, more camber data points during the test, setting the left and right front wheels to the same camber angle for each test, and the introduction of GPS sensor data to assist with individual lap analysis.

The results of the second round of testing once again showed the strong correlation between wheel camber angle and indicated tyre temperatures. Figures 40 and 41 were constructed using the data in Tables 7 and 8, by calculating the percentage difference between the inner and outer tyre temperatures for the two front tyres, thereby effectively measuring the temperature gradient across the tyre.

The vehicle setup on the digital wheel alignment equipment revealed some inaccuracies in the basic construction of DibaOne, such as differences in left and right wheelbase, compliance in the suspension linkages, which produced uncontrolled wheel camber and toe changes under load, and most significantly a large difference between left and right castor angles. The left castor angle was measured at 3.3°, while the right castor angle was 2.7°, which means a difference of 0.6° between left and right. The problem with this castor variance was that it could not be adjusted out of the vehicle, as it was a fundamental function of the manufacturing accuracy of the suspension A-arms and frame mounting points. The significance of this variance in castor was that even though static camber was set reasonably accurately and symmetrically, dynamic camber would be different between left and right wheels on the track. The higher castor value on the left front steering axis, produced more negative camber on a right turn than the lower castor value would on a right turn. In addition, suspension compliance, previously mentioned, also influenced the results of the wheel camber tests, and for these reasons, the front left and right wheel camber test results were analysed separately.

An analysis of Figure 40, which showed data for the left front tyre, revealed that the ideal camber point was between -1.5° and -2.0°, while Figure 41 revealed the ideal camber point for the right front wheel to be less than -1.5°. Extrapolating this graph, one could infer that the ideal camber point lay between -1.0° and -1.5°. These differences between the ideal static camber settings for left and right front wheels, rather than being inaccuracy in the data, confirmed the previous assertion that the difference in castor angles produced different dynamic camber levels when on the track. The ideal static camber setting as revealed by the tyre temperature data therefore reflected the need to compensate for this dynamic camber variation between the front left and right wheels. It can therefore be inferred that if the castor angles could be corrected, to a symmetrical value of say 3.0°, the ideal static camber setting would be -1.5°, the average between the recorded values for the left and right wheels.

These static camber test results compared favourably with the Continental tyre data shown in Figure 14 which indicated an Ideal tyre camber for maximum grip to be -1.5°, as it revealed the best compromise between lateral force in both lateral directions (towards and away from the camber inclination angle).

5.3 Tyre Pressures

As discussed in Chapter 2, tyre pressure management is crucial to effective tyre performance, as a particular tyre will provide the optimum contact patch pressure distribution on the track only when the internal pressure is optimised. A tyre's internal pressure is however influenced by the operating temperature of the tyre, which increases from its "cold" condition at ambient temperature, to its "warm" condition during extended operation. Various operating conditions such as acceleration, braking and cornering serve to increase the temperature of the tyre due to increased frictional heat generated between the track and the tyre, as well as internal stresses in the tyre itself. Assuming that the volume of gas in the tyre does not change significantly, the relationship between the tyre internal pressure and temperature is largely proportional, with an increasing tyre carcass temperature producing a rise in tyre pressure. Tyre temperature testing on DibaOne was however conducted by measuring the tyre surface temperature, and not the carcass temperature, and the first step in establishing the ideal tyre pressures was to analyse the relationship between the tyre temperature and the corresponding tyre pressure. The test methodology for tyre pressure testing required the setting of hot tyre pressures, between subsequent laps on the circuit, and the hot versus cold tyre pressure correlation had to be determined.

Figure 42 shows the results of measuring tyre pressures in cold versus hot conditions, and the average tyre internal pressure increase was measured as 10Kpa. Tyre pressure testing was therefore started at the upper limit of tyre pressures, less 10Kpa, and after tyre warm-up tyre pressures were re-checked to the upper limit of 100Kpa. In order to eliminate the possibility of cold ambient air reducing the tyre internal temperature when increasing tyre pressures from 60Kpa to 100Kpa, the researcher elected to start at the maximum value of 100Kpa and reduce tyre pressures on each successive run until reaching 60Kpa.

Figure 44 illustrates the results of the tyre pressure tests in terms of a percentage difference between the centre tyre temperature and the average of the inner and outer temperatures. A higher centre tyre temperature is said to indicate an over-inflated tyre, while a lower tyre centre temperature is said to indicate an under-inflated tyre. Successive track tests were performed at 10Kpa increments ranging from a hot tyre pressure of 100Kpa down to 60Kpa.

The test results in Figure 44 showed an unexpected trend, as the ideal tyre pressure line did not reach the 0% mark, seemingly indicating tyre over-inflation. Although this result does not conform to general wisdom, regarding the analysis of tyre pressures using tyre temperature data, the lowest point on the graph, where the tyre temperatures were closest to uniform, lay at the 80Kpa level, therefore indicating the most suitable hot tyre pressure, measured at a front static camber of -0.8°. This would correlate to an optimum cold tyre pressure of 70Kpa.

The reasons for this unexpected result are most likely related to the application in which the tyres find themselves, which is a lightweight (330Kg) single-seater car on a relatively low-speed (less than 100Km/h) circuit. Typical race car tyre testing would be conducted on heavier (over 1000Kg) racing car operating at maximum speeds exceeding 200Km/h. These race cars typically run wider tyres with harder rubber compounds than those found on the Continental Formula Student tyre.

Despite conducting tyre warm-up before testing, there was also a detectable upward trend in tyre average temperatures over the five tyre pressure tests, due to the gradual build-up of the tyre carcass temperature, thereby also having an influence on the tyre temperature results.

5.4 G-G Diagram

The "G-G" boundary, at which a particular vehicle can achieve maximum acceleration in any direction, is a combination of all plotted resultant accelerations measured on a vehicle negotiating a given track. This G-G diagram is a useful indicator of the overall performance potential of a particular vehicle, and provides objective data to guide the performance enhancement or tuning process of the racing car. A G-G diagram is by nature a scatter-plot of hundreds of data points, which need to be analysed as a whole, and utilising significant insight into both the vehicle and track configuration. Due to the myriad of factors influencing the extent of the G-G boundary, it was not feasible to establish direct correlations between, for example wheel camber angles and the maximum G-G boundary. The G-G diagram for DibaOne was, however a very useful tool to evaluate the vehicle's performance, and a number of interesting results could be drawn from this diagram.

Figure 45 and 46 show the clockwise and anti-clockwise G-G diagrams for DibaOne on a typical race track test of approximately five laps. A clear shift can be seen when comparing these two graphs, indicating the effect of track layout on the recorded data, where the clockwise circuit, having more right-hand corners, has a higher G-G boundary to the left. The opposite is true of the anti-clockwise G-G boundary. Analysing the maximum values of acceleration on the G-G boundary, namely:

- Maximum lateral acceleration = 1.8G
- Maximum longitudinal acceleration = 0.6G
- Maximum deceleration = 1.4G (braking)

revealed that DibaOne had a significant amount of lateral grip when cornering, and could benefit from a boost in engine performance to utilise this available grip for longitudinal acceleration. Braking deceleration levels were also lower than the maximum lateral acceleration, indicating either an inadequate, braking system or, more likely, inexperienced drivers, who brake too early in the corners. This factor is one of the major challenges when designing and racing a Formula Student car, as in most cases, professional or experienced racing drivers are not available to fully explore the performance capabilities of the car.

The above data was also useful in establishing design objectives (Appendix B) for DibaTwo, as a lighter car with a lower center of gravity, and higher available engine performance would make far better use of the available grip in the Continental Formula Student tyres.

5.5 Understeer Gradient

The understeer gradient is a standardised ISO test, developed to measure the cornering balance of a particular car by recording the lateral acceleration and steering angle, while negotiating a circular skid pad at increasing speeds, until the vehicle over or understeers.

DibaTwo was tested on the VWSA skid pad for this purpose, recording values for two different skidpad diameters, namely 30m and 50m. The results were somewhat disappointing however, due to the poor quality of the surface of the skidpad, which suffered from loose stones and severe undulations. The result of these limitations was that when the vehicle approached the limit of adhesion, it was either destabilised by a bump in the track, or lost grip on the stones. Comparing Figures 47 and 48 shows the limited results obtained on the VWSA skidpan, compared to a plot of steering angle versus lateral acceleration measured during a track test at the Celso Scribante Short Circuit.

Of further interest is the lack of symmetry in the data, revealing different cornering performance on left versus right corners for DibaOne. Figure 48 highlights this lack of symmetry in the solid versus dashed trend lines on the graph, revealing that for a given level of lateral acceleration, a higher steering angle was required when turning right, compared to turning left. This data correlates well with driver feedback, as both drivers noted that the car turns into a left hand corner much better than into a right hand corner, while higher levels of understeer were experienced on right hand corners compared to left hand corners. This phenomenon can be explained by the lack of symmetry in the steering geometry as previously discussed in Chapter 5.2, as well as lack of symmetry in spring and damper settings, resulting in unequal load transfer when cornering left or right.

5.6 Tyre Dynamic Load Distribution

The frictional force required to transmit tractive or cornering forces is proportional to the vertical load on the tyre. For a given tyre and track, it follows that the greater the vertical load on the tyre, the more grip a vehicle will have. The role of the suspension system is therefore to optimally balance the loading at the respective tyre contact patches, while controlling the variation in tyre camber with suspension movement to ensure that the tyre contact patch pressure distribution is optimised [4].

Static versus dynamic load distribution results are shown in Chapter 4, where a static load transfer of up to 16Kg was measured due to steering castor and KPI angles (Figure 50). Dynamic load transfer was measured by comparing the average tyre temperatures and displaying them as a percentage of the total temperature of the tyres, in order to find the portion of the load (proportional to tyre temperature) carried by each tyre.

Figure 51 shows the variation in load distribution with time, providing some insight into the dynamic load transfer occurring in the vehicle on the track. With four wheeled vehicles, load distribution is typically split diagonally, similar to a table rocking on the two longest legs, and Figure 51 bears this out, as the front left and rear right tyres were loaded higher (diagonally across from one another) than the front right and rear left tyres. Turning into a corner enhances this effect, due to the castor and KPI angles of the steering, which tend to lift the inside front wheel in a corner.

5.7 GPS Track Data

Initial GPS data tests on the Celso Scribante Short Circuit were conducted driving at race pace, however an analysis of the data proved to be difficult due to the inaccuracy of the GPS data (Figure 52). The small track combined with the high speed of the vehicle, and the relatively low sampling rate of the sensor (10Hz) produced gaps in the GPS data which made it difficult to plot the track accurately.

A GPS reference lap was then recorded to more accurately plot the co-ordinates of the track, by driving slowly (<10km/h) around the circuit. The results, as shown in Figure 53, were far more accurate, and formed the basis of future testing.

One of the features of the MoTec i2 software is the ability to overlay data channels, including vehicle performance data versus GPS track data. These plots allowed the analysis of vehicle speed or lateral acceleration at various points on the track and could be used to assess driver performance, or track analysis. The maximum speed and maximum lateral acceleration points for the track could therefore be determined for future reference.

5.8 Research Conclusion

The main research problem, stated at the beginning of this research study was to develop an objective and repeatable measurement system, which could provide the required data to make reliable inferences regarding the shortcomings of a particular vehicle suspension setup, and provide guidance for potential improvements. The aforementioned results and discussion clearly show that dynamic tyre temperature measurement is a useful and reliable tool for use in the suspension setup of a racing vehicle.

Tyre operating temperatures were determined, along with camber and tyre pressure settings, based on recorded tyre temperature data. In addition, the G-G boundary, understeer gradient, tyre dynamic load distribution and GPS data were analysed for DibaOne providing the basis for enhancing overall vehicle dynamic performance. A summary of the significant research outcomes is shown in Table 10 below.

Tyre Temperatures	
Tyre warm-up time	**3.51min**
Tyre operating temperature	**43.04°C**
Camber/Castor	
Front wheel camber angle	**-1.5°**
Steering castor angle	**3°**
Tyre Pressures	
Tyre pressure increase from cold to hot	**10KPa**
Tyre operating pressure - hot	**80KPa**
Tyre operating pressure - cold	**70KPa**
G-G Diagram	
Maximum lateral acceleration	**1.8G**
Maximum longitudinal acceleration	**0.6G**
Maximum decelleration	**1.4G**
Weight Distribution	
Static weight transfer @ 24° steering angle	**16Kg**

Table 10: Research Result Datasheet for DibaOne

The research hypothesis for this study stated that tyre temperatures could be used to determine the optimum suspension setting for a race vehicle, and the above research outcomes proved this hypothesis to be true.

5.9 Opportunities for Future Research

This research study served to open a new chapter of research at the Nelson Mandela Metropolitan University, as it was the first study of its kind focussing on motor vehicle dynamics. It is the expressed wish of this researcher that this study will inspire and motivate future students to embark on automotive related research due to its relevance to our university and local automotive industry cluster.

The modular nature of the research equipment employed in this study provides opportunities for future research in this field, as the test equipment used can be transferred to future Formula Student vehicles for further vehicle dynamic research. This equipment can provide the backbone for future related research projects, requiring dynamic vehicle performance measurement.

Future research opportunities, expanding on the experience gained in this study, include the following topics:

- Researching additional variables affecting suspension dynamic performance, such as wheel toe and caster settings, anti-roll stiffness front and rear, spring rates, bump and rebound damping settings.

- Measuring force inputs into suspension by applying strain gauges to critical suspension components in order to accurately measure force inputs. This data would be useful to better design and simulate new components in this application.
- Researching the correlation of MSC Adams simulation results with real world testing of vehicle dynamics to enhance the accuracy and usability of vehicle simulation results.
- Researching the correlation of computational fluid dynamics analysis of aerodynamics using appropriate software to vehicle testing, for optimisation of down-force versus aerodynamic drag.
- Researching the enhancement of vehicle dynamic performance of an electrically-powered formula student vehicle.

6. References

[1] 2011 Formula SAE Rules. SAE International. 2010.

[2] Formulastudent.de. [Homepage]. Pat's Corner: Car Setup. [cited 15 November 2009]. Available from: http://www.formulastudent.de/academy/pats-corner/advice-details/article/pats-column-car-set-up

[3] Milliken WF. Race car vehicle dynamics. Warrendale, Pa.: SAE International. 1995.

[4] Rouelle C. Vehicle Dynamics and Data Acquisition Seminar. Cologne Germany. 14-16 November 2010.

[5] Nunney M J. Light and heavy vehicle technology. Oxford : Butterworth-Heinemann. 2007.

[6] Smith C. Tune to win. Fallbrook California: Aero Publishers. 1978.

[7] Pashley T. How To Build Motorcycle Engined Race Cars. Veloche Publishing. 2008

[8] Pacejka HB. Tyre and Vehicle Dynamics. 2nd ed. Butterworth-Heinemann. 2006.

[9] Information about Continental's Formula Student / Formula SAE tire. 2011

[10] About MD Adams 2011. MD Adams 2011 Products. 2010

[11] Scarborough C. Focus Thermal Imaging Cameras Case Study. Racetechmag. 2009

[12] Conant F., Hall G., and Walter J. Surface Temperature of Running Tires Using Infrared Scanning. SAE Technical Paper 700475. 1970

[13] Trivisonno N. Thermal Analysis of a Rolling Tire. SAE Technical Paper 700474. 1970

[14] Longacreracing.com [Homepage]. [cited 26 September 2012]. Available from http://www.longacreracing.com

[15] MoTeC Pty Ltd. MoTeC ADL3/EDL3 User Manual. V 1.1 May 2009

[16] Texense.com [Homepage]. [cited 26 September 2012]. Available from http://www.texense.com

Appendix A: 2011 Continental Formula Student Tyre

The Continental Formula Student tyre for 2011 had a new carcass construction which provided:

- Better handling due to increased responsiveness and precision
- Better braking & traction performance on track, increased tangential stiffness
- Most efficient use of the new tread compound, noticeable by longer stability on the rear axle

New tread compound provides:

- Lower optimum working temperature, leading to:
- Higher grip with cold tire temperatures
- Faster warm-up, especially on colder days
- Reduced overheating on hot days in the endurance counteracted by the new carcass construction

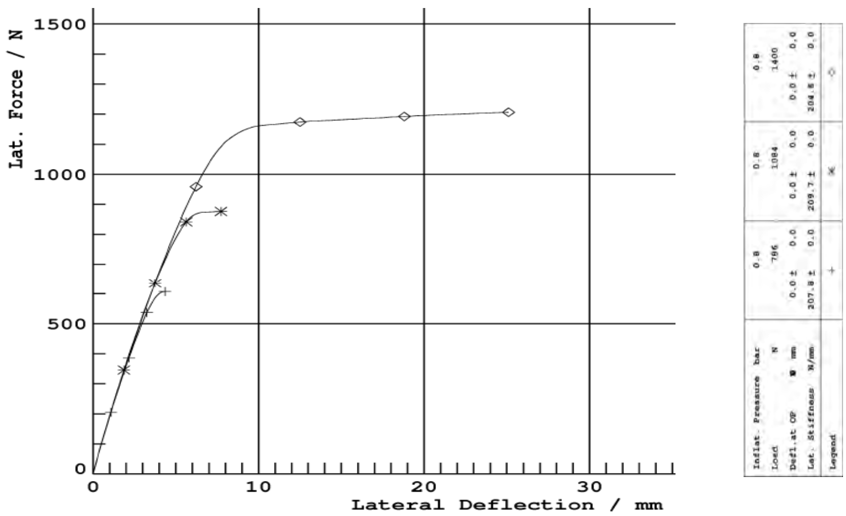

Figure 54: Continental Formula Student Tyre Lateral Spring Stiffness

Source: Information about Continental‘s Formula Student / Formula SAE tire. 2011 [9]

The lateral stiffness of the tyre provides an indication of tyre flex under cornering loads. Figure 54 above indicates a linear stiffness up to 1100N of sideways force with a vertical tyre load of 1400N. Lateral stiffness therefore varies from 204 to 209 N/mm depending on the vertical load applied.

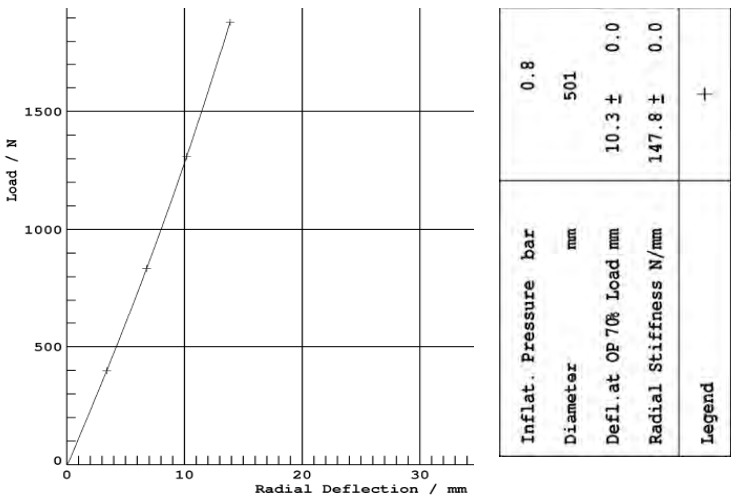

Figure 55: Continental Formula Student Tyre Radial Spring Stiffness

Source: Information about Continental's Formula Student / Formula SAE tire. 2011 [9]

Radial spring stiffness indicates the amount of tyre flex under vertical loads, and as shown in Figure 55 above, a radial stiffness of 147N/mm was measured. This means that with a static load of around 600N per tyre when the car is stationary, it will deflect around 4mm when inflated to 0.8bar. Actual tyre loads vary greatly as load is transferred during cornering, and much higher loads will be experienced.

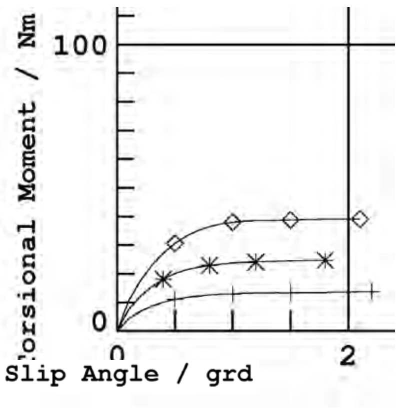

Inflat. Pressure bar	0.8	0.8	0.8
Load N	805	1103	1402
Slip Ang.at Nm0 grd	0.0 ± 0.0	0.0 ± 0.0	0.0 ± 0.0
Tors.Stiffness Nm/grd	36.4 ± 0.0	64.6 ± 0.0	93.9 ± 0.0
Legend	+	✳	◇

Figure 56: Continental Formula Student Tyre Torsional Stiffness

Source: Information about Continental's Formula Student / Formula SAE tire. 2011 [9]

Torsional stiffness, as shown in Figure 56 above, is the tyre's resistance to twist, as in the case of steering the front wheels when the car is stationary. The torsional stiffness also affects the tyre's dynamic slip angle, as a lower torsional stiffness will result in higher slip angles.

Appendix B: Formula Student Vehicle Design Priorities

In terms of vehicle design priorities, the experience of testing and racing the first formula student vehicle resulted in significant changes to key specifications on the next generation vehicle. The focus shifted from basic reliability, to more ambitious performance-based objectives. The following design priorities were established in the design of DibaTwo:

- Light weight
- Low centre of gravity
- Improved aerodynamics and styling
- Better and more balanced handling
- Better ergonomics
- More efficient electronics
- Improved fuel efficiency
- More professional design
- Competitive with top Formula Student teams
- Introduction of renewable materials and electric powertrain

Appendix C: Optimum K Simulation Results for DibaOne

Simulations performed using Optimum K software provided insights into the kinematic performance of DibaOne's suspension. Of particular interest for this study were the camber variation graphs for heave and roll conditions (Figure 57 and 58), showing for example that 30mm of suspension bump movement produced 0.8° of front camber change, and for 2° of roll the front wheel camber changed by 1.5°.

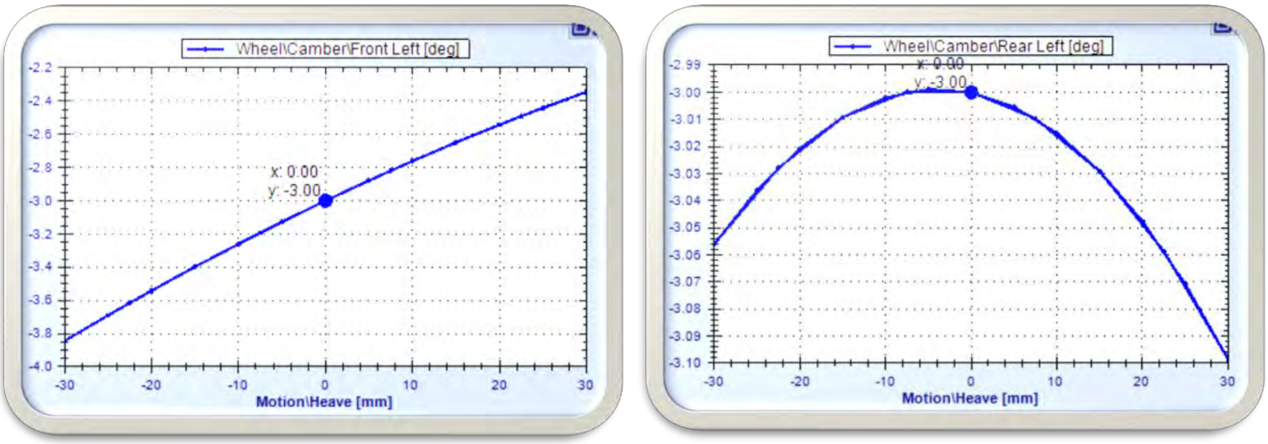

Figure 57: Camber Variation in Heave

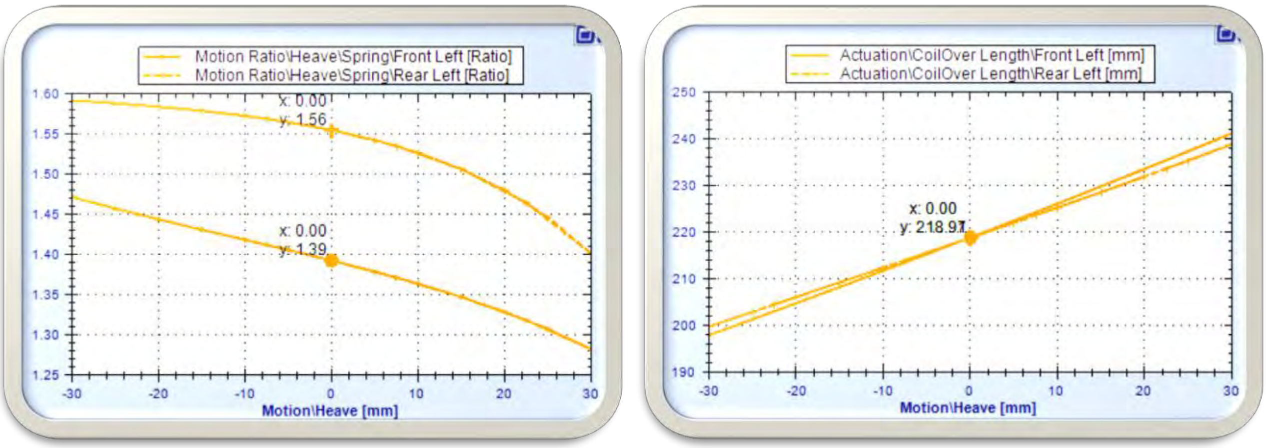

Figure 58: Shock Damper Movement in Heave

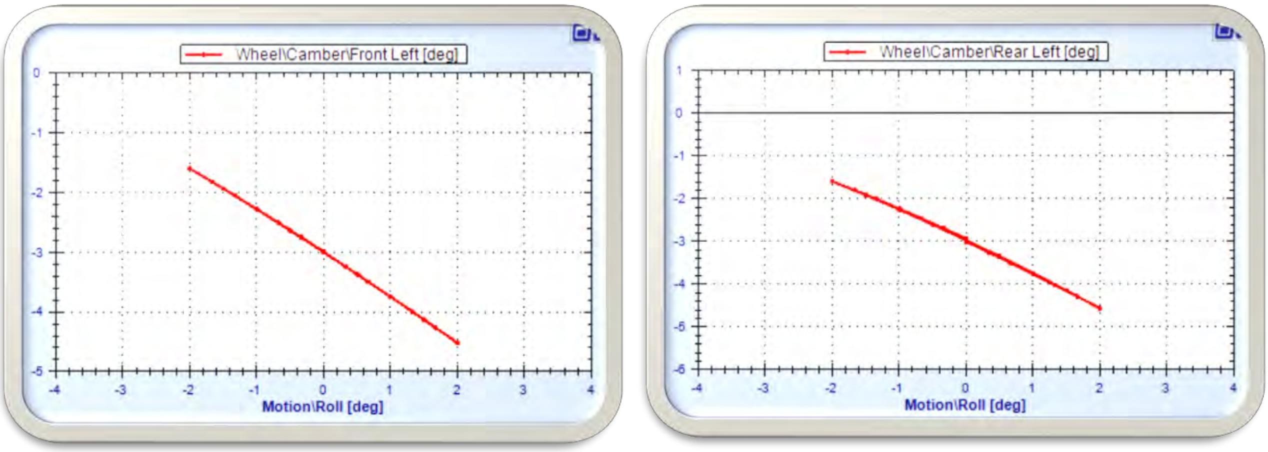

Figure 59: Camber Variation with Roll

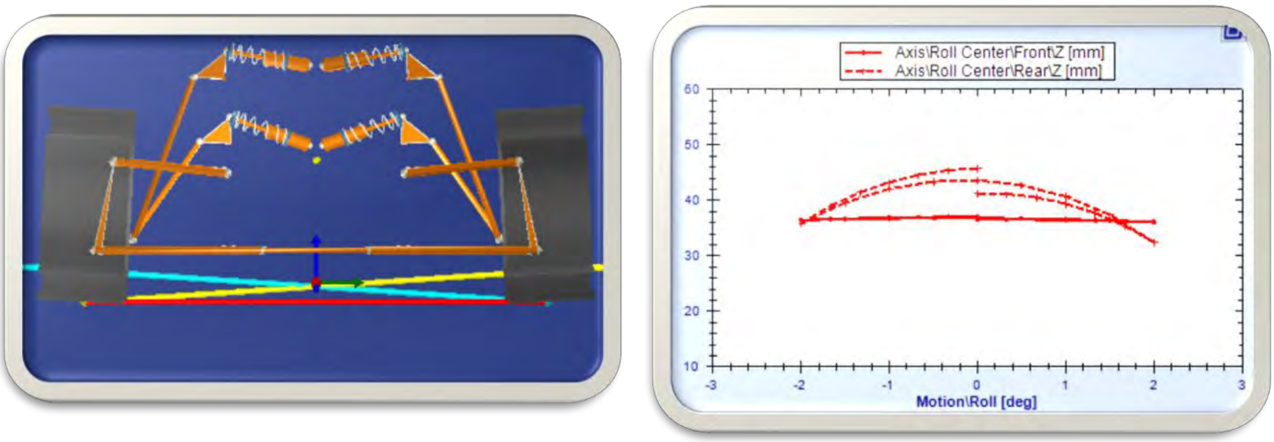

Figure 60: Roll Centre Height

Appendix D: Tyre Warm-Up Temperature Test Data

The graphs shown below in Figure 61 to 66 illustrate the results of the six tyre warm-up tests conducted on DibaOne. As previously explained, data analysis was restricted to the two front tyres, and a smoothed curve for each tyre temperature channel is shown in the upper window of the graph. The “Tyre Temp FL Avg” and “Tyre Temp FR Avg” channels were each calculated by averaging the three temperature sensor readings (inner, centre and outer) of the tyre. The lower window shows a calculated average between the front left and right tyre average temperatures, as well as the track surface temperature. For each window, the MoTec I2 software shows the lowest, highest and average temperatures in the top right hand side, for the displayed graph. The vertical axis is measured in °C and the horizontal axis in seconds.

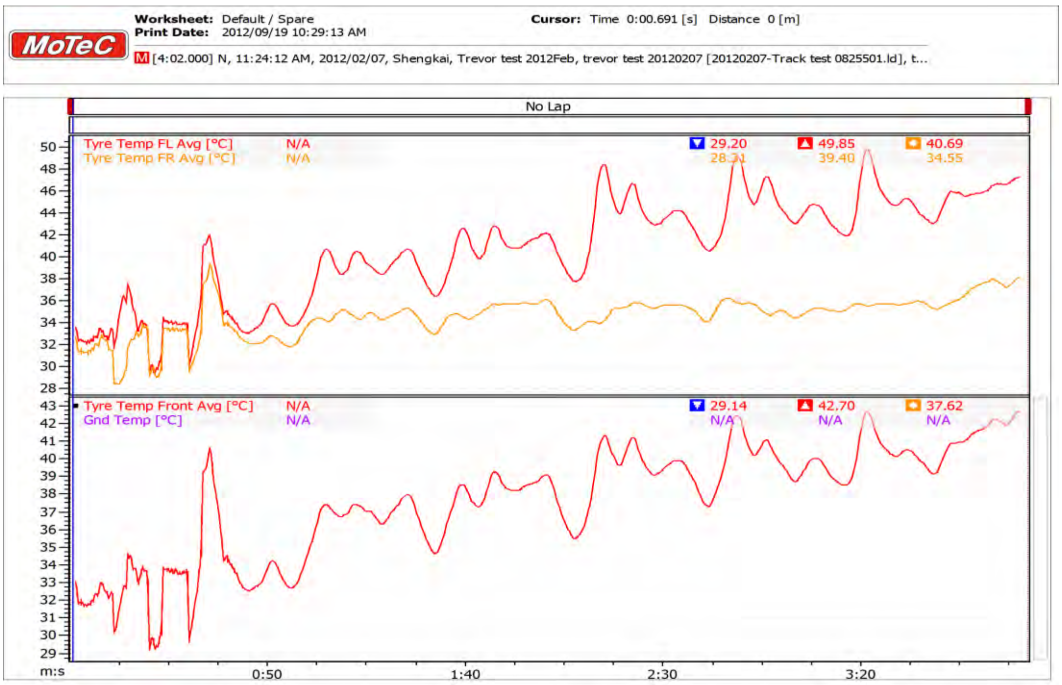

Figure 61: Tyre Warm-up Test 1

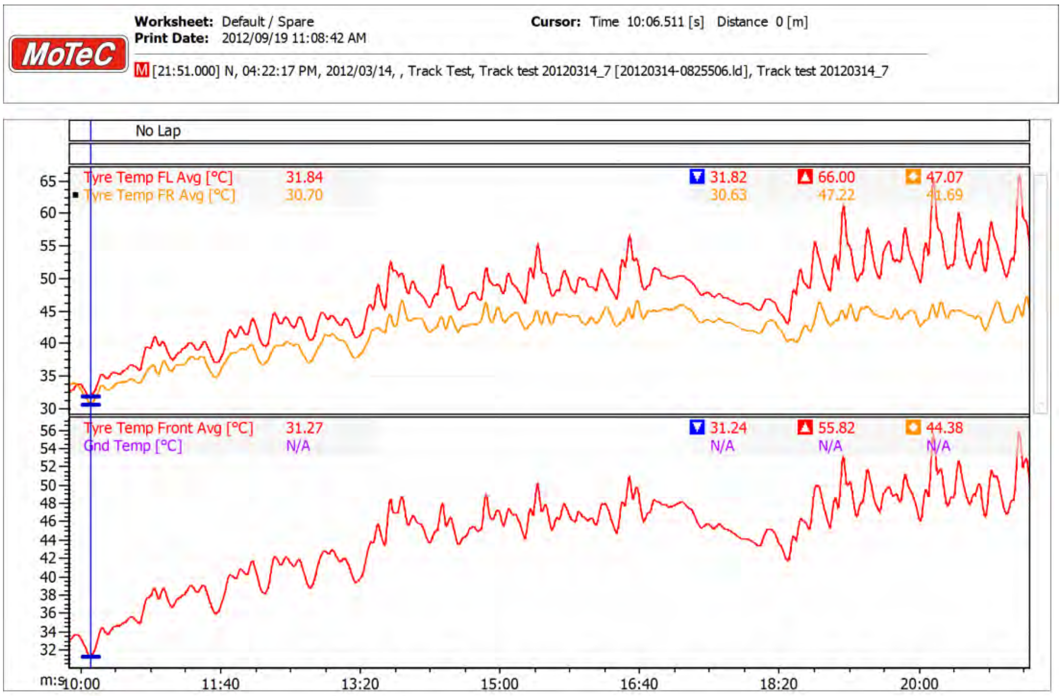

Figure 62: Tyre Warm-up Test 2

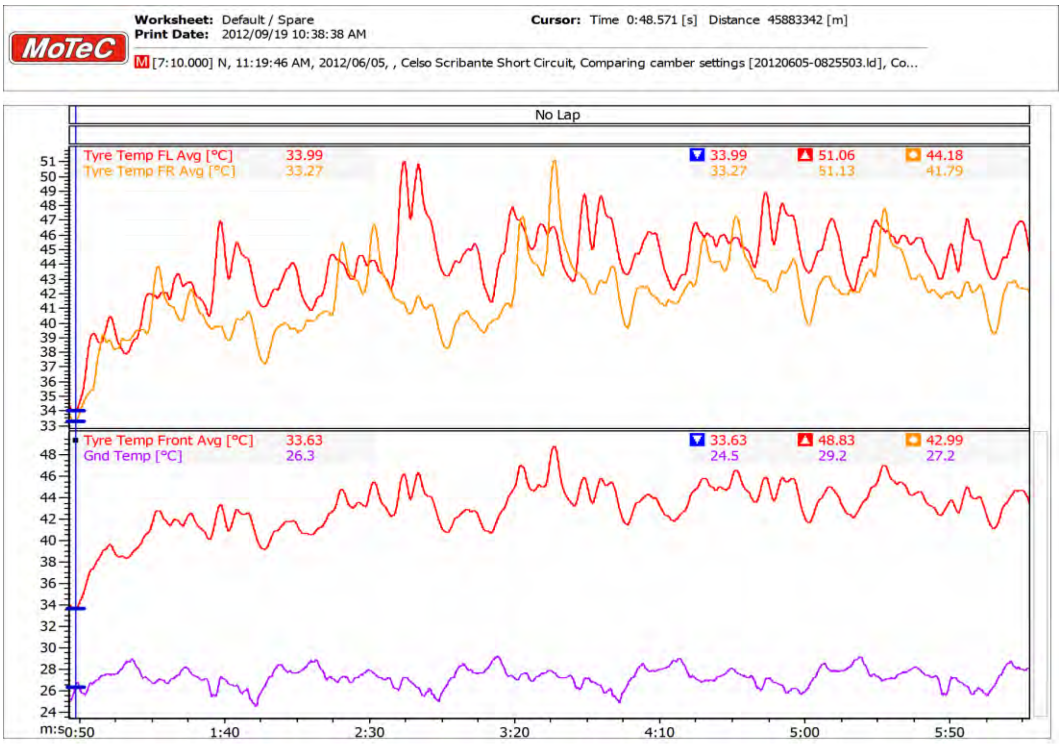

Figure 63: Tyre Warm-up Test 3

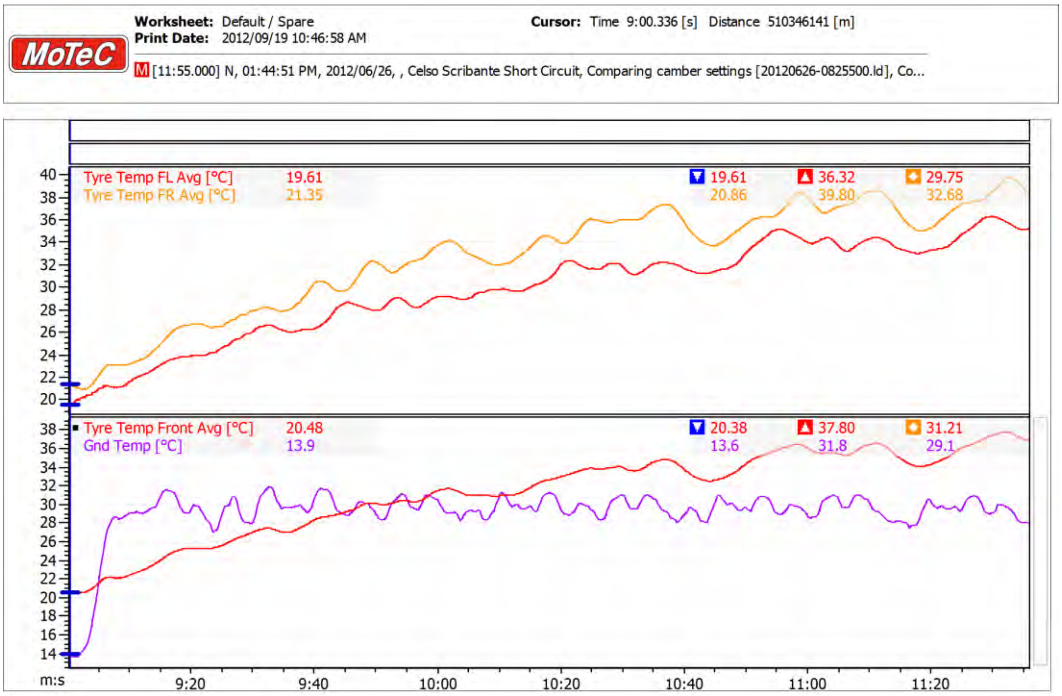

Figure 64: Tyre Warm-up Test 4

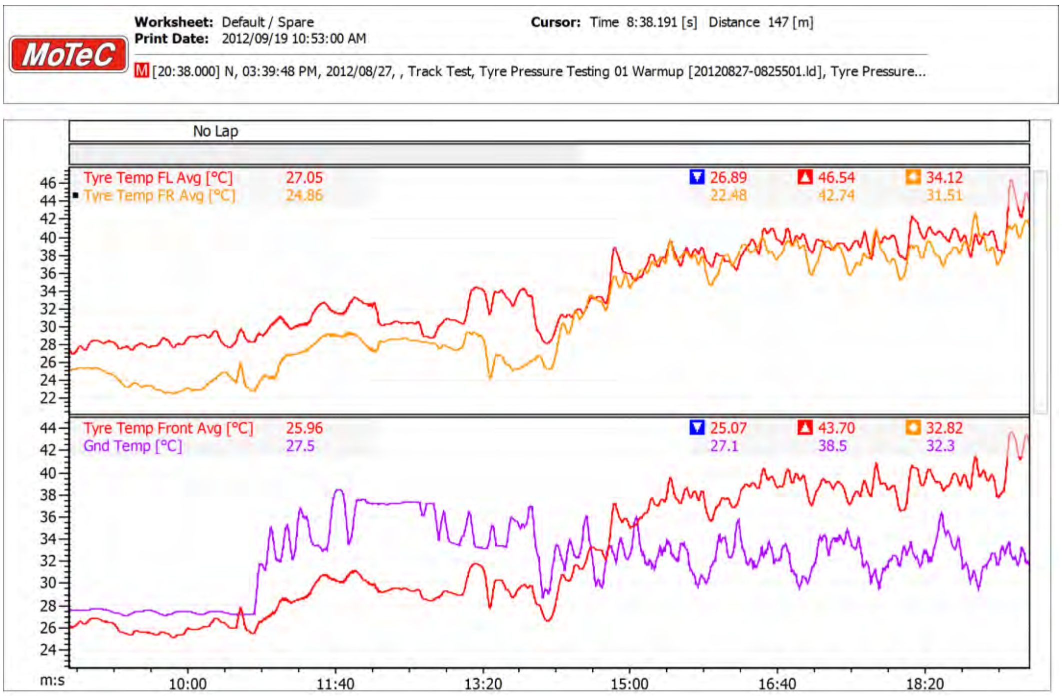

Figure 65: Tyre Warm-up Test 5

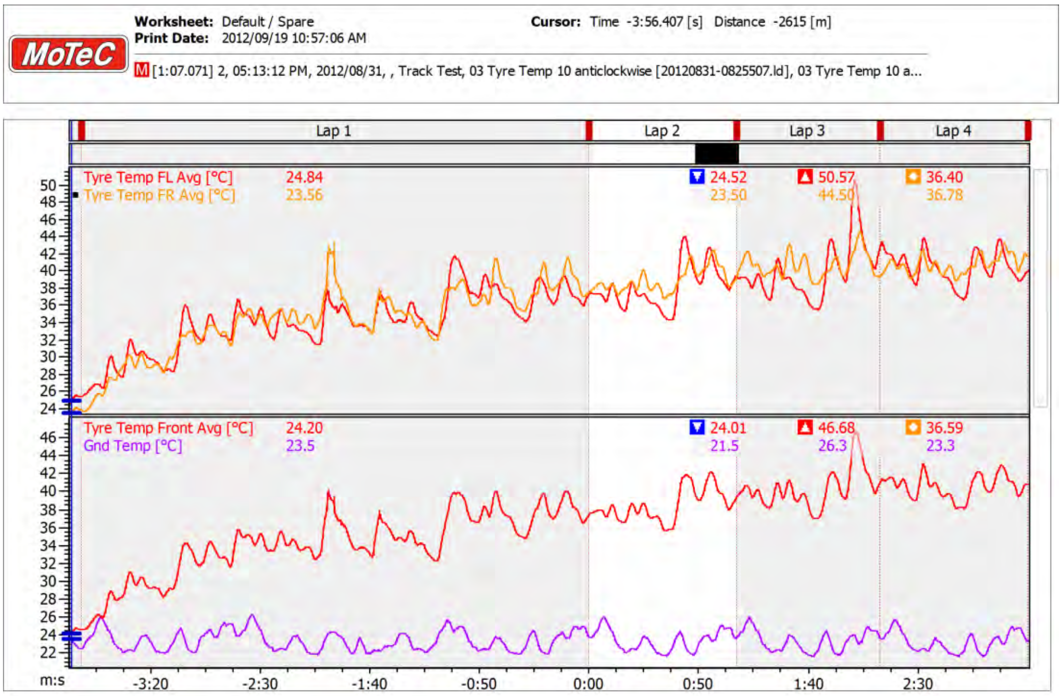

Figure 66: Tyre Warm-up Test 6

Appendix E: Tyre Operating Temperature Test Data

The graphs shown below in Figure 67 to 72 illustrate the results of the six tyre operating temperature tests conducted on DibaOne. As previously explained, data analysis was restricted to the two front tyres, and a smoothed curve for each tyre temperature channel is shown in the upper window of the graph. The “Tyre Temp FL Avg” and “Tyre Temp FR Avg” channels were each calculated by averaging the three temperature sensor readings (inner, centre and outer) of the tyre. The lower window shows a calculated average between the front left and right tyre average temperatures, as well as the track surface temperature. For each window, the MoTec I2 software shows the lowest, highest and average temperatures in the top right hand side, for the displayed graph. The vertical axis is measured in °C and the horizontal axis in seconds.

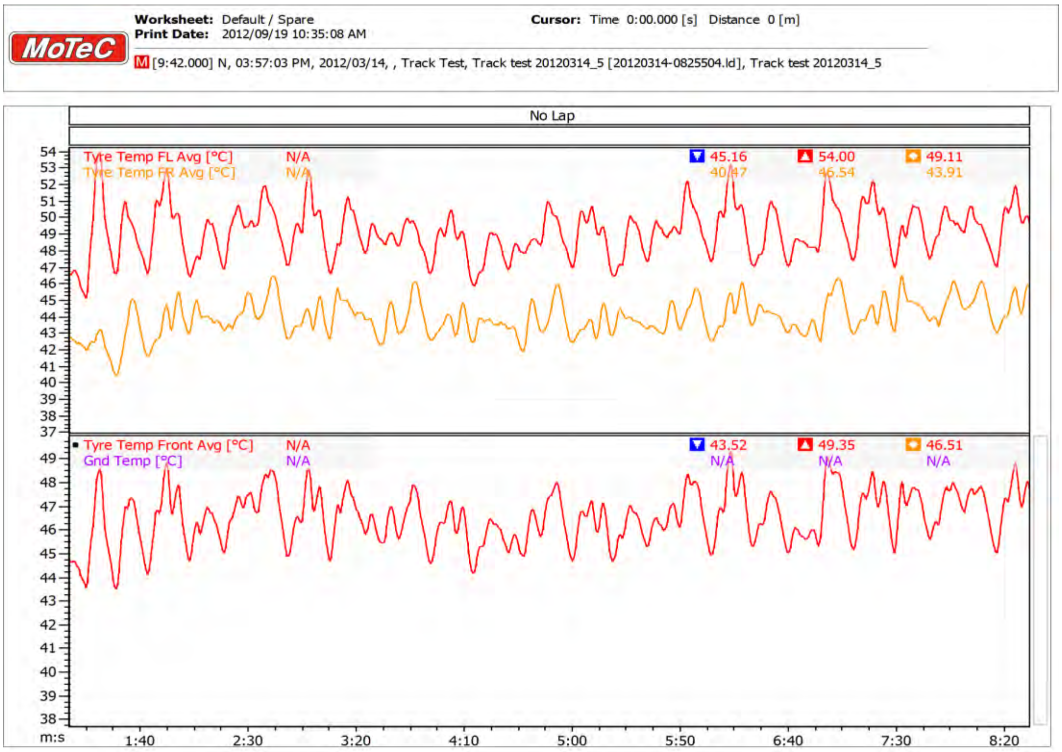

Figure 67: Tyre Operating Temperature Test 1

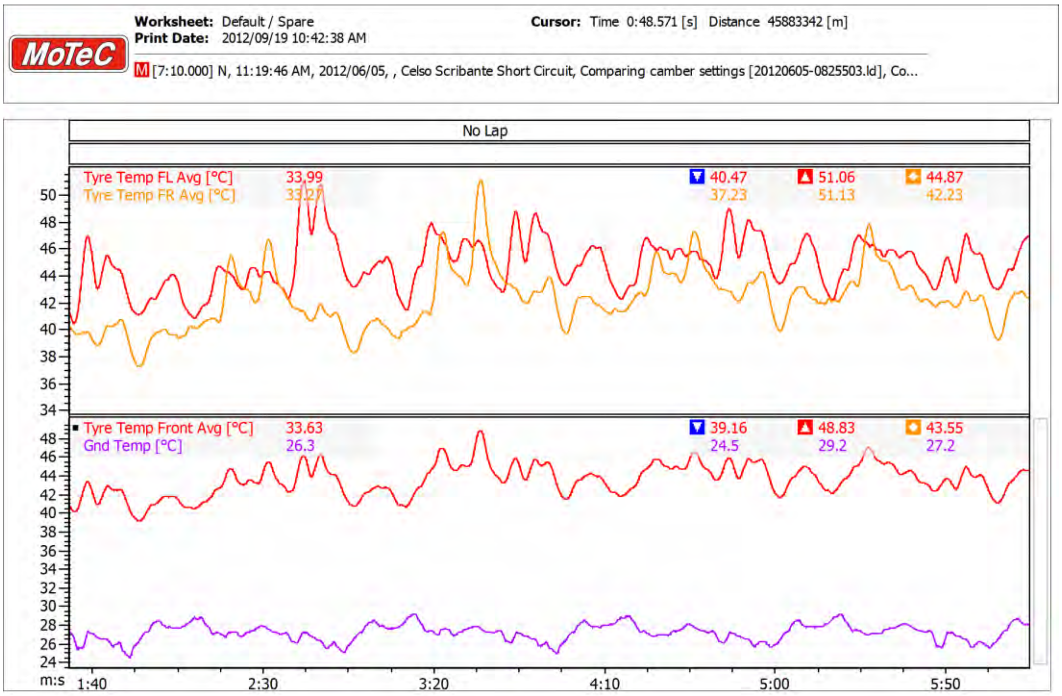

Figure 68: Tyre Operating Temperature Test 2

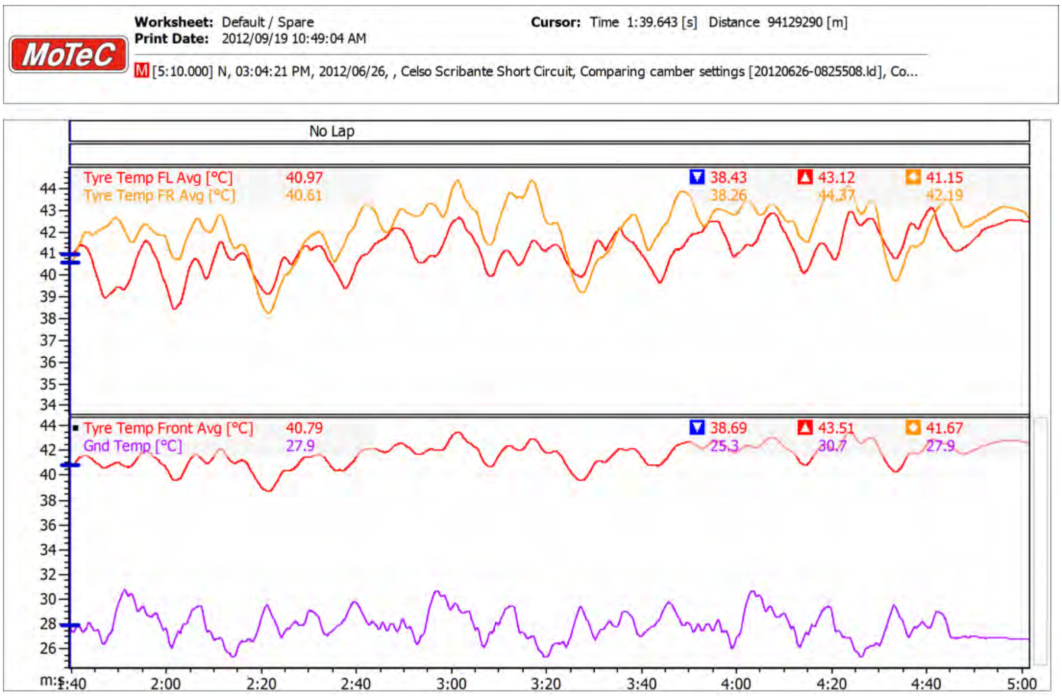

Figure 69: Tyre Operating Temperature Test 3

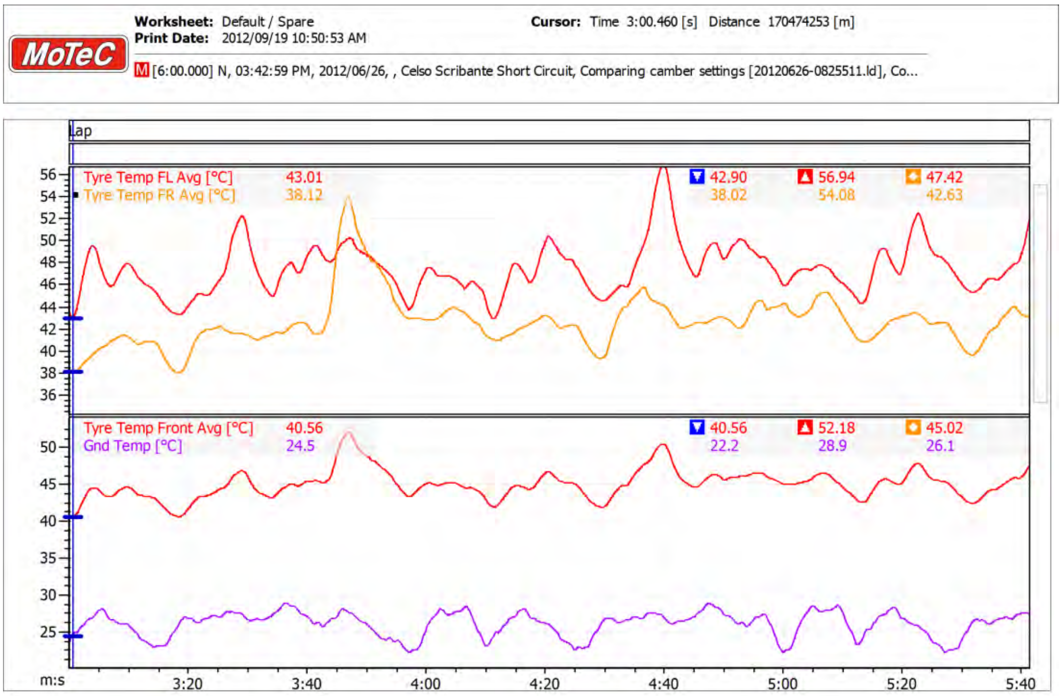

Figure 70: Tyre Operating Temperature Test 4

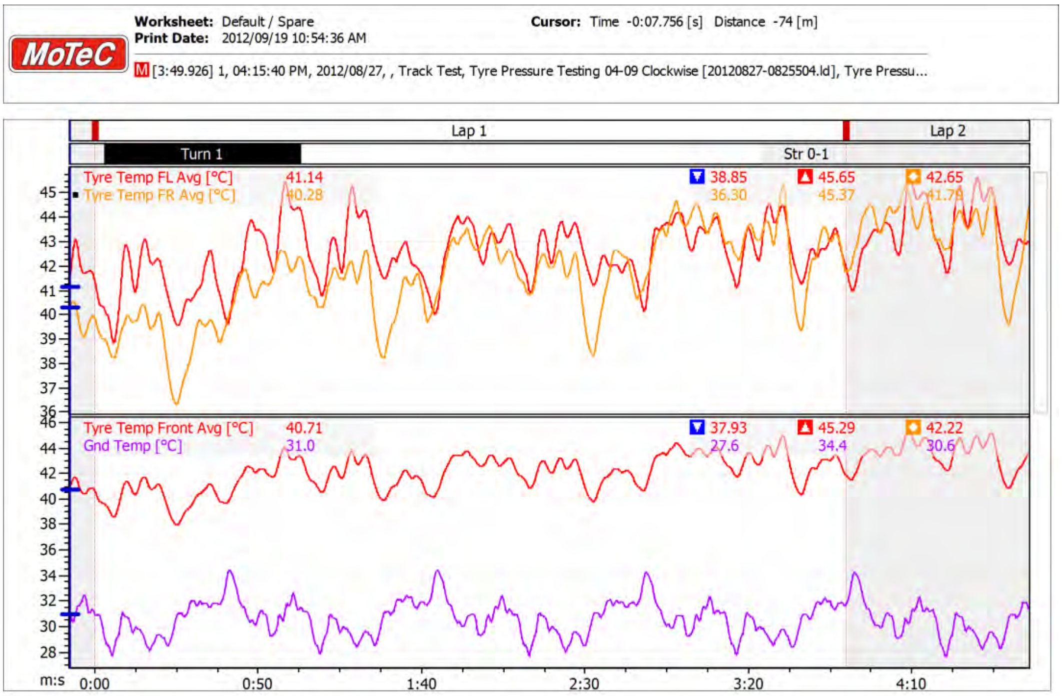

Figure 71: Tyre Operating Temperature Test 5

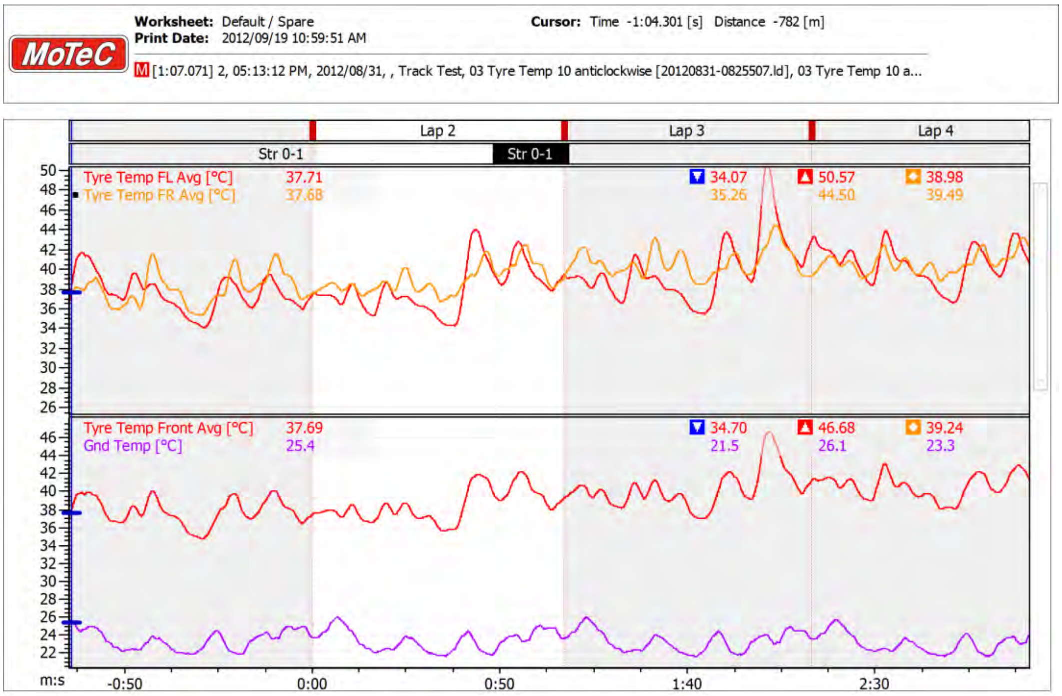

Figure 72: Tyre Operating Temperature Test 6

Appendix F: Vehicle Setup Datasheet for Wheel Camber Test

Figure 73 below shows the setup parameters for DibaOne used during the wheel camber tests. All parameters reflected on this datasheet were kept constant during the test, except for the adjustment of front wheel camber angle.

NMMU Racing Setup and Testing Record

Date	20-Jun-12		
Test Objective	Tyre temperatures vs front wheel camber		
Test Location	Celso Scribante Short Circuit		
Weather conditions	Good	Driver	
Test Responsibility	Trevor Stroud	Driver Weight	

LH Front	Front	RH Front
Camber **-1.0° to -3.0°**	Ride Height **145mm**	Camber **-1.0° to -3.0°**
Castor **3.3°**	Springs **200**	Castor **2.7°**
Toe **-4.7° (out)**	Damper Setting - Bump **14 clicks**	Toe **-4.3° (out)**
Corner Weight **90.0 Kg**	Damper Setting - Rebound	Corner Weight **92.0 Kg**
Tyre Pressure **80KPa**	Anti-Roll Bar **Fitted**	Tyre Pressure **80KPa**

LH Rear	Rear	LH Rear
Camber **-0.8°**	Ride Height **150mm**	Camber **-0.5°**
Toe **3.1° (in)**	Springs **400**	Toe **3.1° (in)**
Corner Weight **93.0 Kg**	Damper Setting - Bump **17 clicks**	Corner Weight **99.0 Kg**
Tyre Pressure **80KPa**	Damper Setting - Rebound	Tyre Pressure **80KPa**
	Anti-Roll Bar **Fitted**	
Overall Weight No Driver:	Front & Rear Sprockets	Overall Weight **374.0 Kg**

Figure 73: Setup and Test Record Sheet - Camber Test

Appendix G: Wheel Camber Test Data

The graphs shown below illustrate the results of the wheel camber tests conducted during round one and two on DibaOne. As previously explained, data analysis was restricted to the two front tyres, and a smoothed curve is shown for each tyre temperature channel. Three windows are shown, reflecting the front right tyre temperatures in the upper window, along with track surface temperature, the front left tyre temperatures in the middle window, and the tyre camber % indicator channels in the lower window. The tyre camber % indicator graph is calculated by finding the percentage difference between the inner and outer tyre temperature channels, and provides an indication of whether a tyre has too much or too little camber. A high positive percentage indicated too much positive camber, while a low negative percentage indicated too much negative camber. For each window, the MoTec I2 software shows the lowest, highest and average temperatures in the top right hand side, for the displayed graph. The vertical axis is measured in °C, except for the lower window which is measured in percent. The horizontal axis is measured in seconds.

Round one test data is shown in Figures 74 to 77, while round two test data is shown in Figures 78 to 85.

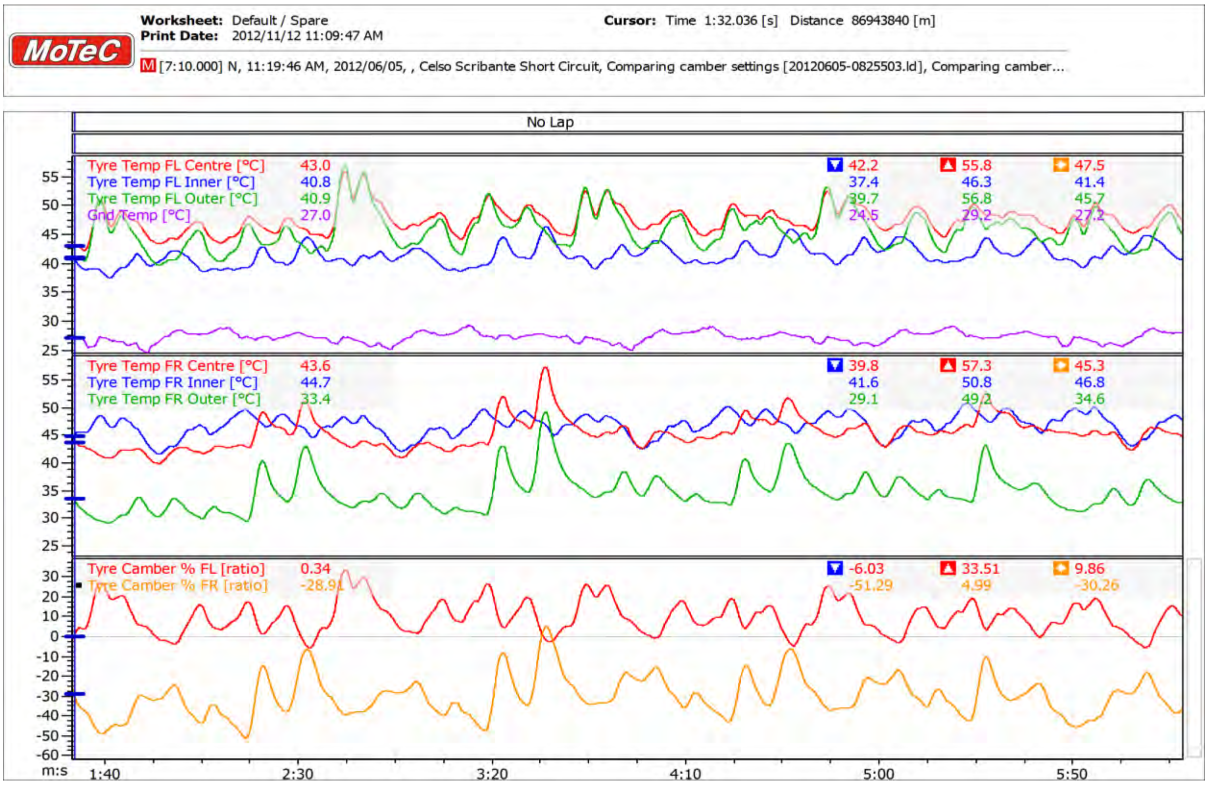

Figure 74: Camber Test Round 1, -1.2°(LH), -1.7°(RH) Camber, Clockwise Circuit

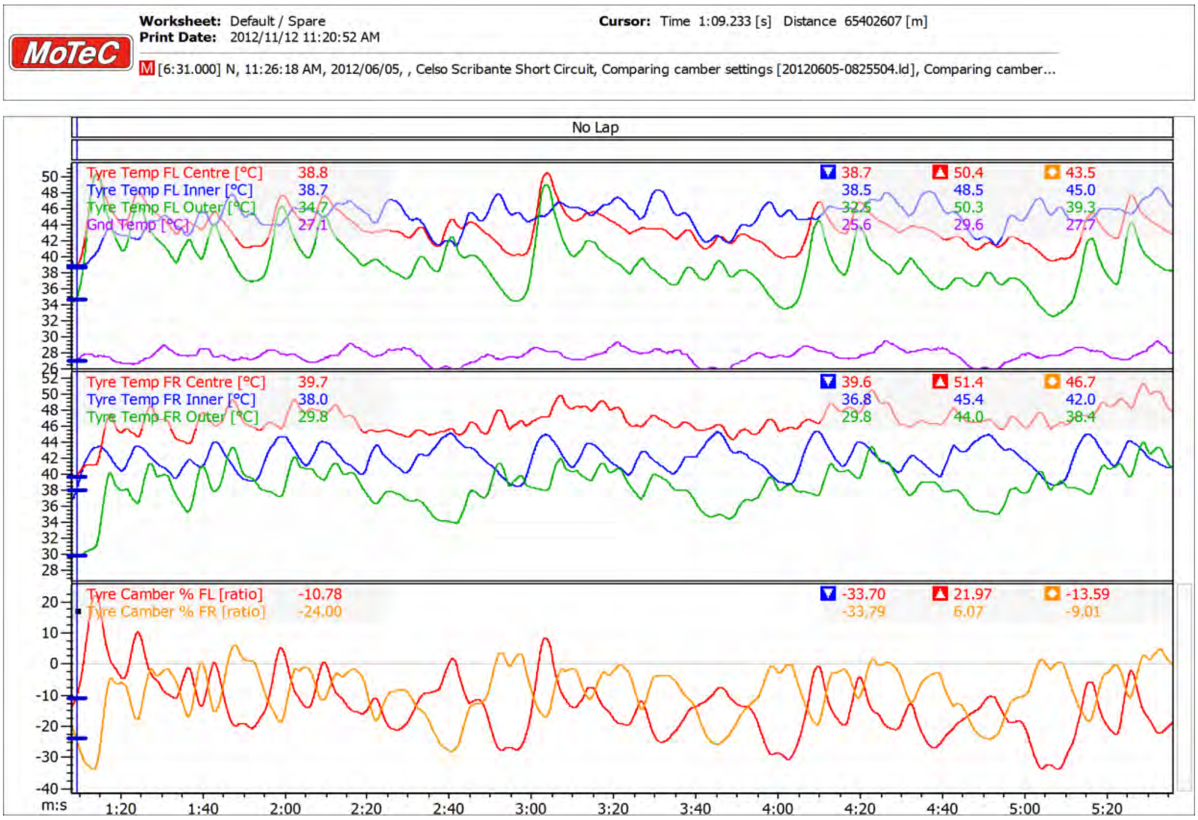

Figure 75: Camber Test Round 1, -1.2°(LH), -1.7°(RH) Camber, Anti-Clockwise Circuit

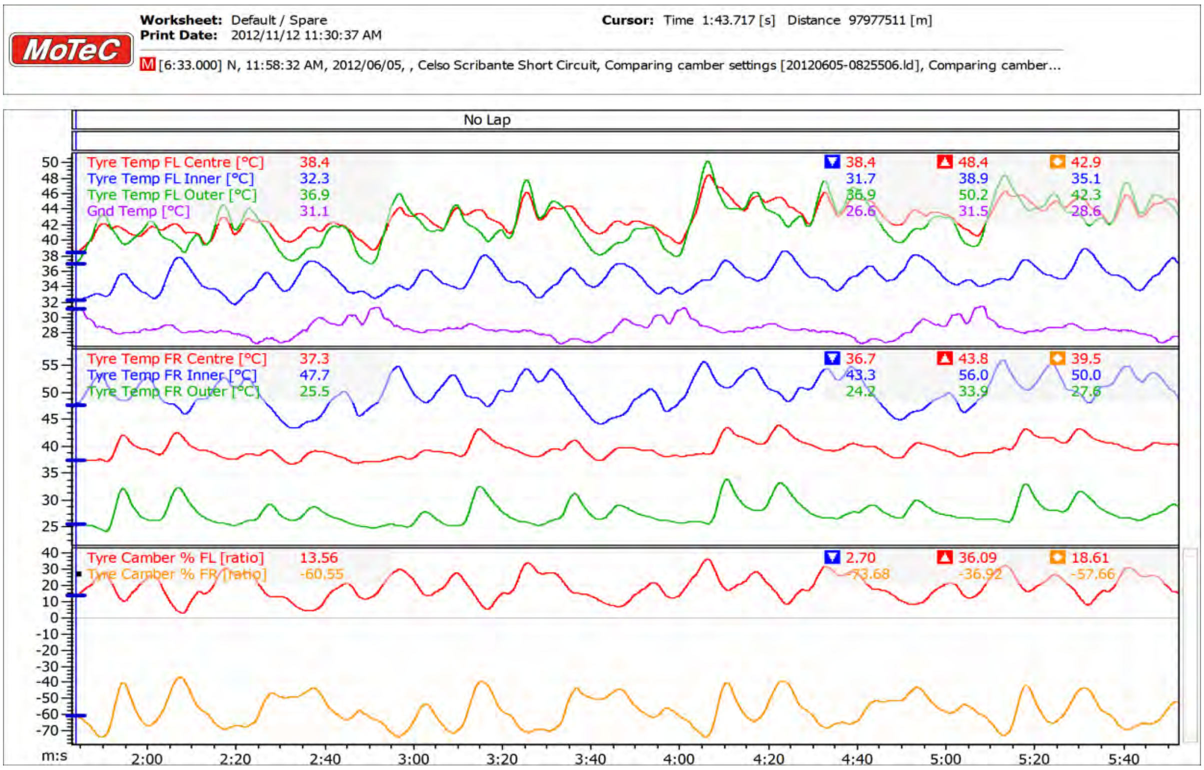

Figure 76: Camber Test Round 1, 0°(LH), -3.0°(RH) Camber, Clockwise Circuit

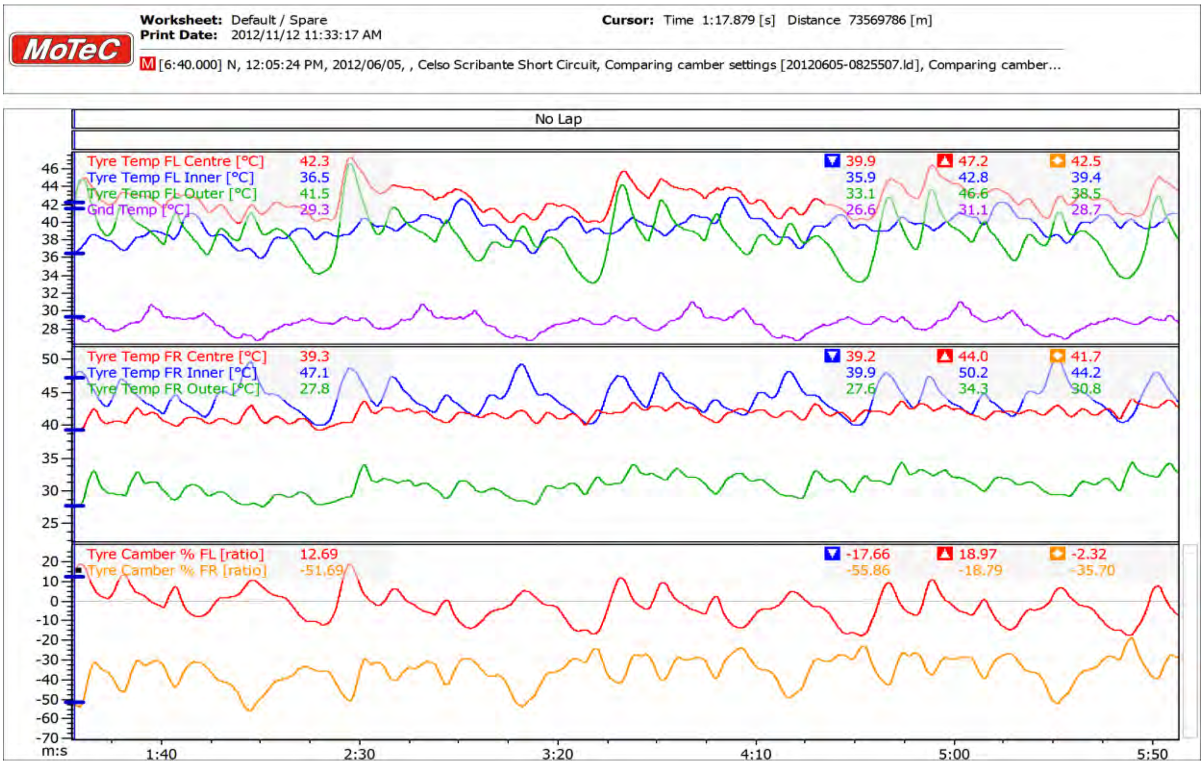

Figure 77: Camber Test Round 1, 0°(LH), -3.0°(RH) Camber, Anti-Clockwise Circuit

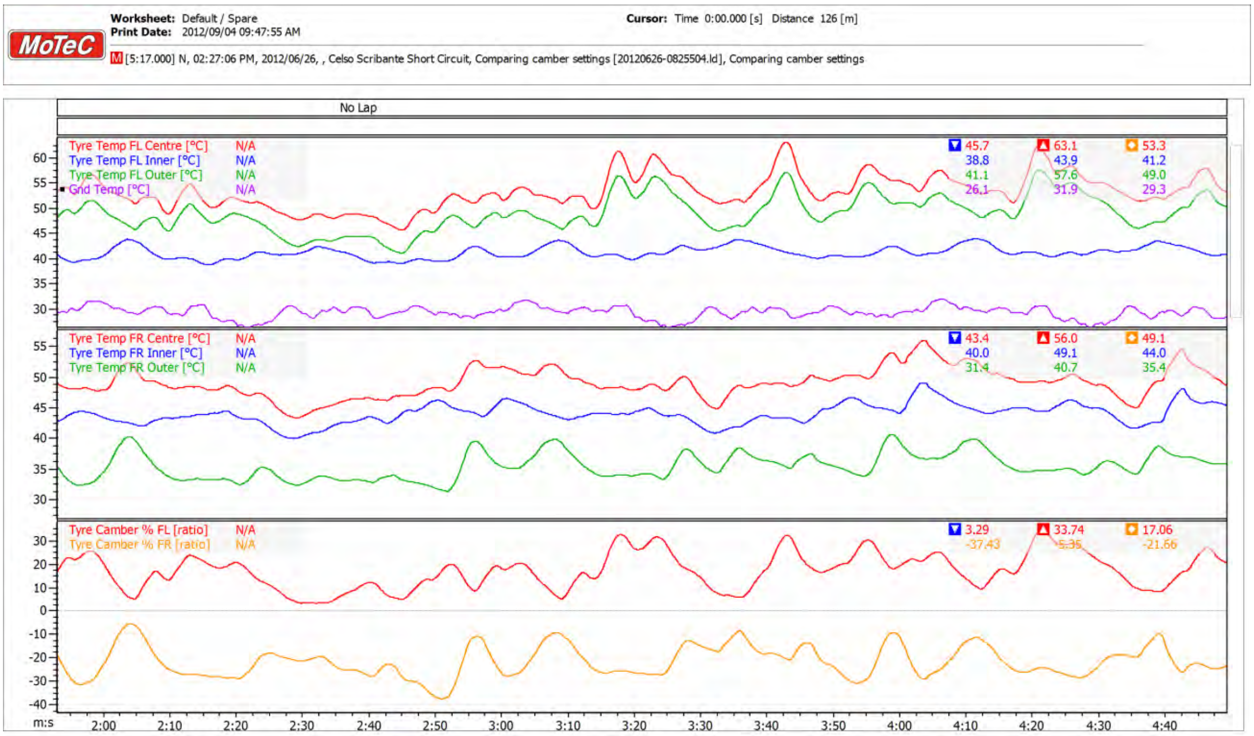

Figure 78: Camber Test Round 2, -1.5° Camber, Clockwise Circuit

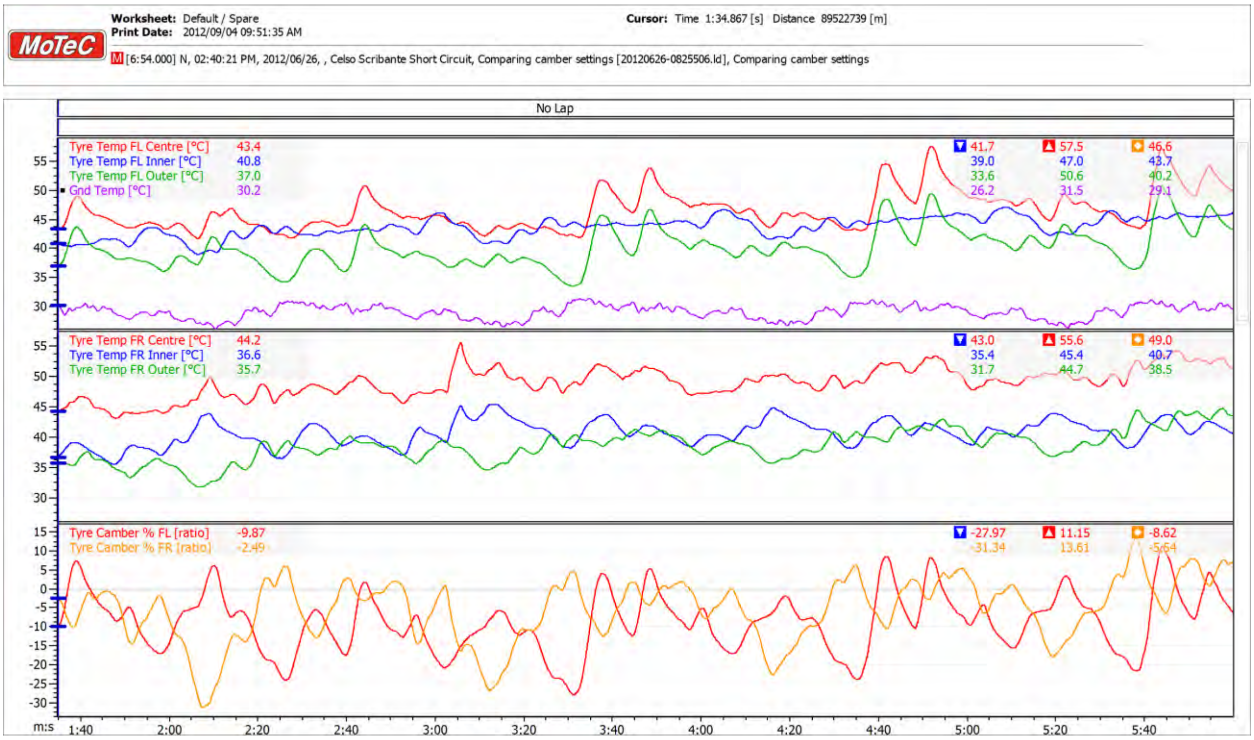

Figure 79: Camber Test Round 2, -1.5° Camber, Anti-Clockwise Circuit

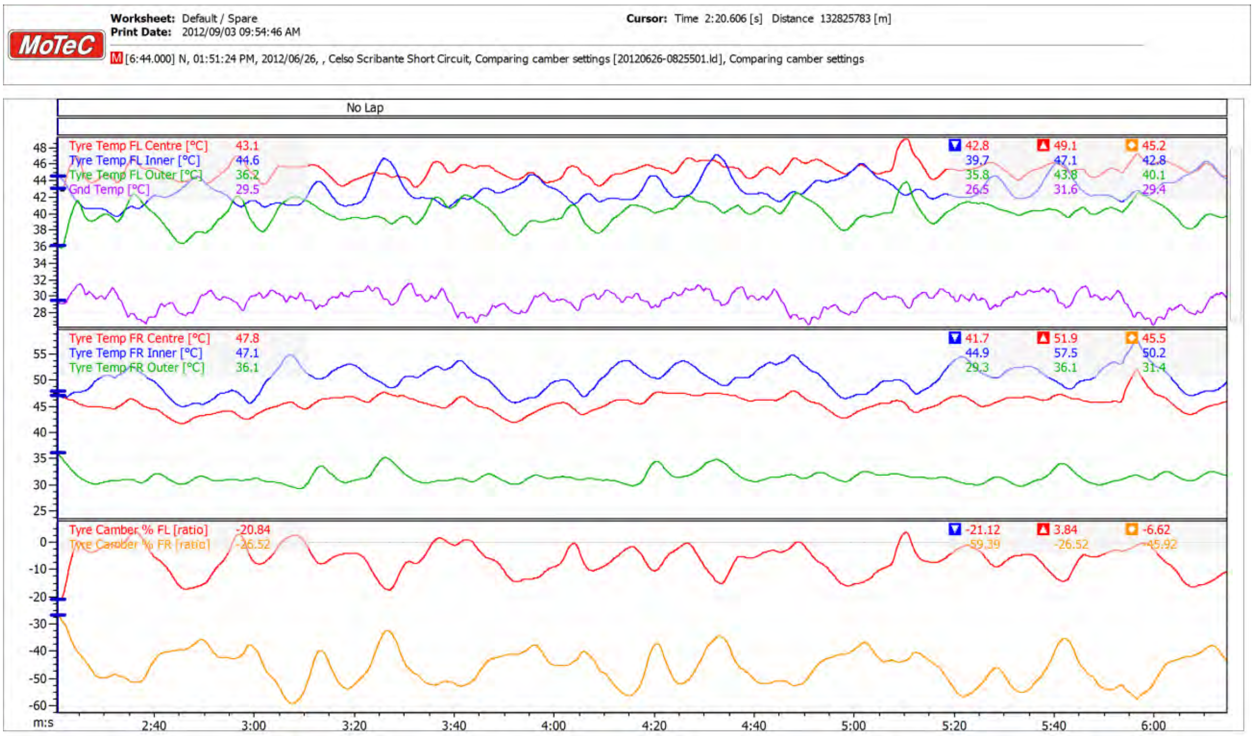

Figure 80: Camber Test Round 2, -2.0° Camber, Clockwise Circuit

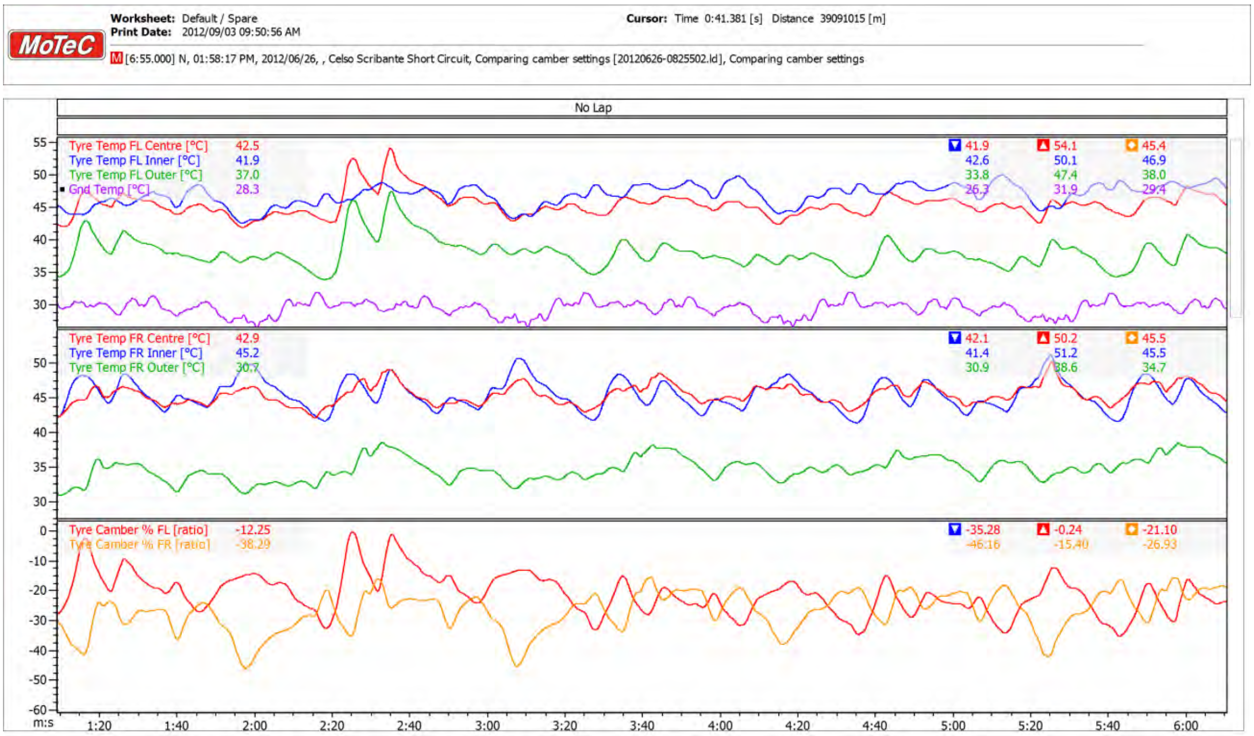

Figure 81: Camber Test Round 2, -2.0° Camber, Anti-Clockwise Circuit

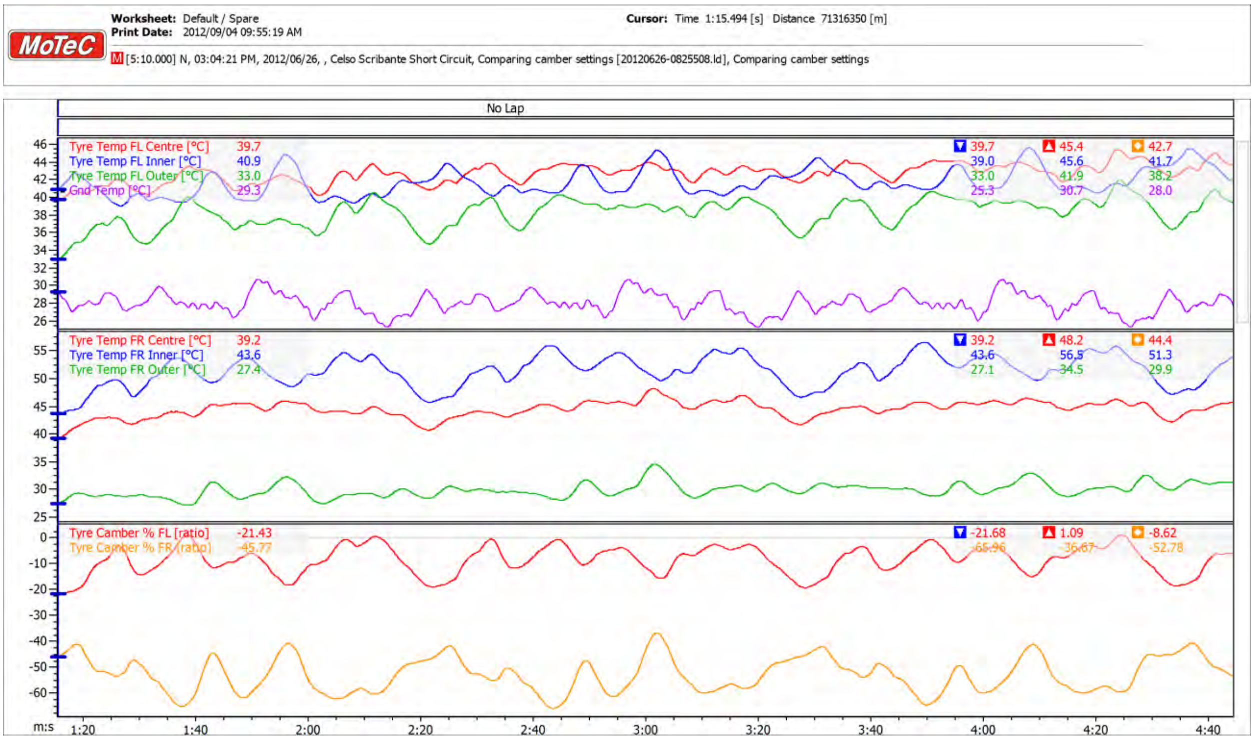

Figure 82: Camber Test Round 2, -2.5° Camber, Clockwise Circuit

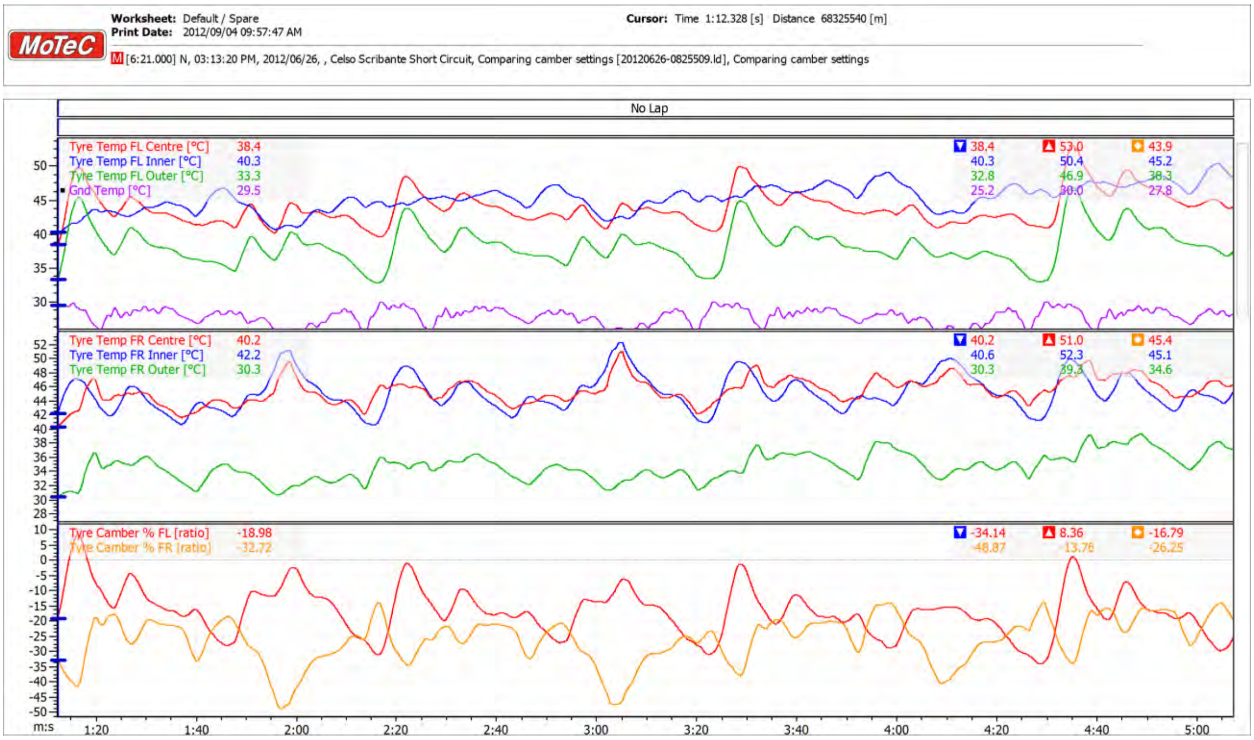

Figure 83: Camber Test Round 2, -2.5° Camber, Anti-Clockwise Circuit

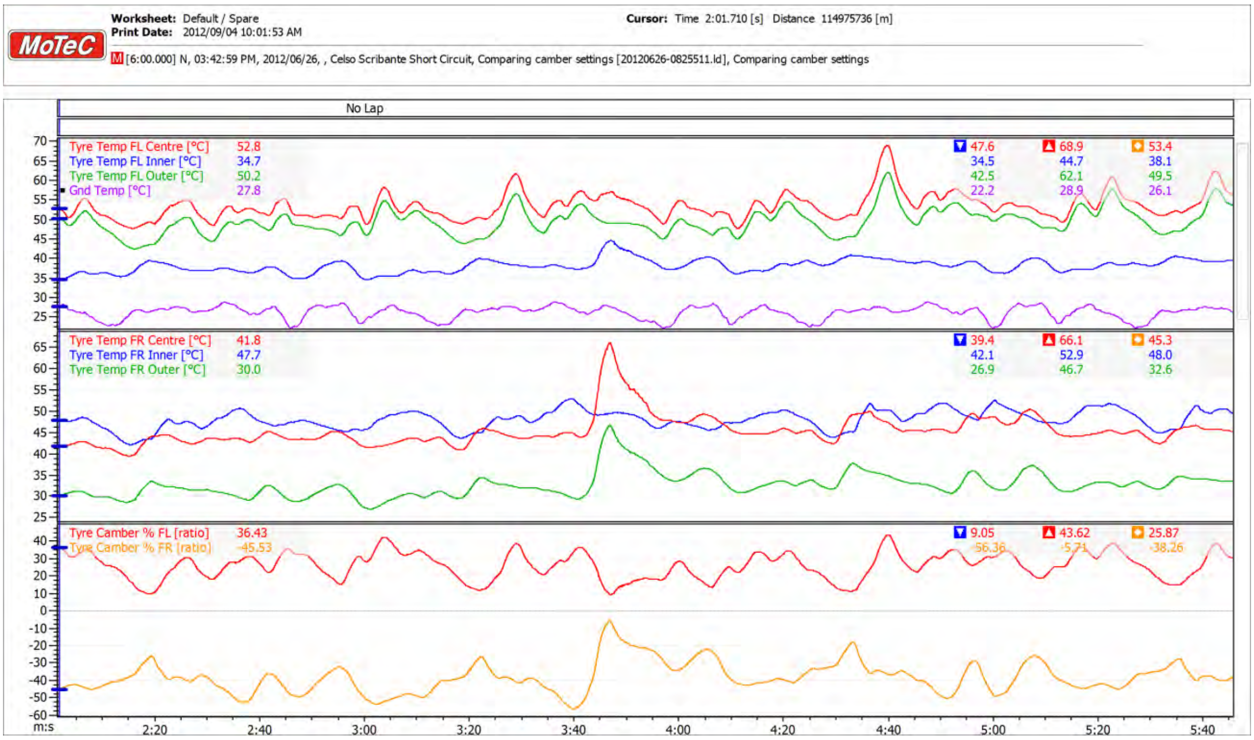

Figure 84: Camber Test Round 2, -1.0°(LH), -3.0°(RH) Camber, Clockwise Circuit

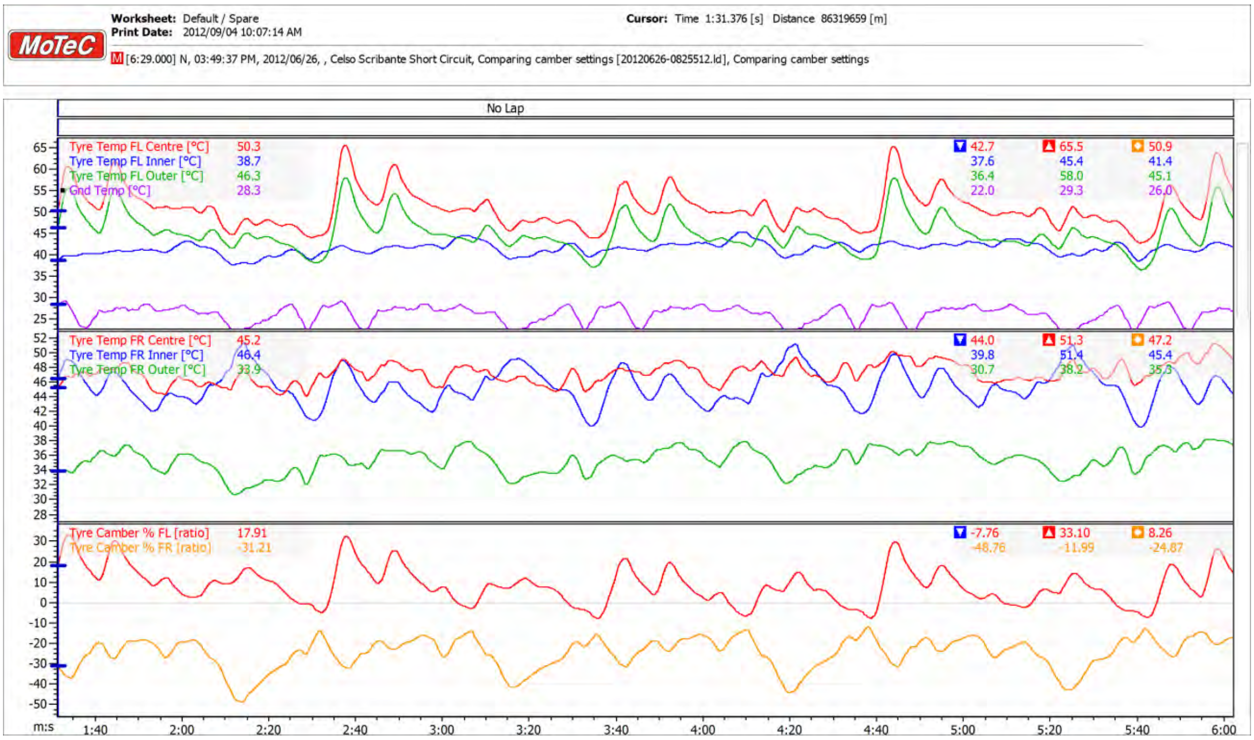

Figure 85: Camber Test Round 2, -1.0°(LH), -3.0°(RH) Camber, Anti-Clockwise Circuit

Appendix H: Vehicle Setup Datasheet for Tyre Pressure Test

Figure 86 below shows the setup parameters for DibaOne used during the tyre pressure tests. All parameters reflected on this datasheet were kept constant during the test, except for the adjustment of tyre pressures. Wheel camber was set -0.8° and all four tyre pressures were adjusted for this test.

NMMU Racing Setup and Testing Record

Date	06-Aug-12		
Test Objective	Tyre temperatures vs front wheel camber (no body)		
Test Location	Celso Scribante Short Circuit		
Weather conditions	Good	Driver	
Test Responsibility	Trevor Stroud	Driver Weight	

LH Front	Front	RH Front
Camber	Ride Height	Camber
-0.7°	**145mm**	**-0.8°**
Castor	Springs	Castor
3.3°	**200**	**2.7°**
Toe	Damper Setting - Bump	Toe
-4.7° (out)	**14 clicks**	**-4.3° (out)**
Corner Weight	Damper Setting - Rebound	Corner Weight
72.0 Kg		**73.0 Kg**
Tyre Pressure	Anti-Roll Bar	Tyre Pressure
60-100KPa	**Fitted**	**60-100KPa**

LH Rear	Rear	LH Rear
Camber	Ride Height	Camber
-0.8°	**150mm**	**-0.8°**
Toe	Springs	Toe
3.1° (in)	**400**	**3.1° (in)**
Corner Weight	Damper Setting - Bump	Corner Weight
93.0 Kg	**17 clicks**	**91.0 Kg**
Tyre Pressure	Damper Setting - Rebound	Tyre Pressure
60-100KPa		**60-100KPa**
	Anti-Roll Bar	
	Fitted	
Overall Weight	Front & Rear Sprockets	Overall Weight
No Driver:		**329.0 Kg**

Figure 86: Setup and Test Record Sheet – Tyre Pressure Test

Appendix I: Tyre Pressure Test Data

The graphs shown below illustrate the results of the tyre pressure tests conducted on DibaOne. All four tyre pressures were set for this test and tyre temperature data for all four tyres were measured. A smoothed curve is shown for each tyre temperature channel and the top two windows show the front tyre temperature detail.

The lower window shows the tyre pressure percentage channels, which were calculated by subtracting the centre tyre temperature channel from the average of the inner and outer channels, and converting to a percentage. These percentage channels give an indication of whether the tyre is over inflated (positive percentage value) or under inflated (negative percentage value). For each window, the MoTec I2 software shows the lowest, highest and average temperatures in the top right hand side, for the displayed graph. The vertical axis is measured in °C, except for the lower window which is measured in percent. The horizontal axis is measured in seconds.

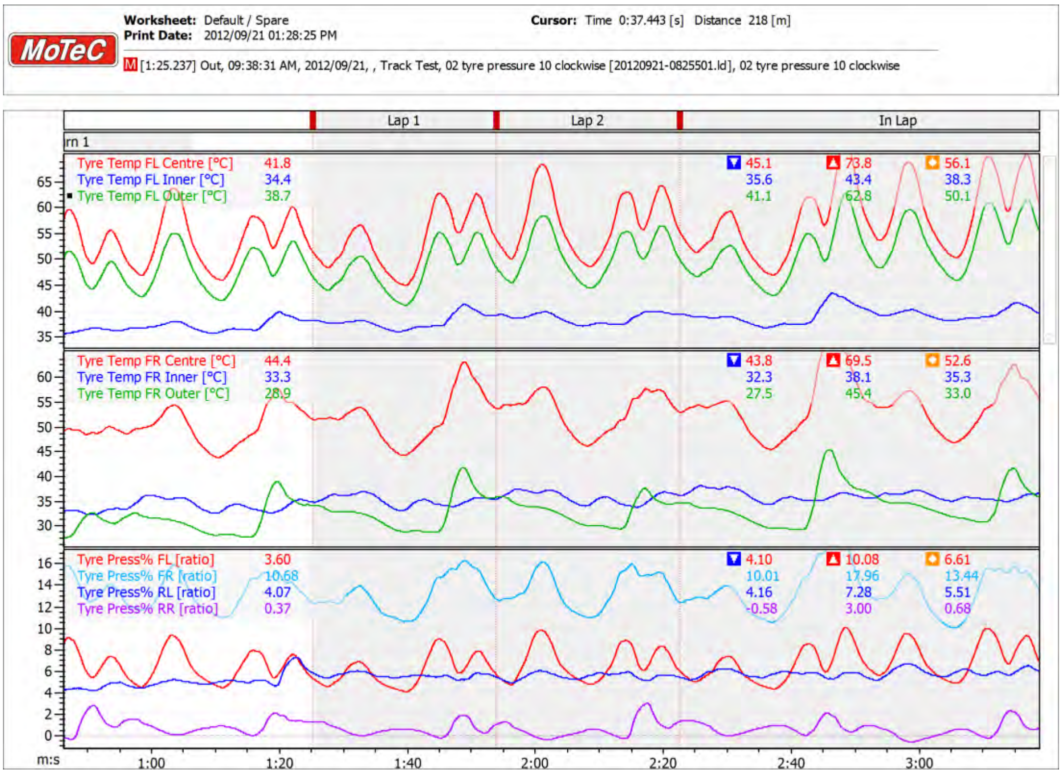

Figure 87: Pressure Test 100kPa Clockwise Circuit

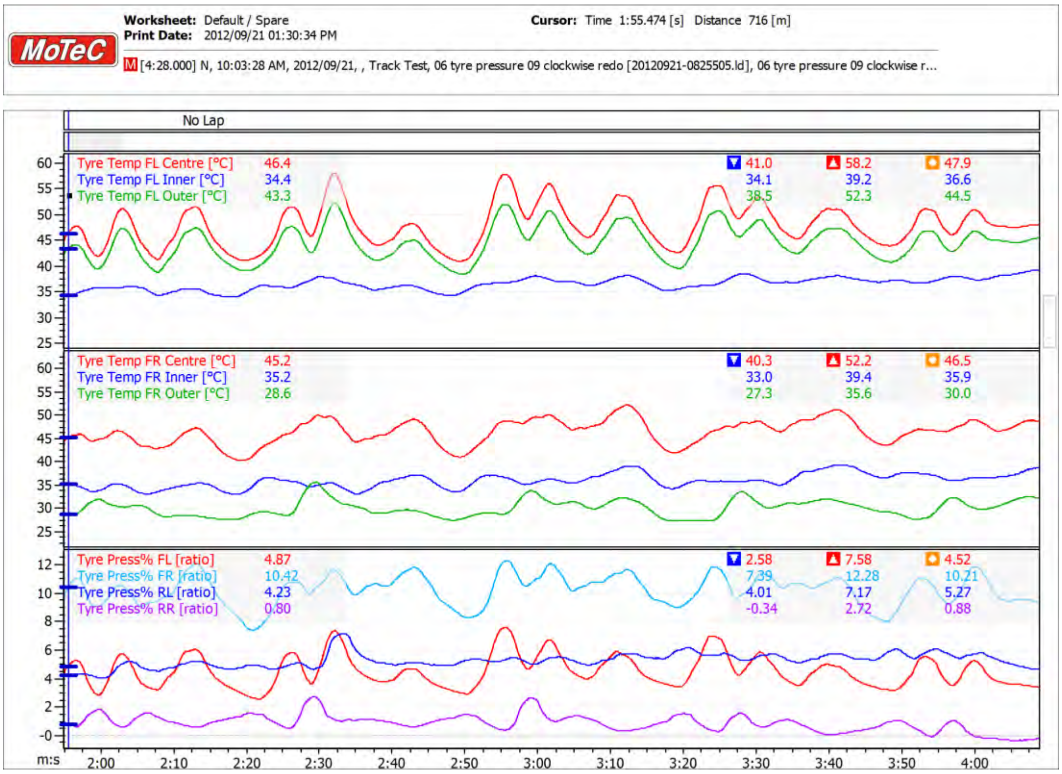

Figure 88: Pressure Test 90kPa Clockwise Circuit

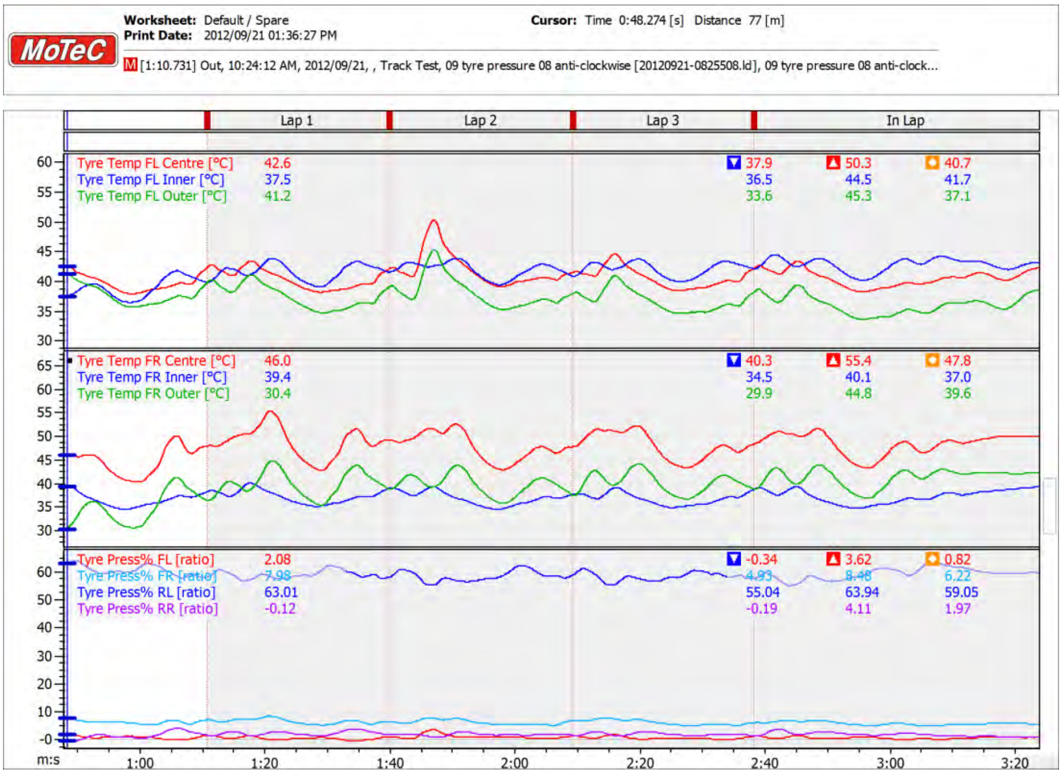

Figure 89: Pressure Test 80kPa Anti-Clockwise Circuit

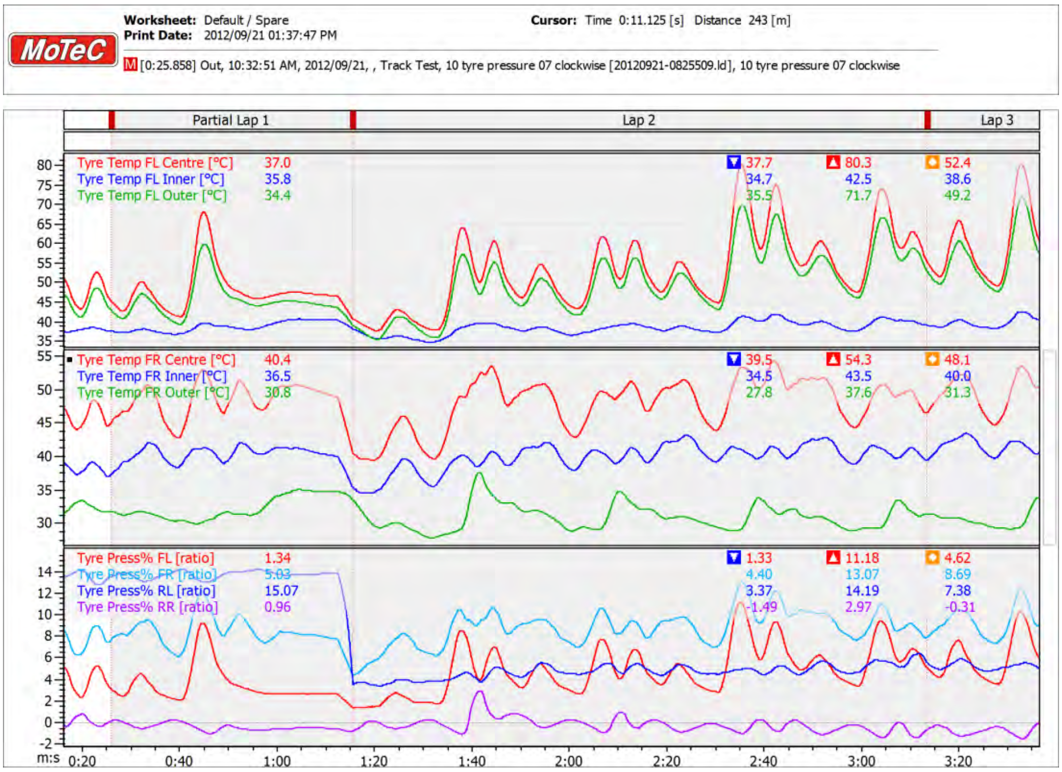

Figure 90: Pressure Test 70kPa Clockwise Circuit

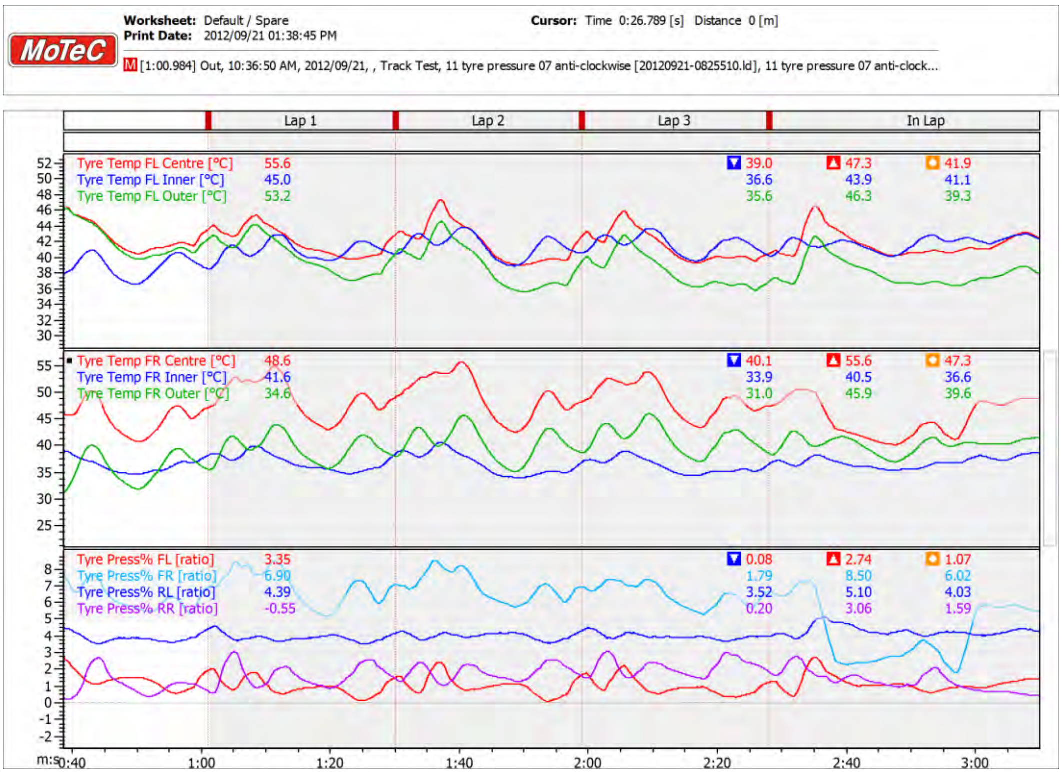

Figure 91: Pressure Test 70kPa Anti-Clockwise Circuit

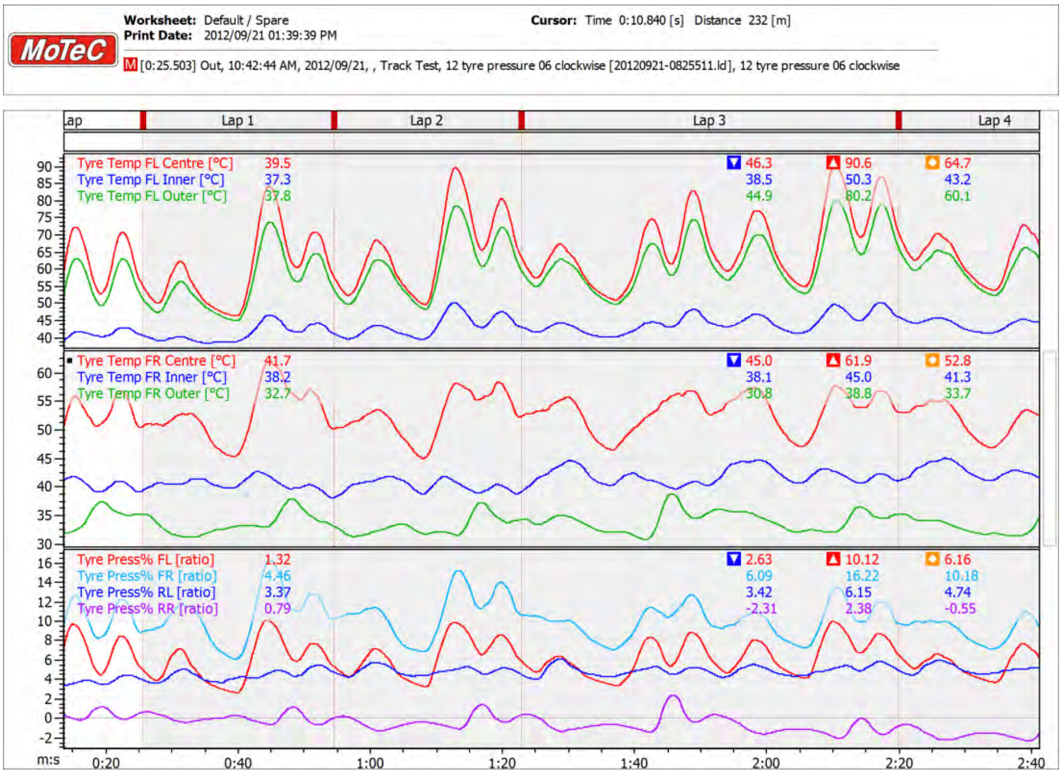

Figure 92: Pressure Test 60kPa Clockwise Circuit

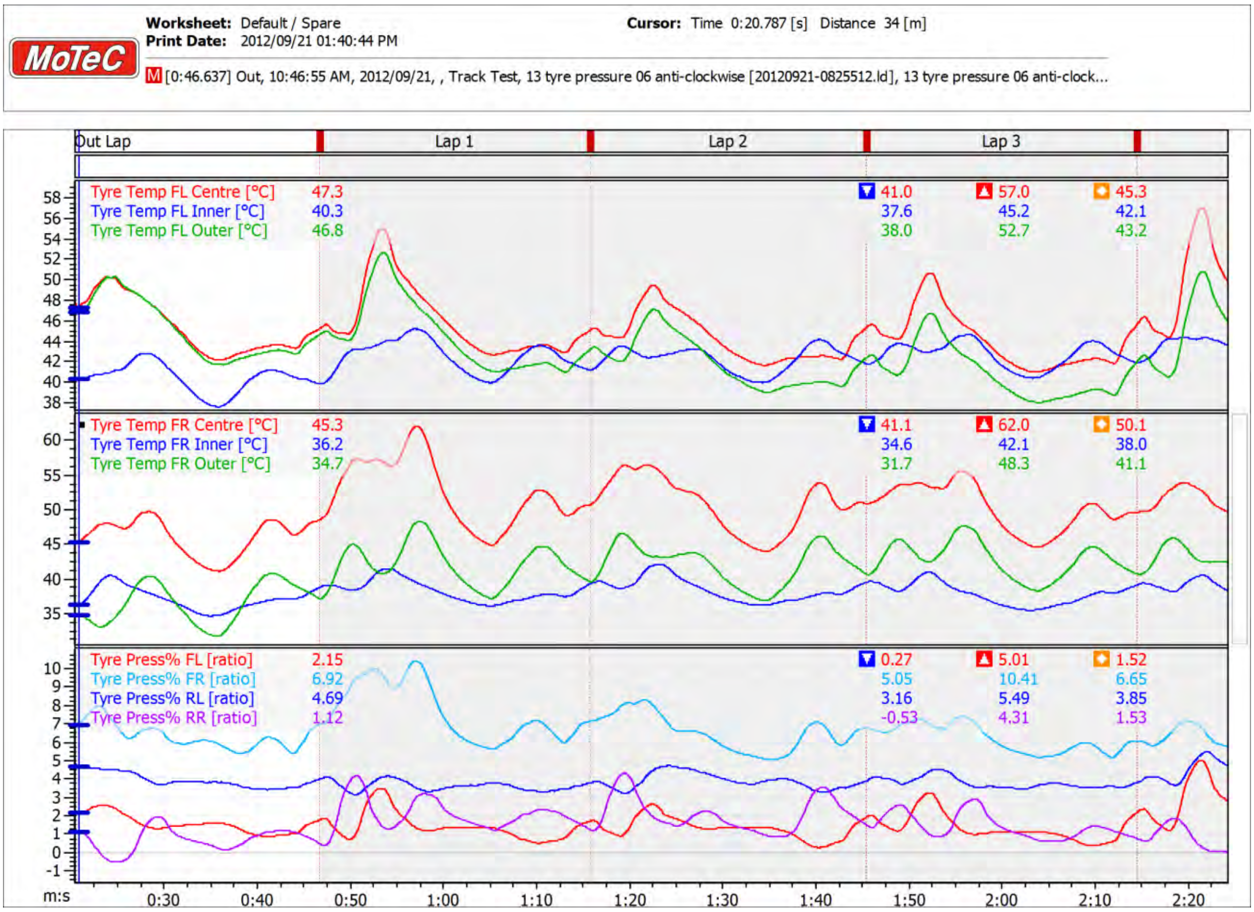

Figure 93: Pressure Test 60kPa Anti-Clockwise Circuit